U.S. DEPARTMENT OF THE INTERIOR
U.S. GEOLOGICAL SURVEY

Composition of Co-Rich Ferromanganese Crusts and Substrate Rocks from the Marshall Islands, Cruise KODOS 97-4

James R. Hein[1], Jai-Woon Moon[2], Kyeong-Yong Lee[2], Ki-Hyune Kim[2], Leanne Roberts[1], Malia Burrows[1], Sung Hyun Park[2], Jennifer Dowling[1], Youn-ji Choi[2], Susan E. Zielinski[1], Sang-Bum Chi[2], Laura Benninger[1], Hyun-Sub Kim[2], and Cheong-Kee Park[2]

Open File Report 98-375

1998

[1]U.S. Geological Survey, 345 Middlefield Rd., MS 999, Menlo Park, CA, 94025, USA
[2]Korea Ocean Research and Development Institute, P.O. Box 29, An San, 425-6000, Seoul, Korea

INTRODUCTION

Three northwest Pacific seamounts were studied in the Marshall Islands Exclusive Economic Zone (EEZ) during the KODOS 97-4 cruise, which took place from 23 August to 6 September, 1997 aboard the R.V. Onnuri (Figs. 1-4). Cruise KODOS 97-4 (Table 1) marked a renewed effort to study seamount mineral deposits that had started with three USGS-KORDI cooperative cruises aboard the R.V. Farnella, one each in the years 1989-1991. The primary objectives of the KODOS 97-4 cruise were to (1) map the distribution of thick Fe-Mn crusts on Lomilik Seamount and determine the geologic and oceanographic conditions that promoted growth of thick crusts (Fig. 3). Reconnaissance sampling and mapping on Lomilik Seamount were completed in 1989 during the first cooperative USGS-KORDI cruise aboard the R.V. Farnella (Hein, Kang, et al., 1990). During that cruise, the thickest (180 mm) shallow-water crust ever recovered from the ocean basins was collected from the summit of Lomilik Seamount; and (2) reconnaissance sampling and mapping of two volcanic edifices that had not previously been studied, Lemkein Seamount and Litakpooki Ridge (Figs. 2, 4). Representative ferromanganese oxyhydroxide crusts (Fe-Mn crusts) and substrate rocks from the dredge hauls taken on those three edifices were analyzed for this study, which extends our previous work on Fe-Mn crusts collected in and around the Marshall Islands (Hein et al., 1988; Hein, Kang, et al., 1990; Hein, Ahn, et al., 1992; Hein et al., 1997a).

Shipboard operations included three dredges on Lemkein Seamount, ten dredges, eight CTD stations, and two camera surveys on Lomilik Seamount, and two dredges on Litakpooki Ridge (Tables 2-4; Figs. 1-4). Of the 15 dredges attempted, 12 provided usable Fe-Mn crust samples. In addition, 1059 km of 12 kHz and 3.5 kHz bathymetric surveys were carried out, 524 km of which also included 12 channel, 300 cubic inch airgun profiles on Lomilik Seamount (Table 3). An important objective of the cruise, swath bathymetric mapping of Lomilik Seamount, was not accomplished because of equipment problems. Swath bathymetry should be completed during a follow-up cruise in 1998 and those data will then be combined with data presented here to fully address objective 1 listed above. A relatively good bathymetric map was prepared from a grid survey of Lomilik Seamount using 12 and 3.5 kHz lines (Fig. 3).

Lemkein Seamount is located between four atolls in the south-central Marshall Islands and Litakpooki Ridge is located at the southwestern margin of the Marshall Islands EEZ (Fig. 1). The bathymetry of those two edifices, especially Lemkein, is poorly known (Figs. 2, 4). Lomilik Seamount is located among a large group of seamounts to the west of Anewetak Atoll in the western Marshall Islands. Our bathymetry reveals a flat-topped edifice with a gently sloping summit located on the southwest margin of a broad, gently sloping summit terrace that, to the north, abruptly steepens in slope at 2200 m water depth, but drops off more gradually to the east and west (Fig. 3). The summit and summit terrace form a 40 km by 15 km rectangular shape in plan view. The summit is at about 1350 m water depth with the seamount base at 4600 m. Most dredge samples were collected from the terrace and from a small scarp that separates the terrace from the summit. The thickest crusts were collected from that scarp and somewhat thinner crusts from the summit terrace, whereas the thinnest crusts were collected from the middle and upper steep flanks of the seamount. The lowermost flanks were not sampled.

As seen on bottom videos, Lomilik summit terrace supports a thin blanket of foraminiferal ooze between outcrops of basalt and volcaniclastic rocks. The first deep-sea camera line (DSC1) is a north-to-south profile across the summit terrace to the summit. Rock outcrops comprise a larger area than do sediments from about 2100 m to 2050 m water depth, then sediment cover is greater than outcrop coverage from about 2050 m to 1880 m, and finally only sediment was seen from 1880 m to 1480 m at the summit. The second deep-sea camera line (DSC2) is a east-to-west profile across the upper summit platform. Rock outcrops characterize the platform at water depths of 1560 m to 1535 m,

sediments from 1535 m to 1445 m, rock outcrops alternating with sediment from 1445 m to 1435 m, and again solely rock outcrops from 1435 m to 1355 m at the summit. Sediment cover on the entire platform is thin as determined by seismic profiles and bottom video and, as found elsewhere, Fe-Mn crusts likely exist under the thin blanket of sediment (Yamazaki, 1993; Yamazaki et al., 1993).

CTD casts taken at about six hour intervals over the same locations show significantly different oxygen contents and temperatures at the same water depths (Table 4). For example, at the summit of Lomilik Seamount, the 5° C isotherm shifted from 900 m water depth to 950 m then to 875 m over a 13 hour period. Likewise, the water depth of the lowest oxygen content shifted by as much as 35 m. These rapid changes highlight the dynamic oceanographic environment that occurs over seamounts in terms of currents and internal tides.

This report presents data for all dredge hauls, including sample descriptions, detailed chemical (major, minor, platinum group, and rare earth elements) and mineralogical analyses of bulk Fe-Mn crusts, individual crust layers, and substrate rocks collected during cruise KODOS 97-4. Correlation coefficients are used to determine relationships between elements and associations of elements with mineralogical phases.

METHODS

X-ray diffraction was completed on a Philips diffractometer using Cukα radiation and a curved-crystal carbon monochromator. Abundances of major oxides and Ba, Sr, Y, Zr, Nb, and Rb in substrate rocks were determined by X-ray fluorescence spectroscopy (XRF; Taggart et al., 1987); Fe(II) by colorimetric titration (Peck, 1964); CO_2 by coulometric titration (Engleman et al., 1985); H_2O^+ by water evolved at 925°C as determined coulometrically by Karl-Fischer titration (Jackson et al., 1987); H_2O^- by sample weight difference at 110°C for greater than one hour (Shapiro, 1975); F and Cl by specific ion electrode, S by combustion and infrared spectroscopy (Jackson et al., 1987), and C by induction furnace; Y, U, Th, and rare earth elements (REEs) by inductively coupled plasma-atomic emission spectrometry-mass spectrometry (ICP-MS); and Au, Sc, Cr, Co, Ni, Zn, As, Se, Br, Mo, Ag, Sb, Cs, Ba, Ta, W, Ir, and Hg by neutron activation analysis (NAA; McKown and Millard, 1987). Low totals for phosphorite samples occur because of the high F, Cl, and S contents, which are not included in the totals.

For Fe-Mn crusts, the concentrations of Mn, Fe, Si, Al, Mg, Ca, Na, K, Ti, P, Ag, Ba, Be, B, Co, Cu, Ge, Li, Mo, Nb, Ni, Pb, Rb, Sc, Sn, Sr, V, Zn, and Zr were determined by ICP; Bi, Cd, Ga, In, Tl, Y, REEs, and platinum group elements (PGEs) by ICP-MS (Aruscavage et al., 1989; Lichte et al., 1987a,b); As, Au, Br, Cr, Cs, Hf, Sb, Se, Ta, Th, U, and W by NAA; and Te by graphite furnace atomic-absorption spectroscopy. The usual Pearson product moment correlation coefficient was used to calculate the correlation coefficient matrices.

SUBSTRATE ROCK DESCRIPTIONS AND COMPOSITION

Substrate rocks in decreasing order of abundance are breccia, basalt, limestone, phosphorite, volcaniclastic mudstone, siltstone, and sandstone, and hyaloclastite (Tables 5, 6). As seen in hand samples, breccias most commonly consist of basalt clasts in a carbonate fluorapatite (CFA) cement and less commonly a Fe-Mn oxyhydroxide cement; the breccias are matrix supported. Many breccia samples have Fe-Mn oxyhydroxide coatings on the basalt clasts, which may extent into the CFA cement as impregnations and dendrites. Volcanogenic clasts in breccias and volcaniclastic rocks are commonly replaced by clay minerals, iron oxides, and zeolites. Other minor breccia clast types include Fe-Mn

crust fragments, phosphorite, and rarely ironstone. Some breccia samples from dredge D7 (Lomilik Seamount) contain large bedding-parallel vugs that are filled with geopedal CFA, probably after foraminiferal sand.

Basalt collected in most dredge hauls was probably clasts in breccia that were removed during the dredging process, as evidenced by CFA cement attached to some basalt fragments. Basalts range from gray, massive, and moderately altered to brown and completely altered. Vesicles are most commonly filled with CFA and less commonly with iron oxide, zeolite, or calcite. In dredge D3 (Lemkein Seamount), pillow basalt wedges have layered, dark-brown, hydrothermally(?) altered chill margins that were completely altered to clay minerals and zeolites. Basalt and breccia from dredge D12 (Lomilik Seamount) contain large (to 10 mm), pristine feldspar crystals. CFA infills fractures in breccias and basalts.

Most limestones are composed of foraminifera and are white, pale brown, or cream colored. They are commonly peppered with Fe-Mn hydroxide grains and are poorly consolidated. Clastic reef limestones consist of rounded to angular carbonate clasts and foraminifera with calcite cement and moldic porosity; some samples (D11-17-1A; D11-20A; Lomilik Seamount) have incipient CFA cement.

Mudstones are laminated and differentially phosphatized. Phosphorites are white, pale pink, pale brown, and brown. Phosphorites are mostly replaced carbonates, but also consist of replaced volcanic and volcaniclastic rocks. Volcaniclastic sandstones and siltstones are bedded and yellow-brown to red-brown. These clastic rocks are cemented by clay minerals, zeolites, and CFA. Ironstone is dark brown and formed by replacement of fine-grained volcaniclastic-bioclastic breccia.

The only age control for the three seamounts sampled is an Eocene or Oligocene age for phosphatized foraminiferal limestone collected from Lomilik Seamount in 1989 (Hein, Kang, et al., 1990).

X-Ray Diffraction Mineralogy

Primary volcanogenic and sedimentary minerals include plagioclase, pyroxene, magnetite, and calcite; and secondary minerals include CFA, smectite, calcite, phillipsite, goethite, hematite, barite, and K-feldspar (Table 7). Secondary CFA is the most abundant mineral in these samples and occurs in 64% of the samples as a major or moderate constituent, regardless of rock type (Table 7).

Bulk breccias consist chiefly of CFA, with moderate to minor amounts of plagioclase, K-feldspar, smectite, calcite, phillipsite, goethite, δ-MnO_2, and barite (Table 7). The freshest basalts consist chiefly of plagioclase, pyroxene, magnetite, CFA, and smectite. The most altered basalts lack all primary minerals and are composed of one or more of phillipsite, smectite, CFA, goethite, and hematite. These are the same minerals, with or without plagioclase, that comprise the volcaniclastic rocks. Basalt sample D3-10A (Lemkein Seamount) is completely altered to CFA and smectite and is very hard, whereas sample D15-12A (Litakpooki Ridge) is completely altered solely to smectite and is soft; both samples maintain relict basalt textures. Chill margin rinds on pillow basalt fragments may be completely altered to phillipsite. Vesicles are filled with CFA, phillipsite, smectite, goethite, or calcite.

Limestones are composed chiefly of calcite, with minor K-feldspar, goethite, and CFA in some samples (Table 7). Calcite is primary and the other minerals are due to various admixtures of volcanogenic grains and their alteration products, or to cementation and replacement. All gradations exist from unaltered limestone to phosphorite with relict limestone textures, especially CFA-replaced foraminiferal sands.

Phosphorite samples are composed of CFA with lesser amounts of plagioclase, K-feldspar, calcite, smectite, and phillipsite (Table 7). Many samples are composed solely of

CFA. Ironstone samples are composed of goethite and have been partly replaced by late-stage CFA.

Chemistry

The most P_2O_5 rich CFA-replaced sedimentary rocks have CaO/P_2O_5 ratios of 1.58 to 1.66 (Table 8), whereas theoretical chemical compositions for CFA range from 1.5 to 1.6 (Manheim and Gulbrandsen, 1979). The slight excess Ca over P in some KODOS 97-4 samples may be due to additional Ca associated with minor contamination by volcanogenic plagioclase, phillipsite cement (an alteration product of volcanic debris), and to relict calcite in the phosphatized limestone. However, several samples (D7-7A, D13-13A, D13-17A; Table 8) with ratios between 1.60 and 1.66 are very pure, indicating that CaO/P_2O_5 ratios between 1.58 and 1.66 are characteristic of uncontaminated marine CFA. Ratios in that range have been found in many of our previous studies (e.g., Hein, Kang, et al., 1990; Hein, Ahn, et al., 1992; Hein et al., 1993). The mean CaO/P_2O_5 ratio of 1.63 is very near the most cation- and anion-substituted francolite (1.62) end of the fluorapatite (1.32)-CFA range (Manheim and Gulbrandsen, 1979; McClellan and van Kauwenbergh, 1990). Similarly, the F/P_2O_5 ratios (0.11-0.13) are closer to the most substituted francolite (0.148) end of the range than the fluorapatite end (0.089) for five of the seven samples for which we have F data. The mean Sr content for the five purest phosphorite samples is 925 ppm, near the low end of the range (900-1600 ppm) found for other central Pacific phosphorite samples (Hein et al., 1993). The normalized REE patterns of pure phosphorite samples show a seawater-type pattern with large negative Ce anomaly, small positive Gd anomaly, and heavy REE enrichment (Table 9; Fig. 5). These identical patterns indicate that the CFA was derived from seawater. A small amount of contamination by smectite significantly decreases the magnitude of the Ce anomaly in the phosphorite (Table 8; Fig. 5; sample D11-8A).

Smectite occurs in major to moderate amounts in 14% of the samples analyzed, and is especially abundant in the strongly altered basalts. Only one sample with abundant smectite (D33-19-1A) was analyzed and has relatively high Si, Al, Fe, and Zr contents, indicative of an iron-rich montmorillonite.

Phillipsite is also a common mineral, occurring in major to moderate abundances in 16% of the samples, primarily in breccias and the altered chill margin of basalts. Two samples measured for chemistry that are dominantly phillipsite (D3-5-1A, D3-14A) have Si/Al ratios of 2.0 and 2.3, which are below the range for most marine phillipsites (2.3-2.8), but within the range for phillipsites formed in mafic igneous rocks (1.3-2.4; Kastner, 1979). These nearly pure KODOS phillipsite samples have the highest Al_2O_3 contents of any rocks analyzed here and the maximum TiO_2 content of 4.8%. With moderate amounts of smectite accompanying the phillipsite (samples D4-5A, D12-2-2A), alumina contents decrease and the silica/alumina ratio increases. The highest K_2O contents and high TiO_2, Nb, Rb, and Cr contents occur in these mixed phillipsite-smectite samples.

Most samples of basalt and basalt clasts in breccia are altered to smectite and goethite and are rarely replaced by phosphorite and phillipsite. Alteration is best characterized by increases in Fe_2O_3 and water and decreases in FeO and K_2O contents (Table 8). Volcaniclastic mudstones and hyaloclastites have compositions comparable to highly altered basalts.

One ironstone sample was analyzed (Table 8) and consists of 35% Fe, which represents about 55% FeOOH in the form of goethite. The remainder of the sample is composed predominantly of Ca, P, and CO_2, representing calcite and CFA (compare Tables 7 and 8). The silica/alumina ratio is the lowest (2.2) of all samples analyzed, which indicates that the excess Al may be acquired by adsorption onto the goethite. Ironstones have been found on many seamounts in the central Pacific and their origin has been attributed to hydrothermal activity that occurred during the Cretaceous when most of the seamounts formed (Hein et al., 1994).

FERROMANGANESE CRUSTS

Fe-Mn crusts studied here vary in thickness from a patina to 130 mm (Tables 5, 6). The total thickness of some crusts is unknown because the substrate rock and some of the lowermost part of the crust were not collected, for example in dredge D9 (Lomilik Seamount). In that dredge, the thickest crust is 110+ mm. The thickest crust average from the various dredge hauls is 70+ mm collected from Lomilik Seamount in dredge D7 (Tables 5, 6). Thicker crusts are composed of two or more layers, five being the maximum and three being the most common. The most common bedding sequence is an uppermost massive black layer (layer 1), which is underlain by a black porous layer that is stained reddish, or contains large vugs in some samples (layer 2), which in turn is underlain by a dense, massive, black, phosphatized layer (layer 3). Layer 2 may contain abundant infiltered carbonate ooze, while layer 3 may contain CFA-filled veins and vugs in addition to being impregnated by CFA. Most crusts greater than 60 mm thick have a phosphatized older crust generation.

The growth rates and ages of nonphosphatized, or very mildly phosphatized bulk crusts and crust layers were determined using the empirical equation of Puteanus and Halbach (1988), which is based on Co contents and assumes a constant flux of Co in space and time, and that of Manheim and Lane-Bostwick (1988), which uses Mn, Fe, and Co contents (Table 10). Using the Puteanus and Halbach (1988) equation produces growth rates that range from 1.7 to 9.9 mm/Ma (mean 4.8 mm/Ma) for bulk crusts and 2.0-12.6 mm/Ma (mean 5.2 mm/Ma) for crust layers. In contrast, growth rates determined by the Manheim and Lane-Bostwick (1988) equation are much slower, with a range for bulk crusts of 0.4-2.7 mm/Ma (mean 1.2 mm/Ma) and for crust layers a range of 0.6-3.2 mm/Ma (mean 1.3 mm/Ma). The later growth rates are much more in line with those determined by U-series and Be isotopes, which range from <1-10 mm/Ma, but mostly fall within the range of 1-3 mm/Ma (Hein et al., 1998). Using the slower growth rates, the age range for the beginning of growth of bulk crusts is 6-93 Ma. The 93 Ma age is based on bulk crust chemical data for the 71 mm-thick crust D8-1. However, when crust layer data for D8-1 are used, the age of initiation of crust growth is only 58 Ma, probably a more accurate estimate of the true age of initiation of crust growth. That would leave 71 Ma as the oldest age (D13- 1) for initiation of crust growth, which is probably close to the age of the seamount on which the crust formed. In contrast, the other ages for initiation of crust growth are much younger than the age of the volcanic edifices on which they grew. Marshall Islands seamounts range in age from about 76-138 Ma old, ages of 76-86 Ma being most common (Davis et al., 1989; Lincoln et al., 1993). The fast growth rates determined by the Puteanus and Halbach (1988) equation produce unreasonably young ages for initiation of crust growth, especially for the thick crusts, the maximum age being only 17 Ma for initiation of crust growth.

X-Ray Diffraction Mineralogy

Great care was taken in sampling crusts for chemical and mineralogical analyses. All contamination from recent sediments was removed, which was especially critical in porous crust layers. Also, special attention was paid to obtaining a clean separation of the lower crust layers from the substrate. Any minerals or elements determined to exist in the various crust layers were incorporated into those layers during deposition or diagenesis and are not due to sampling procedures or post-depositional infiltration of sediment. Finally, encrusting organisms and other debris were cleaned from the crust surfaces before

subsampling. Bulk always refers to the entire crust thickness, whether composed of layers or not.

δ–MnO_2 (vernadite) contents of crusts range from about 78% to 100% (Table 11). δ–MnO_2 has only two X-ray reflections at about 2.42Å and 1.41Å. X-ray amorphous Fe oxyhydroxide epitaxially intergrown with the δ–MnO_2 is also a dominant phase in these crusts, but is not included with the crystalline phases listed in Table 11. Part of this X-ray amorphous iron phase crystallized to goethite in seven of the bulk crusts and six of the individual layers analyzed. In the individual layers, goethite was present mostly in the innermost layer, indicating that those layers have undergone the most advanced diagenetic alteration. An additional sample (D8-1C) may contain Fe hydroxide in the form of lepidocrocite. CFA occurs in 30% of the bulk crusts and 27% of the layers analyzed. Crust layer samples contain up to 22% CFA, always within the innermost one or two layers of the crust. CFA is not found in the outer layers of thick crusts or in thin crusts. Several thick crusts (D4-1, 70 mm; D7-9, 65 mm; D13-1, 85 mm) are very unusual in that they do not contain CFA, which usually occurs in the innermost layers of crusts over about 60 mm thick. Also unusual is the thin crust D4-2A (18 mm thick), which contains CFA; however, the CFA occurs as a contaminant from the substrate that could not be completely removed from the base of the crust--the CFA does not impregnate the crust as in the other CFA-bearing samples.

Quartz occurs in 40% of the crusts analyzed, 44% in bulk crusts and 36% in crust layers (Table 11). Quartz is always less than or equal to about 2%. Plagioclase (trace to 2%) was found in only three samples. The quartz and some of the plagioclase are of eolian origin, carried by the westerlies from Asia, as there is no local or regional source for quartz in the west-central Pacific. The Marshall Islands are south of the main westerly wind belt which is reflected in lower quartz contents compared to crusts from higher latitudes (Hein et al., 1985, 1987; Hein, Kang, et al., 1990). The remainder of the plagioclase, as well as the smectite, phillipsite, K-feldspar, heulandite, and calcite were reworked from local outcrops and incorporated into the crusts during precipitation of the Fe-Mn oxyhydroxides. Smectite occurs in about 20% of the bulk crusts and layers analyzed.

Calcite occurs in only two crusts; one is a thin (2 mm) bulk crust (D14-1A) attached to a limestone substrate and the calcite is due to our inability to get a clean separation from the substrate limestone; the other is a medium thickness (33 mm) bulk crust that is extremely porous and consequently, it was difficult to clean all the infiltered carbonate sediment from the crust.

Chemistry

Sixty-two Fe-Mn oxyhydroxide samples were analyzed for chemical composition including 27 bulk crusts, 33 crust layers, 1 breccia cement, and 1 clast from a breccia (Tables 12-17). Data are presented both with hygroscopic water (Table 12) and on a hygroscopic water-free basis--that is normalized to 0% H_2O^- (Tables 13, 14). Hygroscopic water varies from 6% to 25% (to 30% in other samples from the region) and consequently can affect the contents of all other elements. Sample compositions normalized to 0% H_2O^- can be more meaningfully compared and also more closely represent the grade of the potential ore. The following discussion is confined to water-normalized chemical data.

Bulk Crusts: The mean Fe and Mn contents of the 27 bulk crust samples are 15.1% and 21.4%, respectively (Tables 13, 15). The mean Fe/Mn ratio (0.71) is comparable to the mean ratio for the entire central Pacific region (0.72; Hein et al., 1992), but is higher than the ratio for the entire Marshall Islands EEZ (0.64; Hein et al., 1998), and lower than the ratio for the area to the northwest of the Marshall Islands EEZ (0.76; Hein et al., 1997a). The mean Mn content is less and the Fe content somewhat less compared to bulk

crusts from the entire Marshall Islands EEZ, 16.9% and 26.3%, respectively. The mean contents of the economically important metals Co (0.54%), Ni (0.37%), and Pt (0.33 ppm) are less than the mean contents of 0.79%, 0.57%, and 0.63 ppm, respectively, for the entire Marshall Islands EEZ. The mean Co and Ni contents are less and Pt about the same compared to mean contents for the equatorial Pacific. Phosphorus, a potential byproduct for mining, has a mean value of 1.1%, comparable to the central Pacific mean of about 1%, but lower than the mean content of 1.8% for crusts from the entire Marshall Islands EEZ. Analysis of a large number of thick crusts lowers the mean contents of many metals, and that is probably why this study shows mean concentrations below the regional and Marshall Islands means for Co and Ni. Studies that include only analyses of thin crusts yield mean concentrations higher than those of regional means (for example, Pichocki and Hoffert, 1987; see Hein et al., 1992 for discussion). The Co+Ni+Cu mean content for all bulk crusts is 1.00% and the maximum mean percent is 1.69%. If Pb is added to that group of elements, the mean content is 1.11% and the maximum mean content is 1.83%. The mean content of Co+Ni+Cu decreases with increasing crust thickness, for example the mean is 1.20% for crusts ≤10 mm thick, 1.03% for crusts ≤50 mm thick, and 0.94% for crusts ≥65 mm thick. That decrease in metals is controlled by Co and Pb contents because mean Cu contents increase with crust thickness, 447 ppm for ≤10 mm thick crusts versus 852 ppm for crusts ≥65 mm thick. The relationship of Co+Ni+Cu to Fe and Mn contents can be seen on a Bonatti et al. (1972) diagram (Fig. 6), on which the KODOS 97-4 data fall in the range typical for central Pacific Fe-Mn crust data (Halbach et al., 1982; De Carlo et al., 1987; Hein et al., 1998).

Other metals of potential economic interest that are concentrated in the Fe-Mn crusts include Bi (mean 34 ppm), Te (51 ppm), Tl (173 ppm), W (85 ppm), and Zr (542 ppm). Only recently have crusts been analyzed for those elements. Tellurium contents are remarkably high compared to the lithospheric mean Te content of about 1 ppb--51,000 times enrichment for the Fe-Mn crust mean of 51 ppm and 79,000 times enrichment for the maximum Te content of 79 ppm in bulk crusts. The interesting aspect is that the mean contents of all these elements, Bi, Te, Tl, W, and Zr increase in thick crusts, such as, they are 30, 46, 161, 73, and 357 ppm in ≤10 mm thick crusts and 37, 54, 180, 92, and 514 ppm, respectively, in ≥65 mm thick crusts. Mean contents of Ca, P, Ba, Be, Mo, Sb, Sr, Rh, and especially Pt increase in thick crusts, whereas As, B, Cl, Cr, Th, and Ru decrease as do Co, Ni, and Zn as mentioned above. This means that the ore grade for the rare metals increases with tonnage (thickness), the reverse of the situation of Co in crusts, the chief metal of economic interest. This decrease in grade with increase in tonnage is typical for metals of interest in most types of ore deposits. The increases in Ca and P contents are the result of phosphatization of the older generation of thick crusts.

The composition of an Fe-Mn oxyhydroxide cement (D7-7C; Table 13) taken from a breccia sample is similar to those of bulk crusts, but does have several notable differences including lower contents of Fe, Mn, Cl, Co, Cu, Ni, Tl, W, and Zr and higher contents of Ca, P, Ba, Bi, Pb, and Te. Those differences can be attributed to intense phosphatization and diagenesis of the cement. Likewise, an Fe-Mn oxyhydroxide clast (D13-5) from a breccia sample has a composition similar to those of bulk crusts, with the notable exceptions of lower Fe, Mn, Cl, Co, and Ni contents and higher Ca, P, Ba, Bi, Cu, Pb, and Zr contents. Again, those differences indicate phosphatization and especially strong diagenetic processes in the clast. The significant difference between the clast and the cement is the twice as high Cu content in the clast, probably reflecting its higher degree of diagenesis.

Crust Layers: Individual layers from nine crusts were analyzed: Two crusts were split into five layers, two crusts into four layers, and five crusts into three layers (Tables 13, 16). Most crust profiles show increases of Ba, Be, Cu, and Zn and decreases of Pb and Co contents from the surface layer of the crusts through the innermost layer. In addition, Ca and P are more abundant in the inner, phosphatized parts of crusts, and Mn and Fe in

the outer parts of crusts. Phosphorus remains relatively constant in thin crusts and increases significantly in the lower layers of thick crusts. Other elements show no trends with depth in the crusts, or decrease with depth in some crusts and increase with depth in others. Platinum also typically increases with depth in thick crusts, although Pt was not measured on enough layers to demonstrate that relationship here. These trends generally indicate that there is a decrease of manganophile elements with depth in the crusts accompanied by increases in elements characteristic of the residual biogenic phase (see section on Interelement Relationships). Non-phosphatized crust layers generally have higher trace metal contents relative to Fe and Mn contents than do phosphatized crust layers (Fig. 6B).

Platinum Group Elements and Gold

Eight bulk crusts and nine crust layers were analyzed for Au and PGEs (Table 14). Palladium contents (mean <4.5 ppb) are below the lithospheric mean content of 10 ppb, whereas all other PGEs are enriched over their mean lithospheric content: Os (mean <2.7 ppb) and Ir (5.3 ppb) are 3-5 times enriched, Ru (mean 17 ppb) and Rh (mean 20 ppb) 5-32 times, and Pt with a mean content of 327 ppb is 31-122 times enriched over its mean lithospheric content. Even with the strong enrichments of Pt, the maximum (611 ppb) content measured in this study is less than the mean contents found in previous studies of crusts in the Marshall Islands and areas to the north. The mean Pt content for the Marshall Islands EEZ is 634 ppb (Hein et al., 1998), whereas that reported by Hein, Kang, et al. (1990) for 20 seamounts in the Marshall Islands is 666 ppb. Crusts from the area to the northwest of the Marshall Islands EEZ have a mean Pt content of 501 ppb, and those from a large area of the northwest Pacific have a mean Pt content of 777 ppb (Usui and Someya, 1997). The reason for the low Pt contents measured in this study is unknown. Platinum contents increase with crust thickness and of the eight bulk crusts analyzed, only half were thick and only four of the nine layers were from the phosphatized, older part of the crusts, where the Pt contents are typically the highest. However, this does not fully explain the low Pt contents and the unusual distribution of PGEs. One crust (D7-1; Table 14) had four layers analyzed for PGEs and shows an unusual pattern where the highest Pt content (317 ppb) occurs in one of the outer, non-phosphatized layers (13-28 mm), rather than in one of the innermost layers, which is the more typical distribution pattern. Another thick (85 mm) crust (D13-1) also has an unusual pattern where the highest Pt content, the maximum measured here, occurs in the innermost layer, which is not phosphatized. That sample also has the highest Ir, Pd, Rh, and Ru contents measured in this study.

Enrichment of PGEs in the inner parts of crusts is common for central Pacific crusts. The highest Pd and Ru concentrations occur in crusts from the Yap and Mariana arcs, as do other elements indicative of clastic input. As shown in previous studies, Pt, Ir, and Rh are derived predominantly from seawater, whereas Pd and much of the Ru are derived from clastic debris, the remainder of the Ru being derived from seawater. The extraterrestrial component (meteorite debris) in the bulk crusts is small. However, meteorite debris may be concentrated locally in the crusts by formation of dissolution unconformities, or by proximity of the crust to meteorite fallout during formation of the layer. Localized extraterrestrial debris-rich horizons, however, do not alter the overall hydrogenetic signature of the PGEs. In addition, the PGE ratios are non-chondritic, with Fe-Mn crust compositions showing more than an order of magnitude more Pt relative to Ir and Rh relative to Ir. More likely, Pt is a redox sensitive element and its changing concentration reflects changing redox conditions and diagenesis (see Hein et al., 1997b).

Gold contents vary greatly from <6 ppb to 543 ppb, and is probably near its lithospheric mean for most samples. The high Au content (543 ppb) in sample D15-1A is very unusual in Fe-Mn crusts and, until verified, should be considered with caution. A

duplicate run of sample D15-1A showed the same high Au content. Even the second highest Au content of 51 ppb is unusually high.

Rare Earth Elements

Total REEs vary from about 0.09% to 0.27% (Table 17). The highest REE contents occur in the breccia clast and breccia cement and again highlights the differences of those two samples compared to the crusts. For bulk crusts, the total REE contents range from 0.11% to 0.17%, respectively, with a mean of 0.14%. The range and mean for individual crust layers are somewhat lower than for bulk crusts, 0.09%-0.16% and 0.12% respectively. REE content differences between thick and thin crusts is small, 0.13% and 0.14%, respectively. The five samples for which layers were analyzed show a variety of patterns of REE concentrations with depth in the crusts. The four layers of crust D2-1 generally show a decrease of most elements from the substrate to the crust surface, with the exception of Ce and ΣREEs, which have higher contents in layer 2 than layer 3; and Yb and Lu, which have lower contents in layer 2 than in layer 1. The three layers of crusts D4-1 and D13-1 show nearly the opposite trend with all elements except Ce increasing from the substrate to the crust surface. The five layers from crusts D7-2 and D8-1 show complicated patterns. For crust D8-1, there is an increase in light REE contents from layer 5 next to the substrate through layer 3, then a decrease to the crust surface--that is the contents of light REEs are highest in layer 3 and decrease away from layer 3 both to the substrate and to the crust surface; the heavy REEs generally decrease from layer 5 through layer 4 then increase to the crust surface--that is layer 4 has the lowest contents of the heavy REEs, which increase away from layer 4 to the substrate and to the crust surface. The five layers of crust D7-2 show a pattern with REEs (except Ce) increasing in content from layer 5 next to the substrate through layer 4, then they decrease through layer 3, and then increase again to the crust surface through layers 2 and 1. These various trends are not related to present-day water depth of crust collection nor to phosphatization of the crusts. For crusts from the area northwest of the Marshall Islands, 11 of 13 crusts analyzed showed decreases in REE contents from the substrate to the crust surface (Hein et al., 1997a), as did crust D2-1 here.

Chondrite (Anders and Grevesse, 1989)-normalized REE patterns show moderate to large positive Ce anomalies, small positive Gd anomalies, light REE enrichments, and slight decreases in heavy REEs with increasing atomic number, or flat heavy REE patterns (Figs. 7-15). Post-Archean Australian shale (PAAS; McLennan, 1989)-normalized REE patterns show nearly flat heavy REEs, light REE depletion, and positive Ce and Gd anomalies. There is one exception (sample D7-2E), where a negative Ce anomaly occurs on both chondrite- and shale-normalized patterns. That negative anomaly is the result of strong phosphatization of that crust layer. CFA typically has a REE pattern with a large negative Ce anomaly, as does seawater. A small positive Gd anomaly is typical of hydrogenetic Fe-Mn crusts and of seawater (Hein et al., 1988). In crusts where five layers were analyzed, the largest Ce anomaly occurs in the innermost layer 5, with the second largest anomaly in layer 3. In the crust where four layers were analyzed, the largest Ce anomaly occurs in the innermost layer, with the second largest anomaly in layer 2. In crusts where three layers were analyzed, the largest Ce anomaly occurs in layer 2, the middle layer.

Interelement Relationships

Correlation coefficients coupled with X-ray diffraction mineralogy can be combined to interpret which elements are associated with the mineral phases that make up the Fe-Mn

crusts. We analyzed correlation coefficient matrices for eight datasets including all data included in Table 13, all bulk crusts, bulk crusts ≥65 mm, bulk crusts ≤50 mm, bulk crusts ≤10 mm, and layers for each of four crusts. We present here the matrices for five of those datasets: All bulk crusts, bulk crusts ≥65 mm, bulk crusts ≤50 mm, and two of the four samples for which layers were analyzed (Tables 18-22). We interpret the data for all bulk crusts to indicate the following associations. **Detrital** (aluminosilicate) phase: Si, Al, Fe, K, Sc, Cr, Be, Li, B, Zr, Hf, Ti, Nb, Cu, Th, and Au(?); **Mn-oxyhydroxide** phase: Mn, Co, Ti, K, Mg, Na, Ni, and Nb; **Fe-oxyhydroxide** phase: Fe, As, V, Ba, Cu, Be, and Hf; **CFA** phase: Ca, P, S, and Sr; **residual-biogenic** phase: Na, Sr, Ba, Fe, Sb, Zn, Ga, and Au(?); adsorbed or **loosely bound** phase: Bi, S, Tl, Ni, Mo, Pb, U, Te, W, Cd, Co, and Br. These relationships show a strong affinity of K and Ti for both the detrital and Mn phases and a distribution of Fe among at least three phases. The assigned phases for the rare elements such as Bi, Te, Tl, W, and others are tentative and will be better defined elsewhere using different statistical techniques. In most previous studies, the loosely bound phase was not distinguished, rather two or more of the other five phases were used to define the make-up of crusts.

Only a few differences exist between the datasets of bulk crusts ≤50 mm thick and all bulk crusts. Specifically, the **detrital** (aluminosilicate) phase for bulk crusts ≤50 mm thick includes Mg, but not Nb, Cu, or Th; the **Mn-oxyhydroxide** phase also includes Mo and perhaps B; Mo is typically found as a manganophile element; the **Fe-oxyhydroxide** phase also includes Zr, Br, and perhaps Ti, Nb, and Zn; the **CFA** phase includes Ba and Li, but not Sr; the **residual-biogenic** and **loosely bound** phases are essentially the same. The differences are much greater between the all bulk crusts dataset and the bulk crusts ≥65 mm dataset. As found in other studies (e.g., Hein, Kang, et al., 1990), many of the element associations typically found for Fe-Mn crusts are modified when only thick crusts are considered. It is thought that these major differences are the result of diagenesis that has taken place during phosphatization and maturation of the thick crusts. Element associations for the detrital, CFA, and Fe oxyhydroxide phases are the most similar to those for all bulk crusts, but still have significant differences: The **detrital** (aluminosilicate) phase includes Ba, Sb, and Rh, but not K, Cr, Sc, Be, Cu, or Th; the **Mn-oxyhydroxide** phase only includes Mg and Na, which attests to extensive mobilization of elements associated with that phase; the **Fe-oxyhydroxide** phase includes Pt, but not V, Cu, Be, or Hf; the **CFA** phase is identical; the **residual-biogenic** phase in not discernible; the **loosely bound** phase may be composed of Br, Cl, Co, W, V, Te, Tl, Sb, As, LOI, Cu, and Cr; a **diagenetic** phase may exist, but its associated elements are not clearly defined from the correlation coefficients.

Correlations among layers in single crusts display a range of element associations, from those typical of the all bulk crusts dataset to those typical of the thick crust dataset. An example of the former is the 116 mm-thick crust D7-2, with five layers and strong phosphatization of the lowermost two layers, has the following element associations: **Detrital** (aluminosilicate) phase, Si, Al, Fe, B, Cr, and Th; **Mn-oxyhydroxide** phase, Mn, Co, K, Ti, Cd, Cl, Br, Pb, Te, Tl, and Ga(?); **Fe-oxyhydroxide** phase, Fe, As, V, and U(?); the **CFA** phase, Ca, P, S, and Li; **residual-biogenic** phase, Ba, Na, Zn, Sr, Mo, and Cu; and **loosely bound** phase, Ni, Bi, Ge, Hg, LOI, Co, B, W, Tl, Te, Br, and Cl. An interesting aspect of those associations is the presence of Te and Tl in the Mn phase, indicating their hydrogenetic origin. At the other extreme is the 71 mm-thick crust D8-1 that has five layers and mild phosphatization of the lowermost layer. Very few strong correlations exist and no correlations with at least a 95% confidence level exist for associations among the typical aluminosilicate-phase elements. However, at a lesser confidence level, the **detrital** phase elements may include Si, Al, Fe, Ti, B, Th, and Sc. The **Fe oxyhydroxide** phase includes Fe, As, and Sc; the **Mn oxyhydroxide** phase K,

Mg, Sr, and Na; the **CFA** phase Ca, P, S, Ni, Bi; the **residual biogenic** phase Ba, Cu, Zn, Na, and Sr; and the **loosely bound** phase is not discernible.

These element associations indicate that most of the rare elements that have not been analyzed in previous studies (Te, Tl, W, Bi, Hf, Zr, etc.) are predominantly hydrogenetic in origin and are associated primarily with the loosely bound, residual biogenic, and Mn oxyhydroxide phases. Hf may be associated with the Fe oxyhydroxide and detrital phases, whereas Zr is predominantly part of the detrital phase.

The correlation coefficients also show that the following elements increase with increasing crust thickness, Ca, P, S, Mo, Sr, Zn, and PGEs, whereas Si, Al, K, Ti, B, Co, and Th decrease with increasing crust thickness. These relationships indicate that the CFA phase increases and the detrital phase decreases with increasing crust thickness. It has been noted many times that Co contents, the most important metal of economic interest, decreases with crust thickness.

Correlation coefficients also show that the following elements increase with increasing water depth of occurrence, K, Sc, Th, Hg, and PGEs, whereas Ga, Sr, and Zn decrease with increasing water depth.

RESOURCE CONSIDERATIONS

The commonly cited cut-off grade for potential economic development is 0.8% Co and the cut-off thickness is 40 mm. On a water-free basis, KODOS 97-4 samples have moderate mean Pt (0.37 ppm), Mn (21.4%), Ni (0.37%), Co (0.54%), and Cu (0.09%) contents, with a mean Co+Ni+Cu content of 1.0%. The mean crust thickness is ≥40 mm for six of the 12 dredge hauls (50%) that recovered whole crust samples, some dredge hauls having a much thicker mean than 40 mm. It is not known whether ultimately grade or tonnage (thickness) will be the most important factor in choosing a potential mine site. It is important that several very rare metals, such as the PGEs, increase in grade with increasing crust thickness. Tellurium contents are especially interesting because its lithospheric abundance is about 5 times less than that of Pt, but its concentration in crusts is over 300 times greater than that of Pt. Tellurium needs to be looked at in detail in terms of its resource potential in Fe-Mn crusts.

ACKNOWLEDGMENTS

We thank the captain, crew, and scientific staff of the R.V. Onnuri cruise KODOS 97-4 for excellent support while at sea. We thank Jane Reid, U.S. Geological Survey (USGS) for reviewing this report, and C. Degnan, D. Mosier, and F. Wong of the USGS for help with Fig. 1.

REFERENCES

Anders, E. and Grevesse, N., 1989, Abundances of the elements: Meteoritic and solar. Geochimica et Cosmochimica Acta, v. 53, p. 197-214.

Aruscavage, P.J., Kirschenbaum, H., and Brown, F., 1989, Analytical methods: The determination of 27 elements in ferromanganese materials: *in* Manheim, F.T. and Lane-Bostwick, C.M. (eds.), Chemical Composition of Ferromanganese Crusts in the World Ocean: A Review and Comprehensive Database. U.S. Geological Survey Open File Report 89-020, 200 p. plus 3 appendices.

Chase, T.E. and Menard, H.W., 1973, Bathymetric atlas of the North Pacific Ocean. U.S. Naval Oceanographic Office, Washington, D.C., Publication 1301-2-3.

Cook, H.E., Johnson, P.D., Matti, J.C., and Zemmels, I., 1975, Methods of sample preparation and X-ray diffraction data analysis (X-ray mineralogy laboratory, Deep Sea Drilling Project, University of California Riverside): *in* Hays, D.E., Frakes. L.A., et al., Initial Reports of the Deep Sea Drilling Project, U.S. Government Printing Office, Washington, D.C., v. 28, p. 999-1007.

Davis, A.S., Pringle, M.S., Pickthorn, L-B.G., Clague, D.A., and Schwab, W.C., 1989, Petrology and age of alkalic lava from the Ratak Chain of the Marshall Islands. Journal of Geophysical Research, v. 94, p. 5757-5774.

De Carlo, E.H., McMurtry, G.M., and Kim, K.H., 1987, Geochemistry of ferromanganese crusts from the Hawaiian Archipelago--I. Northern survey areas. Deep-Sea Research, v. 34, p. 441-467.

Engleman, E.E., Jackson, L.L., and Norton, D.R., 1985, Determination of carbonate carbon in geological materials by coulometric titration. Chemical Geology, v. 53, p. 125-128.

Halbach, P., Manheim, F.T., and Otten, P., 1982, Co-rich ferromanganese deposits in the marginal seamount regions of the central Pacific basin--results of the Midpac '81. Erzmetall, v. 35, p. 447-453.

Hein, J.R., Manheim, F.T., Schwab, W.C., and Davis, A.S., 1985, Ferromanganese crusts from Necker Ridge, Horizon Guyot, and S.P. Lee Guyot: Geological considerations. Marine Geology, v. 69, p. 25-54.

Hein, J.R., Morgenson, L.A., Clague, D.A., and Koski, R.A., 1987, Cobalt-rich ferromanganese crusts from the Exclusive Economic Zone of the United States and nodules from the oceanic Pacific: *in* Scholl, D.W., Grantz, A., and Vedder, J.G. (eds.), Geology and Resource Potential of the Continental Margin of Western North America and Adjacent Ocean Basins-Beaufort Sea to Baja California. Circum-Pacific Council for Energy and Mineral Resources, Earth Science Ser., Houston, TX, v. 6, p. 753-771.

Hein, J.R., Schwab, W.C. and Davis, A.S., 1988, Cobalt and platinum-rich ferromanganese crusts and associated substrate rocks from the Marshall Islands. Marine Geology, v. 78, p. 255-283.

Hein, J.R., Kang, J.-K., Schulz, M.S., Park, B.-K., Kirschenbaum, H., Yoon, S.-H., Olson, R.L., Smith, V.K., Park., D.-W., Riddle, G.O., Quinterno, P.J., Lee, Y.-O., Davis, A.S., Kim, S.R., Pringle, M.S., Choi, D.-L., Pickthorn, L., Schlanger, S.O., Duennebier, F.K., Bergersen, D.D. and Lincoln, J.M., 1990, Geological, geochemical, geophysical, and oceanographic data and interpretations of seamounts and Co-rich ferromanganese crusts from the Marshall Islands, KORDI-USGS R.V. Farnella Cruise F10-89-CP. U.S. Geological Survey Open File Report 90-407, 246 p.

Hein, J.R., Ahn, J.-H., Wong, J.C., Kang, J-K., Smith, V.K., Yoon, S-H., d'Angelo, W.M., Yoo, S-O., Gibbs, A.E., Kim, H-J., Quinterno, P.J., Jung, M.-Y., Davis, A.S., Park, B.-K., Gillison, J.R., Marlow, M.S., Schulz, M.S., Siems, D.F., Taggart, J.E., Rait, N., Gray, L., Malcolm, M.J., Kavulak, M.G., Yeh, H.-W., Mann, D.M., Noble, M., Riddle, G.O., Roushey, B.H., and Smith, H., 1992, Geology, geophysics, geochemistry, and deep-sea mineral deposits, Federated States of Micronesia: KORDI-USGS R.V. Farnella cruise F11-90-CP. U.S. Geological Survey Open File Report 92-218, 191 pp.

Hein, J.R., Schulz, M.S., and Gein, L.M., 1992a, Central Pacific cobalt-rich ferromanganese crusts: Historical perspective and regional variability. in Keating, B. H. and Bolton, B. R. (eds.), Geology and Offshore Mineral Resources of the Central Pacific Basin, Springer-Verlag, New York, p. 261-283.

Hein, J.R., Yeh, H.-W., Gunn, S.H., Sliter, W.V., Benninger, L.M., and Wang, C.-H., 1993, Two major Cenozoic episodes of phosphogenesis recorded in equatorial Pacific seamount deposits. Paleoceanography, v. 8, p. 293-311.

Hein, J.R., Yeh, H.-W., Gunn, S.H., Gibbs, A.E., and Wang, C.-H., 1994, Composition and origin of hydrothermal ironstones from central Pacific seamounts. Geochimica et Cosmochimica Acta, v. 57, p. 179-189.

Hein, J.R., Zielinski, S.E., Staudigel, H., Chang, S.-W., Greene, M., and Pringle, M.S., 1997a, Composition of Co-rich ferromanganese crusts and substrate rocks from the NW Marshall Islands and international waters to the north, Tunes 6 cruise. U.S. Geological Survey Open File Report 97-482, 65 pp.

Hein, J.R., Koschinsky, A., Halbach, P., Manheim, F.T., Bau, M., Kang, J.-K., and Lubick, N., 1997b, Iron and manganese oxide mineralization in the Pacific: *in* Nicholson, K., Hein, J.R., Bühn, B., and Dasgupta, S. (eds.) Manganese Mineralization: Geochemistry and Mineralogy of Terrestrial and Marine Deposits. The Geological Society Special Publication No. 119, London, p. 123-138.

Hein, J.R., Koschinsky, A., Bau, M., Manheim, F.T., Kang, J.-K., and Roberts, L., 1998, Cobalt-rich ferromanganese crusts in the Pacific. In, CRC Handbook of Marine Minerals, Cronan, D.S. (Ed.), CRC Press, Boca Raton (in press).

Jackson, L.L., Brown, F.W., and Neil, S.T., 1987, Major and minor elements requiring individual determination, classical whole rock analysis, and rapid rock analysis: *in* Baedecker, P.A. (ed.) Methods for Geochemical Analysis. U.S. Geological Survey Bulletin 1770, p. G1-G23.

Kastner, M., 1979, Zeolites: *in* Burns, R.G. (ed.), Marine Minerals, Mineralogical Society of America Short Course Notes, v. 6, p. 111-122.

Lichte, F.E., Golightly, D.W., and Lamothe, P.J., 1987a, Inductively coupled plasma-atomic emission spectrometry: *in* Baedecker, P.A. (ed.), Methods for Geochemical Analysis. U.S. Geological Survey Bulletin 1770, p. B1-B10.

Lichte, F.E., Meier, A.L., and Crock, J.G., 1987b, Determination of the rare earth elements in geological materials by inductively coupled plasma-mass spectrometry. Analytical Chemistry, v. 59, p. 1150-1157.

Lincoln, J.M., Pringle, M.S., and Silva, I.P., 1993, Early and Late Cretaceous volcanism and reef-building in the Marshall Islands. In, The Mesozoic Pacific: Geology, Tectonics, and Volcanism, Pringle, M.S., Sager, W.W., Sliter, W.V., and Stein, S. (Eds.), American Geophysical Union Geophysical Monograph 77, Washington, D.C., p. 279-305.

Manheim, F.T. and Gulbrandsen, R.A., 1979, Marine phosphorites. *in* Burns, R.G. (ed.), Marine Minerals. Mineralogical Society of America Short Course Notes, v. 6, p. 151-173.

Manheim, F.T. and Lane-Bostwick, C.M., 1988, Cobalt in ferromanganese crusts as a monitor of hydrothermal discharge on the Pacific sea floor. Nature, v. 335, p. 59-62.

McClellan, G.H. and van Kauwenbergh, S.J., 1990, Mineralogy of sedimentary apatites. In, Phosphorite Research and Development, Notholt, A.J.G. and Jarvis, I. (Eds.), The Geological Society, London, p. 23-31.

McKown, D.M. and Millard, H.T., Jr., 1987, Determination of uranium and thorium by delayed neutron counting. *in* Baedecker, P.A. (ed.), Methods for Geochemical Analysis. U.S. Geological Survey Bulletin 1770, p. I1-I12.

McLennan, S.M., 1989, Rare earth elements in sedimentary rocks: Influence of provenance and sedimentary processes: i*n* Lipin, B.R. and McKay, G.A. (eds.) Geochemistry and Mineralogy of Rare Earth Elements. Mineralogical Society of America's Reviews in Mineralogy, v. 21, Washington D.C.

Peck, L.C., 1964, Systematic analysis of silicates. U.S. Geological Survey Bulletin 1170, 89 p.

Pichocki, C. and Hoffert, M., 1987, Characteristics of Co-rich ferromanganese nodules and crusts sampled in French Polynesia. Marine Geology, v. 77, p. 109-119.

Puteanus, D. and Halbach, P., 1988, Correlation of Co concentration and growth rate: A method for age determination of ferromanganese crusts. Chemical Geology, v. 69, p. 73-85.
Shapiro, L., 1975, Rapid analysis of silicate, carbonate, and phosphate rocks--revised edition. U.S. Geological Survey Bulletin 1401, 76 p.
Taggart, J.E., Lindsay, J.R., Scott, B.A., Vivit, D.V., Bartel, A.J., and Stewart, K.C., 1987, Analysis of geologic materials by wavelength-dispersive X-ray fluorescence spectrometry: *in* Baedecker, P.A. (ed.), Methods for Geochemical Analysis. U.S. Geological Survey Bulletin 1770, p. E1-E19.
Usui, A. and Someya, M., 1997, Distribution and composition of marine hydrogenetic and hydrothermal manganese deposits in the northwest Pacific, in Manganese Mineralization: Geochemistry and Mineralogy of Terrestrial and Marine Deposits, Nicholson, K., Hein, J. R., Bühn, B., and Dasgupta, S. Eds., Geological Society Special Publication No. 119, London, p. 177-198, 1997.
Yamazaki, T., 1993, A re-evaluation of cobalt-rich crust abundance on the Pacific seamounts. International Journal of Offshore and Polar Engineering, v. 3, p. 258-263.
Yamazaki, T., Igarashi, Y., and Maeda, K., 1993, Buried cobalt rich manganese deposits on seamounts. Resource Geology Special Issue, v. 17, p. 76-82.

Table 1. Scientific Personnel on R.V. *Onnuri* cruise KODOS 97-4

Jai Woon Moon	Co-chief scientist	KORDI[1]
James R. Hein	Co-chief scientist	USGS[2]
Laura M. Benninger	Sampling	USGS
Sang Bum Chi	Deep Sea Camera	KORDI
Youn-ji Choi	CTD	KORDI
Byung Doo Jang	Observer	KMPC[3]
Hong Sic Kim	Observer	KMPC
Hyun Sub Kim	Sub-Bottom Profiling	KORDI
Kyu Jung Kim	Airgun Seismic	KORDI
Duk Kee Lee	Airgun Seismic	KORDI
Kyeong Yong Lee	Watch Chief	KORDI
Sang Heon Nam	Watch Chief	KORDI
Cheong Kee Park	Seabeam	KORDI
Sung Hyun Park	Sampling	KORDI
Leanne N. Roberts	Data Processing	USGS
Hai Soo Yoon	Airgun Seismic	KORDI
Yong Jeong Yoon	Sampling	KORDI
Susan E. Zielinski	Sampling	USGS

[1]Korea Ocean Research and Development Institute
[2]United States Geological Survey
[3]Korea Mining Promotion Corporation

Table 2. Station and operations for cruise KODOS 97-4

Station	Operation	Seamount
1	D1	Lemkein
2	D2	Lemkein
3	D3	Lemkein
4	D4	Lomilik
5	D5	Lomilik
6	D6	Lomilik
7	D7	Lomilik
8	DSC1	Lomilik
9	DSC2	Lomilik
10	CTD1	Lomilik
11	CTD2	Lomilik
10	CTD3	Lomilik
12	CTD4	Lomilik
10	CTD5	Lomilik
11	CTD6	Lomilik
13	CTD7	Lomilik
14	CTD8	Lomilik
15	D8	Lomilik
16	D9	Lomilik
17	D10	Lomilik
18	D11	Lomilik
19	D12	Lomilik
20	D13	Lomilik
21	D14	Litakpooki
22	D15	Litakpooki

Table 3. Twelve channel, two-150 in^3 airguns, and 3.5 kHz and 12 kHz bathymetry lines

Seamount Name	Line Number	Airgun Volume	Nautical Miles	Kilometers
Lemkein	1	--	24.71	45.77
Lemkein	2	--	14.03	25.98
Lemkein	3	--	24.89	46.10
Lomilik	4	300	26.40	48.88
Lomilik	5	300	26.40	48.89
Lomilik	6	300	26.40	48.90
Lomilik	7	300	26.41	48.91
Lomilik	8	300	06.60	12.23
Lomilik	9	300	17.76	32.89
Lomilik	10	300	06.60	12.23
Lomilik	11	300	17.76	32.89
Lomilik	12	300	17.76	32.89
Lomilik	13	300	26.40	48.89
Lomilik	14	300	26.40	48.90
Lomilik	15	300	26.41	48.91
Lomilik	16	300	26.41	48.91
Litakpooki	17	--	29.75	55.09
Litakpooki	18	--	24.85	46.02
Litakpooki	19	--	34.85	64.54
Litakpooki	20	--	07.96	14.75
Litakpooki	21	--	24.89	46.10
Litakpooki	22	--	10.56	19.56
Litakpooki	23	--	24.78	45.89
Litakpooki	24	--	19.91	36.88
Litakpooki	25	--	34.76	64.38
Litakpooki	26	--	17.92	33.19
Total	--	--	571.57	1058.55

Dash means airguns not used, only 12 and 3.5 kHz system

Table 4. Preliminary oxygen and temperature data from CTD casts, Lomilik Seamount, cruise KODOS 97-4

	Latitude (N)	Longitude (E)	Station Number	Julian Day	Greenwich Mean Time[1]	Lowest O_2 Content (ml/l)	Water Depth at minimum O_2 (m)	Water Depth at Top of OMZ (m)	Water Depth at 10°C Isotherm (m)	Water Depth at 5°C Isotherm (m)
Summit										
CTD 1	11°40.40'	161°40.07'	10	242	1746-1911	~1.07	370	300	275	900
CTD 3	11°40.79'	161°39.80'	10	243	0024-0136	~1.0	315	270	260	950
CTD 5	11°39.86'	161°40.10'	10	243	0545-0658	~1.05	340	305	290	875
Northern Flank										
CTD 2[2]	11°46.33'	161°43.34'	11	242	2001-2310	~1.30	340	340	290	860
CTD 6	11°43.02'	161°46.56'	11	243	0743-1032	~1.40	320	320	280	920
Southern Flank										
CTD 4	11°34.29'	161°36.97'	12	243	0238-0538	~0.99	320	300	260	900
CTD 7	11°37.00'	161°37.00'	13	243	1220-1500	~1.05	370	320	285	900
South of Lomilik										
CTD 8[3]	11°27.09'	161°34.50'	14	243	1609-1813	~1.16	400	320	280	930

[1]Local Time equals GMT minus twelve hours

[2]All CTD data are from the downcast, except for CTD 2, where data are from the upcast because of operational difficulties

[3]CTD 8 is located south of CTD 7; the water depth is deeper at CTD 8 than at CTD 7

Table 5. Dredge summary for cruise KODOS 97-4

Dredge Number	Seamount Name	Water Depth On-Off Bottom (m)	Water Depth Corrected (m)[1]	Recovery (kg)	Max. Crust Thickness (mm)	Ave. Crust Thickness (mm)	Dominant Substrate	Comments
D1	Lemkein	1859-1753	1750-1600	2	10	8	None	Large glass sponge
D2	Lemkein	1732-1692	1725-1650	28	90	60	Breccia	CFA cemented
D3	Lemkein	3210-2480	3180-3090	185	35	<1 (11[2])	Basalt	Hydrothermally altered basalt
D4	Lomilik	2102-1850	2100-1950	71	60	7	Breccia, basalt	Volcaniclastic sandstone
D5	Lomilik	1860-1640	1860-1640	0.1	0	0	Pumice	--
D6	Lomilik	1744-1463	1740-1660	0.1	22	11	Phosphorite	Three pebbles
D7	Lomilik	1912-1476	1800-1550	97	130	70+	Breccia	Mega-crusts
D8	Lomilik	2397-2005	2390-2150	6	75+	50+	None	Incomplete crust thicknesses
D9	Lomilik	1844-1487	2000-1900	19	110+	60+	Breccia	Incomplete crust thicknesses
D10	Lomilik	3650-2162	3500-3200	0	-	-	-	Lost dredge bag
D11	Lomilik	2166-1860	2160-1850	160	55	<1 (26[2])	Foram sandstone	150 kg foram sandstone block
D12	Lomilik	3534-3050	3350-3100	150	4	2	Breccia, basalt	Basalt = clasts from breccia
D13	Lomilik	2390-2142	2350-2250	185	95	61	Breccia	Abundant phosphorite cement
D14	Litakpooki	2505-2492	2505-2492	1.1	3	1	Limestone	Phosphatized; ironstone
D15	Litakpooki	2209-1888	2150-1950	28	80	40	Foram sandstone	Phosphorite

[1]Depth interval from which samples were probably recovered
[2]Number in parentheses based only on the group of samples that contained more than a patina of crust

Table 6. Location and description of dredge hauls, cruise KODOS 97-4

Dredge Number	Latitude (°N)[1]	Longitude (°E)	Total Recovery (kg)	Broken from Outcrop (%)	Talus (%)	Encrusted Rock (%)	Description of Ferromanganese Oxides	Description of Substrate Rocks
D1	09°25.01' 09°23.64'	166°02.93' 166°02.50'	2	100	0	--	Botryoidal surface; 1 massive black layer; thickness: max=10mm, av=8mm	None recovered; large fragments of glass sponge
D2	09°24.60' 09°24.95'	166°03.10' 166°03.69'	28	100	0	100	Botryoidal, granular, & smooth, surface textures; current erosion enhanced relief on some botryoidal surfaces; thick crusts have 3 layers: 1. outer, thin, black, botryoidal; 2. porous black, some with Fe-oxide stain; 3. inner, thick, massive, dense, black with CFA filled (less commonly unfilled) vugs in upper part; thin crusts with one massive black layer; mm-thick crusts on breccia clasts; breccia cement; thickness: max=90mm, av=60mm	95% breccia with altered, brown to reddish brown basalt and minor older breccia and phosphorite clasts commonly all with Fe-Mn oxide crust; cemented by pale brown, yellowish-brown, to cream-colored CFA, less commonly by Fe-Mn oxide; 5% altered yellow-brown hyaloclastite
D3	09°30.86' 09°28.06'	166°04.66' 166°03.87'	185	50	50	20[2]	Granular, smooth, micro-botryoidal, subdued botryoidal, lizard skin, & botryoidal, surface textures; mostly granular patina on rocks; rocks with crusts have mostly 1 massive black layer, less commonly 1 very porous layer with columnar growth; thickest crusts (on nodules with large basalt nucleus) have 3 layers: 1. porous black, 2. massive, 3. porous black, or 2 layers: 1. black massive, 2. black, porous with Fe-oxide stains; dendrites in some substrate rock; thickness: max=35mm, av=11mm on rocks with crusts, av=<1mm for whole dredge haul	35% pale brown altered basalt talus; 35% dark brown basalt nearly completely altered to clay minerals; vesicles filled with zeolites, CFA, or calcite; 15% hydrothermally altered reddish-brown pillow basalt fragments with layered rinds; 10% breccia (with clasts of all basalt types above in differentially phosphatized carbonate matrix; matrix-supported) and hyaloclastite; 4% vesicular, amygdaloidal, & misc. basalts; <1% limestone, phosphorite, and nodules with basalt nucleus

Table 6 continued

D4	11°44.2' 11°42.15'	161°41.9' 161°41.15'	71	40	60	90	1 thick crust (max=60mm, av=55mm) with subdued botryoidal surface with granular overgrowth; 3 layers: 1. massive black, 2. porous with vugs filled with carbonate sand 3. massive black with Fe oxide staining; another crust (10-40mm) with two porous layers, one Fe stained; 3 crust pebbles with no substrate, 16-39mm thick; other crusts ≤3mm with subdued botryoidal, granular, and smooth surfaces; one massive black layer	45% breccia: altered vesicular basalt, Fe-Mn crust, & phosphorite clasts all with Fe-Mn crusts to 3mm in CFA cement; cement supported with more than 1 episode of phosphatizaton; Fe-Mn oxide cement in places; CFA filled fractures; 40% altered, brown, vesicular basalt; vesicles filled with CFA, calcite, & zeolite (?); 12% yellow-brown to red-brown volcaniclastic sandstone; bedded, coarse- to fine-grained; some CFA or calcite cement; 3% phosphorite, massive, cream, brown, pinkish, gray, Mn dendrites; sandstone interbedded with breccia & phosphorite
D5	11°42.12' 11°40.6'	161°40.86' 161°40.4'	0.1	0	100	0	None	Three pumice pebbles
D6	11°41.1' 11°40.3'	161°40.51' 161°40.3'	0.1	33	67	0	1 crust pebble with no substrate; smooth to granular surface; 1 massive black layer; CFA veins; granular patina on phosphorite; max=22mm, av=11mm	1 phosphorite pebble with dense, compact, massive, brown layer & a porous white layer; 1 tan pumice pebble

Table 6 continued

D7	11°39.3' 11°39.12'	161°41.9' 161°40.7'	97	100	0	100	Botryoidal upper surface, granular to microbotryoidal on sides; thicker crusts with 3-6 layers, 3 being most common: 1. massive, black, botryoidal to columnar; 2. porous grading down to vuggy, some samples Fe stained; 3. massive, dense, black, some samples have a central porous layer & others have CFA filled vugs near the top of the layer; 1 crust has an asicular layer between 1 and 2; many thick crusts without substrate have an incomplete layer 3, so thickness is a minimum; thinner crusts have two layers: 1. black botryoidal, rarely laminated; 2. black, massive, rarely porous & vuggy; thickness: max=130mm, av=70+mm	Small amount of breccia with red-brown volcanic clasts in CFA cement, more rarely Fe-Mn oxide cement; large vugs filled with geopedal CFA; minor yellow-brown to red-brown hyaloclastite at the base of layer 3 in a few thick crusts
D8	11°34.12' 11°36.34'	161°42.37' 161°42.02'	6	99	1	No substrate	Surface texture botryoidal, granular on sides; crusts have 3-5 layers most commonly 3: 1. massive, black, botryoidal; 2. porous grading down to vuggy, some samples Fe stained; 3. massive, dense, black, some samples have a central porous layer & others have rare CFA filled vugs; some crusts have an asicular layer between 1 and 2; crusts are without substrate and have an incomplete layer 3=thicker crusts, or are missing layer 3=thinner crusts, so thicknesses are minimums; smooth patina on 2 mudstone talus pebbles & granular patina on phosphorite pebble; thickness: max=75+mm, av=50+mm	No substrate of crusts recovered; 2 laminated brown mudstone pebbles; laminae defined by Fe-Mn oxides, which also form dendrites; 1 phosphorite pebble, yellow-brown, hard, dense, peppered with Fe-Mn oxides; 3 gray pumice pebbles

Table 6 continued

D9	11°36.98' 11°38.51'	161°41.81' 161°39.75'	19	100	0	No substrate	Surface texture botryoidal, granular on sides; crusts have 3-5 layers most commonly 3: 1. massive, black, botryoidal; 2. porous grading down to vuggy, some samples Fe stained; 3. massive, dense, black, some samples have a central porous layer & others have rare CFA filled vugs; crusts are without substrate and have an incomplete layer 3=thicker crusts, or are missing layer 3=thinner crusts, so thicknesses are minimums; thickness: max=110+mm, av=60+mm	No substrate of crusts recovered, nor any other rocks
D10	11°46.71' 11°44.54'	161°43.28' 161°42.18'	0	-	-	-	Lost dredge bag	-
D11	11°36.74' 11°37.72'	161°37.47' 161°37.20'	160	99	1	2	Most limestone with discontinuous granular patina; 4% of dredge detached crusts & <1% with substrate attached; botryoidal surfaces, granular on sides; 1 black columnar layer with Fe staining, or 2 layers: 1. massive black, 2. porous, Fe stained; 1 thick crust has 4 layers: 1. massive brown, Fe stained, 2. black asicular, 3. porous, Fe stained, 4. dense, massive, black; 3 nodules with large volcaniclastic sandstone nucleus and average crust = 20 mm; crusts thickness max=55mm, av=26mm, for whole dredge, av=<1mm	80% forminiferal limestone (carbonate sandstone: very poorly consolidated white, fine-grained, or pale brown, coarse-grained, both lightly peppered with Mn oxides; 5% moderate to well consolidated foraminiferal and shell hash limestones; 5% very fine-grained pale brown mudstone, possibly phosphatized; 5% green-gray to red-brown volcaniclastic breccia interbedded with sandstone and pebbly sandstone; all grains altered, mostly in smectite matrix, rarely CFA cement; 4% detached crusts; <1% crusts on breccia; <1% phosphorite

Table 6 continued

D12	11°46.13' 11°45.83'	161°43.73' 161°42.96'	150	100	0	70 patina 30 crusts	Microbotryoidal, granular, subdued botryoidal, smooth, lizard skin surface textures; current polished on some edges; dominantly 1 black massive layer, less commonly 1 porous black layer; thickness: max=4mm, av=2mm	50% brown breccia with brown vesicular basalt clasts with goethite-filled or unfilled vesicles; lesser amounts of gray vesicular basalt clasts to 150mm; CFA & calcite(?) cement; 50% altered, highly to moderately vesicular basalt; mostly pillow fragments with glassy altered cooling rinds & with large vesicles filled with goethite and small ones unfilled, some lined with calcite(?); some samples with large (to 10mm) elongate translucent feldspar crystals; rare yellow vug fill; some scoria; basalt is probably clasts from the breccia removed during dredging
D13	11°44.69' 11°45.51'	161°35.05' 161°35.18'	185	100	0	100	Botryoidal, subdued botryoidal, microbotryoidal, lizard skin, & smooth surface textures, granular on sides of crusts; dominantly 3 layers: 1. black massive to botyroidal or columnar, 2. porous, vuggy, columnar, may be discontinuous or absent in some samples, 3. porous with Fe staining; this 3rd layer is unlike other places where it is typically black & massive; black & massive crust fragments are found as clasts in the breccia and Mn oxide dendrites are abundant in the CFA cement; a few crusts have a thin very porous upper layer and thick, black, massive lower layer; thickness: max=95mm, av=61mm	90% breccia, yellow-brown to cream colored, composed of vesicular basalt, Fe-Mn crust fragments, and phosphorite clasts in a CFA cement (replaced carbonate); cement-supported; cement is very hard to friable; clasts are surrounded by thin Mn crust and extensive dendrites extend from crust clasts and from the base of the present crust into the CFA cement; 10% altered vesicular basalt, commonly with a chill margin; most likely are clasts separated from the breccia during dredging

Table 6 continued

D14	08°24.74' 08°24.63'	160°36.99' 160°37.05'	1.1	100 (except pumice)	0	100 (except pumice)	Granular surface texture; 1 massive, black, porous layer; punice not encrusted; thickness: max=3mm, av=1mm	65% gray pumice; 30% orange-brown bioclastic limestone composed of shell hash and foraminifera; may be phosphatized; 5% dark brown ironstone, which replaced fine-grained volcaniclastic-bioclastic breccia; mildly phosphatized
D15	08°21.65' 08°19.56'	160°36.86' 160°37.04'	28	>99	<1	100	Small-sized botryoids on surface; granular on sides and undersides; dominantly 3 layers: 1. black, botryoidal, massive, or rarely laminated, 2. porous, columnar, with sediment filled vugs, Fe stained in some, 3. massive, Fe stained; in thinner crusts, layer 3 may be missing; rarely thick entirely dense & massive crusts; dendrites and disseminated Mn oxides in the substrate & lines borings in substrate; thickness: max=80mm, av=40mm	99% foaminifera limestone (carbonate sandstone); white to cream colored, red-brown Fe stain around some borings & granular Mn oxide line others; medium sand size; poorly consolidated, friable; <1% differentially phosphatized limestone; <1% dark brown basalt talus, completely altered to clays and zeolites

[1]Latitudes and longitudes for on and off bottom
[2]30% of rocks with Fe-Mn oxyhydroxide patina and 50% with discontinuous patina

Table 7. X-ray diffraction mineralogy of substrate rocks from KODOS 97-4

Sample	Major[1]	Moderate	Minor/Trace	Rock/Sediment
D2-1F	CFA[2]	–	Barite	Breccia[3] matrix
D3-1A	CFA	–	–	Breccia matrix
D3-1B	CFA	–	Smectite, phillipsite	Phosphorite (limestone)[4] lens in D3-1A
D3-2B	CFA	–	–	Phosphorite breccia
D3-4B	Plagioclase	Pyroxene, CFA	Smectite	Gray basalt
D3-5-1A	Phillipsite	–	Smectite	Hydrothermally altered dark red-brown glassy pillow basalt rind
D3-8-1A	CFA	–	–	Phosphorite rind on basalt
D3-10A	CFA	Smectite	–	Completely altered brown basalt
D3-12-1A	Calcite	–	–	White micrite limestone
D3-12-2A	CFA	–	Plagioclase	Pale-brown phosphorite (limestone)
D3-14A	Phillipsite	–	Smectite	Hydrothermally altered dark red-brown glassy pillow basalt rind
D3-19-1A	Smectite	Phillipsite	Plagioclase, hematite	Highly altered vesicular basalt
D4-5A	Phillipsite	Smectite	Plagioclase?	Bedded volcaniclastic sandstone
D4-7A	CFA, goethite	–	–	Fe-rich phosphorite clast in breccia
D4-7B	CFA	δ-MnO_2	–	Black clast in breccia
D4-7C	CFA	–	–	Breccia matrix
D7-7A	CFA	–	–	Dark fill in large vug in breccia
D7-7B	CFA	–	–	Pale fill in same vug as D7-7A
D8-4A	CFA	K-feldspar	Smectite	Laminated brown mudstone
D11-8A	CFA	–	Smectite	Phosphorite (mudstone)
D11-10-1A	Plagioclase	CFA	Smectite	Green-gray volcaniclastic sandstone
D11-11A	Calcite	Plagioclase, CFA	Smectite	Gray sandstone
D11-14A	CFA	K-feldspar, calcite	Smectite, phillipsite	Red & green breccia
D11-16-1A	CFA	Calcite	K-feldspar	Pale yellow phosphorite
D11-16-2A	CFA	–	–	Brown phosphorite
D11-16-3A	CFA	–	Calcite	Pale brown phosphorite
D11-16-3B	CFA	–	–	Gray phosphorite
D11-17-1A	Calcite	–	CFA	Foraminiferal limestone
D11-17-1B	CFA	Smectite	–	Phosphorite (mudstone) interbedded with D11-17-1A
D11-19A	Calcite	–	–	Foraminiferal limestone
D11-20A	Calcite	–	CFA	Foraminiferal limestone
D12-1-2	Goethite	–	–	Brick-red vesicle fill in D12-1-3
D12-1-3	Plagioclase	CFA, phillipsite	Smectite	Brown to gray pillow basalt fragment
D12-1-4	Phillipsite	–	Smectite	Yellow vesicle fill in D12-1-3
D12-2-2A	Phillipsite	Smectite	–	Brown breccia
D12-3-1A	Labradorite	–	–	Translucent crystals to 10mm long in breccia and basalt
D13-3A	CFA	–	Calcite	Breccia matrix
D13-13A	CFA	–	–	Cream-colored phosphorite
D13-17A	CFA	–	–	Cream-colored phosphorite
D13-27A	Plagioclase	Magnetite, calcite	Smectite	Altered vesicular basalt
D14-1B	Calcite	–	K-feldspar, goethite	Bioclastic reef limestone
D14-2A	Goethite	Calcite, CFA	–	Ironstone (breccia)
D15-8A	Calcite	–	–	Foraminiferal limestone
D15-12A	Smectite	–	–	Completely altered red-brown basalt

[1]Major: ≥25%, Moderate: ≥5% to <25%, Minor: <5%
[2]CFA is carbonate fluorapatite
[3]All breccias are sedimentary, and most are volcaniclastic
[4]Rock types in parentheses are replaced by CFA

Table 8. Chemical Composition of substrate rocks from cruise KODOS 97-4

	D3-1A	D3-1A[1]	D3-4B	D3-4B[1]	D3-5-1A	D3-8-1A	D3-12-2A	D3-14A	D3-19-1A	D4-5A
SiO_2 wt.%	4.20	4.15	45.1	45.2	41.0	2.24	–	33.8	43.1	42.5
Al_2O_3	1.35	1.35	14.0	14.1	16.0	0.57	–	15.0	14.7	12.2
FeO	<0.1	<0.1	1.9	1.9	0.1	<0.1	<0.1	0.1	0.4	<0.1
Fe_2O_3	0.57	0.56	9.69	9.71	15.6	0.35	–	15.0	12.0	18.8
MgO	0.35	0.35	4.36	4.38	2.15	0.38	–	1.67	2.99	2.45
CaO	50.0	49.8	8.13	8.12	0.41	51.8	–	0.38	3.04	0.32
Na_2O	1.05	1.06	3.70	3.69	2.42	0.59	–	2.01	1.97	2.48
K_2O	0.28	0.27	1.75	1.77	2.41	0.08	–	2.60	1.61	4.57
TiO_2	0.152	0.152	3.484	3.468	4.849	0.084	–	4.367	3.832	3.633
P_2O_5	30.7	30.7	1.87	1.87	0.16	31.3	–	0.12	1.69	0.12
MnO	0.07	0.07	0.08	0.08	0.14	0.04	–	0.21	0.13	0.46
LOI	7.40	7.25	5.25	5.30	14.8	10.0	–	25.0	13.2	12.8
Total	96.12	95.71	99.35	99.48	100.04	97.821	–	100.26	98.66	100.33
H_2O^+	2.00	2.1	2.20	2.30	7.50	2.00	2.40	6.60	6.50	6.40
H_2O^-	0.50	0.6	2.90	2.80	5.40	0.40	0.70	20.4	5.30	4.70
CO_2	4.71	4.73	0.28	0.32	0.05	5.21	4.72	0.05	0.22	0.04
C_{total}	1.43	1.42	–	–	–	1.60	1.51	–	–	–
S_{total}	0.640	0.640	–	–	–	0.680	0.650	–	–	–
F	3.56	3.73	–	–	–	4.01	3.74	–	–	–
Cl	0.179	0.175	–	–	–	0.294	0.172	–	–	–
Ba ppm	<20	<20	241	239	236	<20	–	257	102	275
Sr	770	752	453	455	147	1150	–	150	159	132
Y	90	88	49	50	17	131	–	24	47	15
Zr	66	67	159	158	690	36	–	179	487	416
Nb	<2	<2	25	27	78	<2	–	30	61	91
Rb	<2	<2	26	27	37	<2	–	26	28	93
Rock Type	Breccia	Breccia	Basalt	Basalt	Basalt rind	Phosphorite (basalt rind)	Phosphorite (limestone)	Basalt rind	Basalt	Volcaniclastic sandstone

Table 8 continued

	D4-7A	D7-7A	D11-8A	D12-1-3	D12-2-2A	D13-13A	D13-17A	D13-27A	D14-2A
SiO_2 wt.%	6.58	0.23	11.9	37.3	40.2	0.94	0.41	41.9	5.60
Al_2O_3	1.74	0.04	3.77	13.7	13.5	0.17	0.07	13.8	2.60
FeO	<0.1	<0.1	<0.1	2.0	0.1	<0.1	<0.1	1.8	0.1
Fe_2O_3	23.0	0.41	3.15	13.9	16.8	<0.01	0.06	10.3	49.5
MgO	1.15	0.24	1.05	1.74	1.42	0.21	0.34	3.36	1.26
CaO	27.2	53.2	41.1	9.54	1.46	53.3	54.3	10.8	16.4
Na_2O	0.91	0.73	1.14	2.92	3.78	0.72	0.73	2.96	0.48
K_2O	0.63	0.05	0.85	2.20	4.35	0.06	0.04	1.91	0.33
TiO_2	0.253	0.028	0.765	4.439	4.616	0.004	0.017	2.771	0.751
P_2O_5	17.2	32.6	25.6	3.95	0.46	32.2	33.1	1.65	3.14
MnO	6.12	0.31	<0.01	0.15	0.33	0.03	0.05	0.06	0.13
LOI	13.7	8.80	8.50	8.05	13.3	10.2	9.65	8.60	20.0
Total	98.48	96.54	97.73	99.89	99.86	97.83	98.77	99.91	100.29
H_2O^+	6.20	2.00	2.50	3.90	6.80	2.10	2.20	2.80	8.10
H_2O^-	4.60	7.80	2.10	4.60	4.00	1.60	0.30	5.00	1.50
CO_2	3.07	5.23	3.58	0.48	0.35	5.46	5.43	1.95	10.4
C_{total}	–	1.62	0.95	–	0.11	1.78	1.67	–	–
S_{total}	–	0.800	0.540	–	0.050	0.720	0.830	–	–
F	–	3.46	3.03	–	3.24	3.96	3.79	–	–
Cl	–	0.394	0.154	–	0.857	0.503	1.097	–	–
Ba ppm	1160	<20	<20	406	460	<20	61	282	95
Sr	855	891	554	900	204	865	948	578	199
Y	95	386	11	52	53	251	309	30	10
Zr	179	88	102	371	441	85	71	186	178
Nb	6	<2	14	54	46	<2	<2	38	15
Rb	23	<2	10	37	39	<2	<2	56	8
Rock Type	Clast in Breccia	CFA vug fill	Phosphorite (mudstone)	Basalt	Breccia	Phosphorite	Phosphorite	Basalt	Ironstone

[1]Duplicate analysis; LOI = loss on ignition at 925° C; CFA = carbonate fluorapatite; rock type in parentheses was replaced by CFA

Table 9. Rare earth and minor element contents of selected substrate rocks from Table 8, cruise KODOS 97-4

	D3-8-1A	D7-7A	D11-8A	D12-2-2A	D13-17A
Y ppm	143	365	14	49	319
La	61.7	175	22.4	51.6	159
Ce	5.8	16.1	34.9	104	6.4
Pr	8.4	21.1	4.8	8.7	25.9
Nd	40.2	97.0	20.7	39.9	124
Sm	8.0	19.7	4.7	8.4	27.1
Eu	1.83	4.3	1.13	1.93	6.0
Gd	10.7	26.9	3.8	8.5	33.6
Tb	1.5	3.8	0.5	1.1	4.6
Dy	11.3	28.7	2.8	7.2	30.7
Ho	2.8	7.1	0.51	1.48	7.1
Er	9.2	23.1	1.4	4.5	21.3
Tm	1.3	3.2	0.2	0.6	2.7
Yb	8.7	21.1	1.1	4.0	17.4
Lu	1.48	3.5	0.16	0.56	2.7
ΣREEs	316	816	113	291	788
Ce*	0.05	0.05	0.78	1.09	0.02
Y/Ho	51	51	27	33	45
Th	1.1	0.5	1.7	5.2	0.3
U	7.3	8.1	3.4	1.9	5.5
Cr	10	10	<10	680	10
Sc	5	12	3	17	6
Co	9	24	<5	85	10
Zn	<50	<50	70	420	80
As	4	7	5	59	5
Br	13	18	6	30	40
Sb	4.6	4.4	3.0	35.0	3.9
Hf	<1	<1	2	9	<1
Ta	<1	<1	1	3	<1
Au ppb	7	<5	<5	<5	<5
Rock Type	Phosphorite (basalt rind)	CFA vug fill	Phosphorite (mudstone)	Breccia	Phosphorite

Rare earth elements, Y, U, and Th by ICP-MS and minor elements by NAA; Ce* is Ce anomaly = chondrite-normalized 2Ce/La+Pr; in all samples, Ni is <100 ppm, Se <5 ppm, Mo <5ppm, Ag <5 ppm, Cs <3 ppm, W <4 ppm, Hg <1 ppm, and Ir <20 ppb.

Table 10. Calculated growth rates and ages of Fe-Mn crusts, cruise KOSDO 97-4

Sample	Interval (mm)[1]	Type	Growth Rate (mm/Ma)[2]	Crust Age (Ma)	Growth Rate (mm/Ma)[3]	Crust Age (Ma)
D2-1B	0-10	Layer	5.9	1.7	1.4	7.2
D2-1C	10-25	Layer	3.7	5.7	1.2	19.5
D2-1D	25-45	Layer	3.9	10.8	0.8	45.1
D2-4A	0-65	Bulk	3.9	16.8	1.3	51.8
D2-6B	0-10	Layer	2.0	5.1	0.6	16.0
D2-6C	10-18	Layer	3.2	7.6	1.0	23.8
D3-2A	0-14	Bulk	6.8	2.0	2.3	6.0
D3-3A	0-30	Bulk TC	4.6	6.5	1.4	21.2
D3-3B	0-12	Bulk UC	3.3	3.6	1.1	11.3
D3-4A	0-7	Bulk	1.7	4.2	0.4	15.8
D4-1A	0-70	Bulk	9.9	7.1	2.7	25.9
D4-1B	0-15	Layer	5.4	2.8	1.3	11.8
D4-1C	15-36	Layer	10.2	4.9	2.8	19.3
D4-1D	36-55	Layer	12.6	6.4	3.2	25.1
D4-5B	0-5	Bulk	3.8	1.3	0.9	5.6
D4-5B1	0-5	Bulk	3.6	1.4	0.9	5.6
D7-1B	0-13	Layer	2.5	5.3	0.7	17.3
D7-1C	13-28	Layer	4.2	8.8	1.2	30.1
D7-2B	0-9	Layer	3.0	3.0	0.8	11.5
D7-2C	9-45	Layer	4.3	11.5	1.3	38.3
D7-2D	45-56	Layer	5.3	13.6	1.5	45.6
D7-9A	0-65	Bulk	4.0	16.2	1.2	55.7
D7-9B	0-7	Layer	2.0	3.4	0.6	12.2
D7-9C	7-32	Layer	6.5	7.3	1.8	25.9
D7-9D	32-64	Layer	6.7	12.1	1.7	45.1
D7-10A	0-31	Bulk	3.8	8.2	0.9	33.1
D8-1A	0-71	Bulk	4.5	15.6	0.8	93.0
D8-1B	0-7	Layer	2.8	2.5	0.7	10.3
D8-1C	7-32	Layer	4.2	8.5	1.1	32.8
D8-1D	32-36	Layer	4.2	9.5	0.9	37.4
D8-1E	36-61	Layer	11.2	11.7	1.9	50.6
D8-1F	61-71	Layer	7.2	13.1	1.4	57.8
D9-1A	0-105	Bulk	6.8	15.5	1.5	69.4
D9-5A	0-30	Bulk	2.5	12.1	0.7	40.9
D11-1A	0-30	Bulk	9.7	3.1	2.4	12.3
D11-2A	0-30	Bulk	6.9	4.3	2.2	13.8
D12-1-1	0-3	Bulk	2.2	1.4	0.4	7.5
D12-2-1A	0-2.5	Bulk	2.3	1.1	0.8	3.3
D13-1B	0-28	Layer	4.4	6.3	1.1	25.9
D13-1C	28-40	Layer	4.9	8.7	0.9	39.1
D13-1D	40-85	Layer	8.0	14.3	1.4	71.1
D13-2A	0-50	Bulk	7.9	6.3	2.1	23.7
D13-20-1A	0-33	Bulk PSC	2.2	14.9	0.5	69.2
D14-1A	0-2	Bulk	2.9	0.7	0.8	2.6
D15-1A	0-32	Bulk	4.5	7.1	1.4	22.5
D15-1A1	0-32	Bulk	4.4	7.2	1.4	23.0
D15-2A	0-48	Bulk	5.8	8.2	1.2	40.8
D15-2B	0-11	Layer	3.2	3.5	0.9	11.8
D15-2C	11-32	Layer	5.4	7.4	1.5	26.1
D15-2D	32-50	Layer	6.2	10.3	1.1	41.8

[1]Intervals measured from the outer surface of crusts; TC is topside crust, UC is underside crust for encrusted talus debris, and PSC is porous side crust

[2]From equation of Puteanus and Halbach (1988); age of a layer is for the base of that layer

[3]From equation of Manhein and Lane-Bostwick (1988)

Table 11. X-ray diffraction mineralogy of Fe-Mn crusts from cruise KODOS 97-4

Sample	Type & Interval (mm)[1]	δ–MnO_2 (%)[2]	Others (%)
D2-1A	Bulk (0-70)	91	9-CFA
D2-1B	Layer (0-10)	>99	<1-quartz
D2-1C	Layer (10-25)	98	2-smectite
D2-1D	Layer (25-45)	94	6-CFA
D2-1E	Layer (45-70)	82	16-CFA, 2-smectite
D2-4A	Bulk (0-65)	94	6-CFA
D2-6A	Bulk (0-75)	91	9-CFA
D2-6B	Layer (0-10)	97	2-smectite, 1-quartz
D2-6C	Layer (10-18)	100	–
D2-6D	Layer (18-75)	87	13-CFA
D3-2A	Bulk (0-14)	100	–
D3-3A	Bulk TC (0-30)	>98	1-smectite, <1-quartz
D3-3B	Bulk UC (0-12)	97	2-smectite, 1-phillipsite
D3-4A	Bulk (0-7)	100	–
D4-1A	Bulk (0-70)	>98	1-goethite, <1-quartz
D4-1B	Layer (0-15)	97	2-plagioclase, 1-quartz
D4-1C	Layer (15-36)	100	–
D4-1D	Layer (36-55)	99	1-goethite
D4-2A	Bulk (0-18)	>86	12-CFA, 1-goethite?, <1-quartz
D4-5B	Bulk (0-5)	99	1-quartz
D7-1A	Bulk (0-112)	87	13-CFA
D7-1B	Layer (0-13)	99	1-quartz
D7-1C	Layer (13-28)	>99	<1-quartz
D7-1D	Layer (28-74)	85	15-CFA
D7-1E	Layer (74–112)	82	17-CFA, 1-smectite
D7-2A	Bulk (0-116)	>88	11-CFA, <1-goethite?
D7-2B	Layer (0-9)	98	2-quartz
D7-2C	Layer (9-45)	100	–
D7-2D	Layer (45-56)	99	1-CFA
D7-2E	Layer (56-61)	80	19-CFA, 1-goethite?
D7-2F	Layer (61-122)	>77	22-CFA, <1-smectite
D7-7C	Cement in breccia	84	14-CFA, 1-smectite, 1-quartz
D7-9A	Bulk (0-65)	97	2-CFA, 1-goethite?
D7-9B	Layer (0-7)	98	1-quartz, 1-heulandite?
D7-9C	Layer (7-32)	>99	<1-quartz
D7-9D	Layer (32-64)	>99	<1-goethite?
D7-10A	Bulk (0-31)	99	1-quartz
D8-1A	Bulk (0-71)	>99	<1-smectite
D8-1B	Layer (0-7)	>99	<1-quartz
D8-1C	Layer (7-32)	98	1-lepidocrocite?, 1-heulandite?
D8-1D	Layer (32-36)	100	–
D8-1E	Layer (36-61)	99	1-goethite
D8-1F	Layer (61-71)	93	7-CFA
D9-1A	Bulk (0-105)	94	6-CFA
D9-5-1A	Bulk (0-30)	100	–
D11-1A	Bulk (0-30)	>98	1-goethite, <1-quartz
D11-2A	Bulk (0-30)	>98	1-goethite?, <1-quartz?
D12-1-1	Bulk (0-3)	100	–
D12-2-1A	Bulk (0-2.5)	99	1-plagioclase

Table 11 continued

D13-1A	Bulk (0-85)	99	1-quartz
D13-1B	Layer (0-28)	98	2-quartz
D13-1C	Layer (28-40)	96	3-smectite, 1-quartz
D13-1D	Layer (40-85)	>98	1-goethite, <1-smectite
D13-2A	Bulk (0-50)	98	1-quartz, 1-K-feldspar
D13-5A	Clast in breccia	90	9-CFA, 1-quartz
D13-20	Bulk PSC (0-33)	97	1-smectite, 1-calcite, 1-quartz
D14-1A	Bulk (0-2)	96	3-calcite, 1-quartz
D15-1A	Bulk (0-32)	98	1-smectite, 1-quartz
D15-2A	Bulk (0-48)	99	1-goethite?
D15-2B	Layer (0-11)	99	1-plagioclase
D15-2C	Layer (11-32)	100	–
D15-2D	Layer (32-50)	97	2-goethite, 1-quartz

[1]Intervals measured from the outer surface of crusts; TC is topside crust, UC is underside crust for encrusted talus debris, and PSC is porous side crust

[2]Percentages were determined by using the following weighting factors relative to quartz set at 1: δ-MnO_2 70; todorokite 10; birnessite 12 (Hein et al., 1988); carbonate fluorapatite (CFA) 3.1; plagioclase 2.8; calcite 1.65; smectite 3.0; goethite 7.0; phillipsite 17.0; illite 6.0; pyroxene 5.0; halite 2.0 (Cook et al., 1975); the limit of detection for each mineral falls between 0.2 and 1.0%, except the manganese minerals which are greater, perhaps as much as 10% for δ-MnO_2

Table 12. Chemical composition of Fe-Mn oxyhydroxide crusts from cruise KODOS 97-4

	D2-1A	D2-1A[1]	D2-1B	D2-1C	D2-1D	D2-1E	D2-4A	D2-6A	D2-6A[1]	D2-6B	D2-6C	D2-6D	D3-2A	D3-3A
Fe Wt%	8.7	9.0	9.6	12.9	7.6	6.9	10.8	9.3	9.5	11.6	12.2	7.9	16.4	13.8
Mn	18.4	18.4	18.0	19.4	17.0	20.9	21.1	19.2	19.7	21.5	19.5	19.1	21.9	18.4
Fe/Mn	0.5	0.5	0.5	0.7	0.4	0.3	0.5	0.5	0.5	0.5	0.6	0.4	0.7	0.8
Si	1.1	1.0	1.6	2.1	0.7	0.6	1.5	1.1	1.2	1.8	2.0	0.7	3.4	2.8
Na	1.0	1.0	1.0	1.1	0.9	1.2	1.2	1.2	1.1	1.3	1.3	1.2	1.2	1.2
Al	0.2	0.3	0.3	0.4	0.1	0.2	0.3	0.2	0.3	0.3	0.4	0.1	0.6	0.6
K	0.3	0.3	0.3	0.4	0.3	0.4	0.4	0.3	0.3	0.4	0.4	0.3	0.4	0.4
Mg	0.8	0.8	0.7	0.7	0.6	0.8	0.8	0.8	0.8	0.9	0.9	0.8	0.8	0.8
Ca	7.5	7.6	1.7	2.0	4.6	11.7	5.7	6.2	6.2	1.9	1.8	8.3	2.3	1.8
Ti	0.5	0.5	0.6	0.8	0.5	0.4	0.7	0.6	0.6	0.6	0.8	0.5	1.0	0.9
P	2.4	2.4	0.3	0.3	1.2	3.8	1.6	2.1	2.0	0.3	0.3	2.8	0.4	0.3
S	0.3	0.3	0.2	0.2	0.3	0.3	0.2	0.2	0.3	0.2	0.2	0.3	0.2	0.2
H_2O^-	16.5	16.5	21.5	21.9	20.4	17.1	22.7	21.1	21.1	21.9	22.7	19.9	14.1	19.5
LOI	35.8	35.7	40.9	40.7	38.4	34.4	39.5	37.1	37.0	39.7	39.6	35.6	33.3	36.9
As ppm	120	120	170	150	120	95	130	130	120	170	160	120	160	160
B	115	100	144	148	109	91	116	125	105	153	145	94	194	176
Ba	1370	1370	901	1320	1140	1550	1410	1510	1470	1100	1350	1580	1400	1460
Be	1.7	1.9	1.2	2.4	1.7	1.3	1.8	4.9	4.4	4.3	5.4	4.0	2.5	6.8
Bi	35.2	34.8	29.4	36.2	29.5	46.8	31.3	--	--	--	--	--	25.1	--
Br	22	20	20	21	25	19	22	22	20	21	24	21	21	23
Cd	4.2	4.2	4.7	3.7	4.5	4.6	4.3	--	--	--	--	--	3.8	--
Cl	7140	7250	9030	7450	5100	5060	7550	6750	6790	7180	9440	6530	7610	7630
Co	3690	3580	6210	4550	4530	2210	4420	3560	3300	6960	4940	2710	3670	4150
Cr	<10	<10	25	<10	38	<10	18	17	15	<10	<10	20	23	15
Cu	410	448	212	303	408	326	374	493	455	270	446	501	749	1200
Ga	9	7	7	7	8	7	7	--	--	--	--	--	8	--
Ge	32	<10	<10	<10	<10	<10	<10	<10	<10	<10	<10	<10	<10	<10
Hf	6	6	6	5	3	2	4	5	5	--	7	--	8	10
Li	2	2	<1	<1	<1	2	1	2	2	<1	1	1	<1	1
Mo	424	428	444	374	491	423	420	462	435	505	412	496	367	312
Nb	33	35	34	47	32	25	48	28	32	33	40	29	49	46
Ni	3920	4110	3390	3050	4170	4320	3550	3950	3520	3850	3700	4160	2320	2930
Pb	950	962	1130	1110	826	961	919	1010	950	1260	1110	950	814	768
Sb	28	30	28	33	29	22	28	29	27	29	34	26	25	27
Sc	5.7	6.0	3.1	3.1	3.0	2.9	3.1	2.6	2.4	4.0	3.0	2.5	4.6	5.3
Sr	1250	1280	960	1170	1010	1400	1280	1270	1220	1160	1160	1320	1270	1100
Te	35.9	39.0	41.5	50.0	37.8	42.4	39.0	39.8	40.2	40.8	44.6	44.0	27.4	34.8
Th	5.2	4.8	2.4	2.0	<0.5	2.6	<0.5	2.8	3.3	4.8	3.8	3.7	8.3	6.9
Tl	162	167	165	171	200	156	161	--	--	--	--	--	126	--
U	9.3	9.9	12.3	10.1	7.1	7.3	9.3	8.3	8.2	9.7	9.6	7.4	9.4	8.9
V	471	477	535	520	504	408	466	473	486	545	512	453	559	573
W	78	76	95	68	95	67	76	67	65	92	83	64	41	62
Zn	500	516	395	436	488	552	450	511	490	443	483	531	398	454
Zr	319	320	271	423	281	249	387	333	340	296	401	286	545	584
Au ppb	5	--	--	--	5	<5	--	--	--	--	--	--	<5	<5
Hg	<5	<5	<5	<5	<5	<5	<5	<5	<5	<5	<5	<5	<5	<5
Ir	4	--	--	--	4	4	--	--	--	--	--	--	4	4
Os	<2	--	--	--	2	<2	--	--	--	--	--	--	<2	<2
Pd	6	--	--	--	<2	2	--	--	--	--	--	--	<2	4
Pt	310	--	--	--	195	270	--	--	--	--	--	--	135	260
Rh	17	--	--	--	18	14	--	--	--	--	--	--	10	16
Ru	12	--	--	--	10	8	--	--	--	--	--	--	14	20
Interval	0-70	0-70	0-10	10-25	25-45	45-70	0-65	0-75	0-75	0-10	10-18	18-75	0-14	0-30
Type	Bulk	Bulk	Layer	Layer	Layer	Layer	Bulk	Bulk	Bulk	Layer	Layer	Layer	Bulk	Bulk TC

Table 12 continued

	D3-3B	D3-4A	D4-1A	D4-1B	D4-1C	D4-1D	D4-2A	D4-5B	D4-5B[1]	D7-1A	D7-1A[1]	D7-1B	D7-1C	D7-1D
Fe Wt%	14.2	10.4	16.4	11.9	15.2	16.8	13.9	12.1	12.6	7.8	7.9	12.3	12.4	7.2
Mn	19.8	21.5	17.5	15.7	17.5	17.0	12.5	16.7	17.3	10.2	10.0	18.6	16.6	15.2
Fe/Mn	0.7	0.5	1	0.8	0.9	1.0	1.1	0.7	0.7	0.8	0.8	0.7	0.7	0.5
Si	3.3	1.7	3.8	3.3	4.1	2.6	2.7	2.5	2.6	1.2	0.5	2.6	2.2	0.6
Na	1.4	1.1	1.0	1.0	1.1	0.9	1.0	1.0	1.1	1.0	1.0	1.2	1.1	1.0
Al	0.8	0.3	0.9	0.6	0.9	0.6	0.7	0.3	0.4	0.2	0.2	0.4	0.5	0.1
K	0.5	0.4	0.4	0.4	0.4	0.3	0.3	0.3	0.3	0.3	0.2	0.4	0.3	0.2
Mg	0.9	0.8	0.7	0.6	0.7	0.7	0.7	0.6	0.7	0.6	0.6	0.8	0.8	0.7
Ca	1.9	2.1	2.2	1.7	2.0	2.0	9.2	1.8	1.9	7.2	7.2	1.8	1.6	8.7
Ti	0.9	0.9	0.9	0.7	0.9	0.8	0.5	0.5	0.5	0.5	0.5	0.6	0.7	0.3
P	0.2	0.3	0.5	0.3	0.3	0.4	3.5	0.3	0.4	2.5	2.5	0.4	0.3	3.2
S	0.2	0.2	0.2	0.1	0.1	0.2	0.3	0.2	0.2	0.3	0.3	0.2	0.2	0.3
H_2O^-	17.0	18.3	19.5	20.0	23.2	22.5	17.1	~15.1	~15.1	23.5	23.5	23.1	22.8	20.3
LOI	34.6	38.4	36.4	37.4	40.4	40.7	30	33.3	33.3	37	37	41.1	40.9	36.4
As ppm	150	130	160	170	130	170	160	190	200	130	130	180	160	120
B	178	144	161	160	148	157	134	181	180	105	101	141	134	86
Ba	1420	1030	3440	1000	1960	2080	3090	737	773	1440	1430	975	1190	1200
Be	6.5	1.4	3.6	2.1	2.9	4.6	7.5	1.4	1.6	2.2	2.3	4.5	5.2	3.6
Bi	--	30.8	23.5	24.5	24.5	17.7	--	22.4	24.1	--	--	--	--	--
Br	22	23	17	24	19	24	24	23	26	24	21	21	21	24
Cd	--	4.7	3.1	3.3	2.8	3	--	4.1	--	--	--	--	--	--
Cl	7510	7950	6150	7180	7040	7570	6750	7810	7960	6790	6500	7620	7340	6190
Co	5200	8260	2970	3800	2810	2650	1490	4910	5060	2930	2770	5830	4190	2180
Cr	11	29	<10	15	14	<10	22	13	12	12	10	10	14	10
Cu	1440	446	992	641	819	1170	795	347	358	403	388	229	414	419
Ga	--	8	10	8	7	7	--	8	6	--	--	--	--	--
Ge	<10	<10	<10	<10	<10	<10	<10	<10	<10	<10	<10	<10	<10	<10
Hf	10	4	10	7	10	12	10	3	3	5	5	3	8	--
Li	2	<1	1	<1	3	<1	4	1	2	<1	<1	<1	2	1
Mo	339	329	276	317	233	306	241	378	396	368	363	415	347	419
Nb	45	49	60	39	52	64	33	20	25	28	30	36	41	27
Ni	3270	3770	2330	2670	2200	2190	1640	2920	2990	3030	2890	2920	2910	3670
Pb	827	938	803	981	781	702	842	1020	1070	891	867	1210	1090	775
Sb	24	25	39	35	33	44	39	26	26	29	29	27	33	28
Sc	4.3	3.9	4.7	3.8	4.0	4.3	6.7	5.1	5.5	3.1	3.1	3.7	2.9	2.6
Sr	1100	962	1280	943	1140	1190	1330	946	1050	1270	1240	1120	1080	1160
Te	36.8	46.8	44.5	35.8	43.1	40.9	33.5	28.0	28.8	46.0	49.3	41.6	52.2	39.7
Th	4.7	16.0	7.9	8.9	7.0	2.1	6.4	17.0	17.0	6.4	5.9	11.0	8.0	1.1
Tl	--	157	108	104	96.4	117	--	100	106	--	--	--	--	--
U	8.7	9.7	9.3	10.3	8.5	9.3	8.2	11.7	11.3	9.1	8.9	9.4	9.3	8.1
V	662	413	535	487	437	581	447	547	541	465	455	502	490	433
W	70	71	66	68	53	73	43	68	70	51	52	79	77	67
Zn	478	427	473	398	405	532	402	364	373	441	427	368	417	498
Zr	588	301	695	415	629	769	527	298	315	241	274	321	389	235
Au ppb	--	<5	--	--	--	--	--	--	--	39	--	5	<5	<5
Hg	<5	<5	<5	<5	<5	<5	<5	<5	<5	<5	<5	<5	<5	<5
Ir	--	4	--	--	--	--	--	--	--	4	--	4	6	6
Os	--	<2	--	--	--	--	--	--	--	<3	--	2	<2	<2
Pd	--	<2	--	--	--	--	--	--	--	2	--	2	<2	4
Pt	--	150	--	--	--	--	--	--	--	245	--	183	245	205
Rh	--	10	--	--	--	--	--	--	--	17	--	11	18	16
Ru	--	18	--	--	--	--	--	--	--	8	--	16	16	8
Interval	0-12	0-7	0-70	0-15	15-36	36-55	0-18	0-5	0-5	0-112	0-112	0-13	13-28	28-74
Type	Bulk UC	Bulk	Bulk	Layer	Layer	Layer	Bulk	Bulk	Bulk	Bulk	Bulk	Layer	Layer	Layer

Table 12 continued

	D7-1E	D7-2A	D7-2B	D7-2C	D7-2D	D7-2E	D7-2F	D7-7C	D7-9A	D7-9B	D7-9B[1]	D7-9C	D7-9D	D7-10A
Fe Wt%	8.5	10.9	13.1	13.6	12.9	12.5	6.5	8.3	12.7	11.3	10.8	13.3	11.7	11.3
Mn	15.7	18.1	19.0	21.4	19.6	11.3	13.3	15.2	17.2	18.9	18.1	17.1	16.3	15.1
Fe/Mn	0.5	0.5	0.7	0.6	0.7	1.1	0.5	0.5	0.7	0.6	0.6	0.8	0.7	0.7
Si	0.7	1.5	3.4	2.4	1.3	1.0	0.6	1.3	1.8	1.8	1.8	2.4	0.9	2.4
Na	1.0	1.1	1.1	1.2	1.4	1.2	1.1	1.2	1.1	1.2	1.2	1.1	1.0	1.2
Al	0.1	0.3	0.5	0.5	0.3	0.3	0.1	0.5	0.5	0.4	0.3	0.7	0.3	0.6
K	0.2	0.3	0.4	0.4	0.4	0.2	0.3	0.4	0.3	0.4	0.3	0.4	0.2	0.4
Mg	0.6	0.7	0.7	0.8	0.9	0.7	0.6	0.8	0.8	0.8	0.8	0.8	0.7	0.8
Ca	10.6	10.1	2.0	2.2	2.2	13.2	11.0	9.8	2.6	1.7	1.7	1.7	1.6	1.5
Ti	0.4	0.5	0.6	0.8	0.9	0.3	0.3	0.5	0.7	0.7	0.7	0.8	0.5	0.7
P	3.9	3.2	0.4	0.4	0.5	5.1	4.0	3.7	0.6	0.3	0.3	0.3	0.3	0.3
S	0.3	0.3	0.2	0.2	0.2	0.3	0.3	0.3	0.2	0.2	0.2	0.2	0.2	0.2
H_2O^-	18.5	19.1	11.7	~13.8	15.7	6.2	18.8	10.1	22.6	22.9	23.9	23.3	24.1	24.7
LOI	33.6	34.7	31.9	32.1	35.6	21.1	32.8	26.0	42.2	41.3	41.4	41.5	42.9	42.1
As ppm	120	130	190	180	190	190	100	130	160	150	150	170	190	150
B	88	110	183	154	138	119	77	99	124	125	126	130	119	126
Ba	1590	1320	900	1260	1640	1160	1130	1760	1260	1060	1010	1260	1320	999
Be	4.8	2.1	1.6	2.3	3.2	3.1	1.4	2.8	5.5	4.2	3.5	5.6	6.6	1.9
Bi	--	27.7	25.7	32.0	22.9	6.8	29.9	57.9	--	--	--	--	--	27.0
Br	20	21	22	25	25	22	19	17	30	20	21	29	35	21
Cd	--	3.3	4.2	3.9	3.9	2.4	3.4	3.5	--	--	--	--	--	3.7
Cl	5920	7560	8450	9640	8610	7460	6650	6260	8240	9400	9280	8310	9440	7760
Co	2390	2720	5910	4660	4050	1280	1810	3270	4330	6700	6500	3360	3270	4360
Cr	<10	17	20	17	<10	11	<10	16	21	19	22	25	11	20
Cu	233	444	262	503	627	565	405	562	697	377	350	563	844	383
Ga	--	7	9	8	9	6	5	12	--	--	--	--	--	6
Ge	<10	<10	<10	<10	<10	<10	<10	<10	<10	<10	<10	<10	<10	<10
Hf	5	6	5	9	9	7	5	5	8	6	6	11	10	6
Li	<1	<1	<1	1	<1	<1	2	5	<1	<1	2	2	1	2
Mo	369	350	374	372	489	416	354	445	361	375	365	276	511	280
Nb	28	37	41	50	65	42	24	40	44	26	20	58	44	43
Ni	2260	2720	2790	3290	3220	2100	3090	3130	3130	3440	3270	2690	3400	2790
Pb	980	805	1170	1070	872	424	708	1180	922	1150	1090	917	794	919
Sb	26	31	30	37	48	47	26	33	40	29	28	42	51	29
Sc	2.5	3.9	4.2	4.5	2.6	7.4	3.5	7.9	4.8	3.3	2.9	5.2	4.5	3.8
Sr	1390	1300	1110	1230	1390	1390	1210	1450	1090	1060	1010	1100	1020	993
Te	63.8	37.6	45.0	58.2	54.2	43.4	38.0	69.8	61.3	61.1	56.0	65.4	52.8	53.3
Th	7.2	2.6	14.0	8.4	3.2	<0.5	2.2	7.4	7.2	9.0	8.7	6.5	1.1	8.9
Tl	--	115	119	152	177	98	100	100	--	--	--	--	--	123
U	8.9	7.9	9.8	12.6	11.8	12.4	7.3	8.1	9.3	9.0	9.1	10.2	8.7	9.7
V	500	479	600	533	594	545	374	523	466	454	464	430	563	457
W	18	63	72	75	110	82	46	37	88	78	79	78	140	60
Zn	447	397	358	434	495	412	414	519	453	399	378	404	515	356
Zr	257	409	400	488	493	413	243	319	434	333	310	477	431	375
Au ppb	<5	--	--	--	--	--	--	--	--	--	--	--	--	--
Hg	<5	<5	<5	<5	<5	<5	<5	<5	<5	<5	<5	<5	<5	<5
Ir	2	--	--	--	--	--	--	--	--	--	--	--	--	--
Os	<2	--	--	--	--	--	--	--	--	--	--	--	--	--
Pd	2	--	--	--	--	--	--	--	--	--	--	--	--	--
Pt	240	--	--	--	--	--	--	--	--	--	--	--	--	--
Rh	15	--	--	--	--	--	--	--	--	--	--	--	--	--
Ru	4	--	--	--	--	--	--	--	--	--	--	--	--	--
Interval	74-112	0-116	0-9	9-45	45-56	56-61	61-122	Cement	0-65	0-7	0-7	7-32	32-64	0-31
Type	Layer	Bulk	Layer	Layer	Layer	Layer	Layer	in Breccia	Bulk	Layer	Layer	Layer	Layer	Bulk

Table 12 continued

	D8-1A	D8-1B	D8-1C	D8-1D	D8-1D[1]	D8-1E	D8-1F	D9-1A	D9-5A	D11-1A	D11-2A	D12-1-1	D122-1A	D13-1A
Fe Wt%	8.4	10.1	11.2	10.1	10.4	12.4	8.1	11.3	11.3	15.7	15.5	9.4	13.1	11.0
Mn	12.6	16.3	17.0	15.5	15.9	12.2	17.0	16.7	18.1	17.6	18.8	16.7	19.9	13.9
Fe/Mn	0.7	0.6	0.7	0.7	0.7	1.0	0.5	0.7	0.6	0.9	0.8	0.6	0.7	0.8
Si	1.1	1.6	1.8	1.1	1.1	1.2	0.8	1.5	2.0	2.6	2.4	1.6	3.8	2.1
Na	0.9	1.1	1.2	1.1	0.9	1.0	1.2	1.2	1.3	1.2	1.3	1.1	1.4	0.9
Al	0.2	0.2	0.4	0.2	0.2	0.3	0.2	0.3	0.4	0.8	0.6	0.3	1.0	0.5
K	0.3	0.4	0.4	0.3	0.3	0.2	0.4	0.4	0.4	0.4	0.4	0.4	0.6	0.3
Mg	0.6	0.7	0.7	0.7	0.6	0.6	0.7	0.8	0.8	0.9	0.9	0.7	0.9	0.6
Ca	1.3	1.5	1.6	1.5	1.6	1.3	4.5	5.4	1.8	2.0	2.0	1.7	2.5	1.5
Ti	0.5	0.6	0.8	0.7	0.7	0.5	0.5	0.6	0.7	0.9	0.9	0.7	0.9	0.7
P	0.3	0.3	0.3	0.2	0.2	0.3	1.4	1.8	0.3	0.4	0.3	0.3	0.6	0.3
S	0.2	0.2	0.2	0.2	0.2	0.2	0.3	0.3	0.2	0.2	0.2	0.2	0.2	0.2
H_2O^-	24.9	23.7	23.0	~19.5	--	24.7	21.8	19.2	25.8	16.7	19.5	13.1	~21.2	22.3
LOI	43.2	41.1	41.9	37.4	--	44.7	39.6	36.0	43.8	34.5	36.9	35.7	38.9	40.6
As ppm	140	160	150	160	160	180	120	140	140	180	180	160	150	148
B	136	148	139	143	139	140	97	128	126	150	148	146	172	141
Ba	928	874	1190	1300	1230	1200	1340	1340	1070	1720	1860	669	829	1057
Be	2.5	1.4	2.6	3.5	3.4	4.5	2.2	2.7	1.7	4.4	4.3	1.1	4.5	3.2
Bi	29.9	27.1	30.0	25.7	27.0	14.6	43.3	30.5	26.8	24.0	22.9	27.1	--	26.3
Br	23	20	26	29	27	27	23	20	24	25	24	21	23	22
Cd	3.8	4.1	3.4	3.7	4.3	2.9	4.8	3.7	4.1	3.6	3.5	4.7	--	3.9
Cl	8330	7200	7920	8730	8790	9350	8070	7500	7540	8620	7960	7340	7110	7710
Co	3920	5280	4210	4410	4500	2670	3260	3470	5620	3100	3420	7200	6220	3544
Cr	16	13	<10	13	14	14	<10	<10	<10	28	13	<10	61	12
Cu	816	387	647	922	944	1000	1070	683	472	1210	1170	351	388	1385
Ga	6	5	4	5	7	6	6	6	5	8	7	5	--	7
Ge	<10	<10	<10	<10	<10	<10	<10	<10	22	<10	<10	<10	<10	<10
Hf	6	6	6	11	10	10	6	6	5	14	11	4	4	11
Li	1	<1	<1	3	1	2	1	3	<1	4	1	2	4	2
Mo	412	413	400	452	459	456	481	407	374	376	412	349	303	351
Nb	30	32	41	44	43	37	31	39	46	53	61	25	32	37
Ni	3200	3220	3230	3160	3230	2610	4320	3230	3300	2980	2860	3220	2770	2779
Pb	806	1030	940	830	842	602	800	907	1070	884	820	933	890	725
Sb	33	27	31	39	38	42	29	33	27	44	43	24	23	35
Sc	4.6	3.9	4.5	4.0	3.8	6.2	3.8	4.3	3.6	4.1	3.5	4.6	8.9	6
Sr	804	982	1090	1010	978	893	1100	1290	1150	1260	1350	923	1060	904
Te	42.5	34.0	38.8	44.7	41.6	39.7	27.1	36.8	44.2	44.6	39.8	32.6	28.3	37.8
Th	<0.5	6.7	7.9	<0.5	<0.5	<0.5	2.4	5.6	12.0	2.8	2.9	33.0	29.0	4.2
Tl	167	145	155	192	195	137	189	155	150	114	122	146	--	131
U	8.3	10.8	9.1	10.7	11.2	6.7	7.7	8.9	10.6	10.0	9.9	9.3	8.5	8.1
V	515	515	467	571	575	618	449	508	425	586	608	441	459	490
W	83	81	72	84	82	81	81	74	75	95	89	71	40	82
Zn	441	384	443	523	531	527	505	458	392	536	517	369	361	433
Zr	321	290	384	452	460	467	365	415	382	754	698	209	274	506
Au ppb	<5	--	--	--	--	--	--	--	--	--	--	--	--	5
Hg	< 5	< 5	< 5	< 5	< 5	< 5	< 5	< 5	< 5	< 5	< 5	7	6	10
Ir	4	--	--	--	--	--	--	--	--	--	--	--	--	4
Os	2	--	--	--	--	--	--	--	--	--	--	--	--	<2
Pd	6	--	--	--	--	--	--	--	--	--	--	--	--	2
Pt	270	--	--	--	--	--	--	--	--	--	--	--	--	445
Rh	18	--	--	--	--	--	--	--	--	--	--	--	--	22
Ru	14	--	--	--	--	--	--	--	--	--	--	--	--	16
Interval	0-71	0-7	7-32	32-36	32-36	36-61	61-71	0-105	0-30	0-30	0-30	0-3	0-2.5	0-85
Type	Bulk	Layer	Layer	Layer	Layer	Layer	Layer	Bulk	Bulk	Bulk	Bulk	Bulk	Bulk	Bulk

Table 12 continued

	D13-1B	D13-1C	D13-1D	D13-2A	D13-5A	D13-5A[1]	D13-20-1A	D14-1A	D15-1A	D15-1A[1]	D15-2A	D15-2B	D15-2C	D15-2D
Fe Wt%	11.5	10.1	10.9	14.8	11.8	11.6	9.5	13.3	15.9	15.7	11.8	12.9	13.7	11.3
Mn	16.0	13.6	12.6	16.1	16.7	15.6	16.1	17.6	19.6	19.4	13.6	17.4	17.5	12.6
Fe/Mn	0.7	0.7	0.9	0.9	0.7	0.7	0.6	0.8	0.8	0.8	0.9	0.7	0.8	0.9
Si	2.8	2.3	1.6	3.3	1.4	1.3	1.9	3.0	2.7	2.7	2.1	2.3	3.2	1.3
Na	1.0	0.9	0.8	1.1	0.9	0.9	0.9	1.1	1.5	1.6	0.9	1.1	1.2	0.7
Al	0.4	0.5	0.5	0.7	0.3	0.3	0.4	0.6	0.5	0.6	0.5	0.5	0.8	0.3
K	0.4	0.3	0.3	0.4	0.3	0.3	0.3	0.4	0.4	0.4	0.3	0.3	0.4	0.2
Mg	0.7	0.6	0.6	0.7	0.7	0.6	0.7	0.8	0.9	0.9	0.6	0.7	0.8	0.6
Ca	1.6	1.4	1.4	1.7	7.0	7.1	1.9	5.2	2.0	2.0	1.4	1.7	1.8	1.3
Ti	0.7	0.7	0.6	0.8	0.8	0.7	0.7	0.7	1.1	1.1	0.7	0.9	1.0	0.6
P	0.3	0.2	0.3	0.4	2.2	2.1	0.2	0.3	0.4	0.4	0.3	0.3	0.3	0.2
S	0.2	0.2	0.2	0.2	0.2	0.3	0.2	0.2	0.2	0.2	0.2	0.2	0.2	0.2
H_2O^-	21.0	20.4	23.9	21.7	~11.7	--	22.5	~15.8	12.7	13.6	20.3	22.3	17.6	21.7
LOI	38.5	38.4	42.3	38.7	30.2	--	39.8	33.9	31.9	31.9	38	40.7	36	42.2
As ppm	150	130	150	160	150	140	130	160	210	200	160	150	140	170
B	161	136	129	157	129	122	122	169	187	186	157	143	141	143
Ba	978	1020	1110	1410	2040	1820	886	812	1710	1670	1100	1110	1280	1160
Be	2.1	3.0	3.9	7.4	4.9	4.5	1.6	1.3	7.3	6.8	7.4	5.2	6.3	8.1
Bi	28.7	28.2	24.3	--	59.8	59.4	33.5	21.3	27.4	27.2	--	--	--	--
Br	19	22	23	24	19	19	14	22	29	26	26	22	26	25
Cd	4.7	3.4	4.1	--	2.9	3.1	5.3	5.6	5.0	--	--	--	--	--
Cl	6940	7900	8090	7720	6080	5970	5500	10700	10100	9460	8080	7500	8210	8070
Co	4170	3990	3040	3140	3070	2930	6330	5680	4560	4570	3660	5020	3930	3500
Cr	16	<10	10	10	15	12	<10	21	14	11	24	21	<10	21
Cu	587	1260	1890	1120	1090	1010	1060	326	540	558	594	431	648	718
Ga	7	7	7	--	11	9	7	7	8	--	--	--	--	--
Ge	<10	<10	<10	<10	<10	<10	<10	<10	<10	<10	<10	<10	<10	<10
Hf	7	10	13	11	9	9	7	5	8	7	10	5	9	11
Li	<1	1	2	2	1	2	<1	1	<1	<1	<1	1	3	1
Mo	338	316	367	333	408	400	338	281	395	388	301	315	271	339
Nb	40	41	35	50	49	40	44	39	58	51	37	43	52	45
Ni	2660	2930	2800	2350	2390	2280	3680	2880	2870	2910	2360	2740	2710	2280
Pb	924	742	598	787	1570	1540	889	978	1170	1160	893	1050	876	757
Sb	30	32	39	37	53	52	39	22	41	40	37	29	30	40
Sc	4.6	5.0	7.4	5.4	7.3	6.9	3.4	6.0	5.6	5.6	4.6	3.7	4.6	5.2
Sr	1020	868	841	1050	1400	1110	844	1040	1420	1420	895	1050	1090	832
Te	32.4	41.5	39.9	35.2	49.6	52.1	56.7	56.5	44.8	45.4	45.4	40.1	53.9	51.1
Th	6.4	6.9	2.1	5.2	14.0	15.0	10.0	14.0	8.5	9.5	4.8	6.8	9.5	2.3
Tl	136	139	125	--	99.9	103	170	139	158	--	--	--	--	--
U	9.2	10.7	6.7	10.5	9.3	9.5	7.7	8.7	13.4	12.9	10.7	10.4	9.6	7.9
V	526	431	482	512	546	534	425	474	575	575	499	447	445	557
W	70	68	91	82	110	110	66	53	81	78	57	49	45	65
Zn	368	408	476	447	446	438	388	383	483	480	433	396	409	489
Zr	397	542	560	567	549	610	300	403	510	524	423	400	482	458
Au ppb	<5	<5	8	--	--	--	--	--	474	--	--	--	--	--
Hg	18	15	<5	<5	<5	<5	<5	9	<5	<5	<5	<5	<5	<5
Ir	4	4	6	--	--	--	--	--	4	--	--	--	--	--
Os	2	<2	<2	--	--	--	--	--	3	--	--	--	--	--
Pd	4	4	6	--	--	--	--	--	4	--	--	--	--	--
Pt	130	390	465	--	--	--	--	--	285	--	--	--	--	--
Rh	11	21	24	--	--	--	--	--	18	--	--	--	--	--
Ru	16	16	18	--	--	--	--	--	18	--	--	--	--	--
Interval	0-28	28-40	40-85	0-50	Breccia	Breccia	0-33	0-2	0-32	0-32	0-48	0-11	11-32	32-50
Type	Layer	Layer	Layer	Bulk	Clast	Clast	Bulk PSC	Bulk	Bulk	Bulk	Bulk	Layer	Layer	Layer

All Ag contents <0.2ppm; In <0.5ppm; Se <5ppm; Cs <3ppm; Ta <1ppm

[1]Duplicate analysis of sample

Table 13. Hydroscopic water-free (0% H_2O^-) composition of Fe-Mn crusts from Table 12

	D2-1A	D2-1A[1]	D2-1B	D2-1C	D2-1D	D2-1E	D2-4A	D2-6A	D2-6A[1]	D2-6B	D2-6C	D2-6D	D3-2A	D3-3A
Fe Wt%	10.4	10.8	12.2	16.5	9.5	8.3	14.0	11.8	12.0	14.9	15.8	9.8	19.1	17.1
Mn	22.0	22.0	22.9	24.8	21.4	25.2	27.3	24.3	25.0	27.5	25.2	23.6	25.5	22.9
Fe/Mn	0.6	0.6	0.6	0.9	0.5	0.4	0.6	0.6	0.6	0.6	0.8	0.5	0.8	1.0
Si	1.3	1.2	2.0	2.7	0.9	0.7	1.9	1.4	1.5	2.3	2.6	0.9	4.0	3.5
Na	1.2	1.2	1.3	1.4	1.1	1.4	1.6	1.5	1.4	1.7	1.7	1.5	1.4	1.5
Al	0.2	0.4	0.4	0.5	0.1	0.2	0.4	0.3	0.4	0.4	0.5	0.1	0.7	0.7
K	0.4	0.4	0.4	0.5	0.4	0.5	0.5	0.4	0.4	0.5	0.5	0.4	0.5	0.5
Mg	1.0	1.0	0.9	0.9	0.8	1.0	1.0	1.0	1.0	1.2	1.2	1.0	0.9	1.0
Ca	9.0	9.1	2.2	2.6	5.8	14.1	7.4	7.9	7.9	2.4	2.3	10.3	2.7	2.2
Ti	0.6	0.6	0.8	1.0	0.6	0.5	0.9	0.8	0.8	0.8	1.0	0.6	1.2	1.1
P	2.9	2.9	0.4	0.4	1.5	4.6	2.1	2.7	2.5	0.4	0.4	3.5	0.5	0.4
S	0.4	0.4	0.3	0.3	0.4	0.4	0.3	0.3	0.4	0.3	0.3	0.4	0.2	0.2
LOI	42.9	42.8	52.1	52.1	48.2	41.5	51.1	47.0	46.9	50.8	51.2	44.0	38.8	45.8
As ppm	144	144	217	192	151	115	168	165	152	218	207	148	186	199
B	138	120	183	190	137	110	150	158	133	196	188	116	226	219
Ba	1641	1641	1148	1690	1432	1870	1824	1914	1863	1408	1746	1953	1630	1814
Be	2.0	2.3	1.5	3.1	2.1	1.6	2.3	6.2	5.6	5.5	7.0	4.9	2.9	8.4
Bi	42.2	41.7	37.5	46.4	37.1	56.5	40.5	--	--	--	--	--	29.2	--
Br	26	24	25	27	31	23	28	28	25	27	31	26	24	29
Cd	5	5	6	5	6	6	6	--	--	--	--	--	4	--
Cl	8551	8683	11503	9539	6407	6104	9767	8555	8606	9193	12212	8072	8859	9478
Co	4419	4287	7911	5826	5691	2666	5718	4512	4183	8912	6391	3350	4272	5155
Cr	<12	<12	32	<13	48	<12	23	22	19	<13	<13	25	27	19
Cu	491	537	270	388	513	393	484	625	577	346	577	619	872	1491
Ga	11	8	9	9	10	8	9	--	--	--	--	--	9	--
Ge	38	<12	<13	<13	<13	<12	<13	<13	<13	<13	<13	<12	<12	<12
Hf	7	7	8	6	4	2	5	6	6	--	9	--	9	12
Li	2	2	<1	<1	<1	2	1	3	3	<1	1	1	<1	1
Mo	508	513	566	479	617	510	543	586	551	647	533	613	427	388
Nb	40	42	43	60	40	30	62	35	41	42	52	36	57	57
Ni	4695	4922	4318	3905	5239	5211	4592	5006	4461	4930	4787	5142	2701	3640
Pb	1138	1152	1439	1421	1038	1159	1189	1280	1204	1613	1436	1174	948	954
Sb	34	36	36	42	36	27	36	37	34	37	44	32	29	34
Sc	6.8	7.2	3.9	4.0	3.8	3.5	4.0	3.3	3.0	5.1	3.9	3.1	5.4	6.6
Sr	1497	1533	1223	1498	1269	1689	1656	1610	1546	1485	1501	1632	1478	1366
Te	43.0	46.7	52.9	64.0	47.5	51.1	50.5	50.4	51.0	52.2	57.7	54.4	31.9	43.2
Th	6.2	5.7	3.1	2.6	0.6	3.1	0.6	3.5	4.2	6.1	4.9	4.6	9.7	8.6
Tl	194	200	210	219	251	188	208	--	--	--	--	--	147	--
U	11.1	11.9	15.7	12.9	8.9	8.8	12.0	10.5	10.4	12.4	12.4	9.1	10.9	11.1
V	564	571	682	666	633	492	603	599	616	698	662	560	651	712
W	93	91	121	87	119	81	98	85	82	118	107	79	48	77
Zn	599	618	503	558	613	666	582	648	621	567	625	656	463	564
Zr	382	383	345	542	353	300	501	422	431	379	519	354	634	725
Hg ppb	<6	<6	<6	<6	<6	<6	<6	<6	<6	<6	<6	<6	<6	<6
Interval	0-70	0-70	0-10	10-25	25-45	45-70	0-65	0-75	0-75	0-10	10-18	18-75	0-14	0-30
Type	Bulk	Bulk	Layer	Layer	Layer	Layer	Bulk	Bulk	Bulk	Layer	Layer	Layer	Bulk	Bulk TC

Table 13 continued

	D3-3B	D3-4A	D4-1A	D4-1B	D4-1C	D4-1D	D4-2A	D4-5B	D4-5B[1]	D7-1A	D7-1A[1]	D7-1B	D7-1C	D7-1D
Fe Wt%	17.1	12.7	20.4	14.9	19.8	21.7	16.8	14.3	14.8	10.2	10.3	16.0	16.1	9.0
Mn	23.9	26.3	21.7	19.6	22.8	21.9	15.1	19.7	20.4	13.3	13.1	24.2	21.5	19.1
Fe/Mn	0.8	0.6	1.2	1.0	1.2	1.3	1.3	0.8	0.8	1.0	1.0	0.9	0.9	0.6
Si	4.0	2.1	4.7	4.1	5.3	3.4	3.3	2.9	3.1	1.6	0.7	3.4	2.8	0.8
Na	1.7	1.3	1.2	1.3	1.4	1.2	1.2	1.2	1.3	1.3	1.3	1.6	1.4	1.3
Al	1.0	0.4	1.1	0.8	1.2	0.8	0.8	0.4	0.5	0.3	0.3	0.5	0.6	0.1
K	0.6	0.5	0.5	0.5	0.5	0.4	0.4	0.4	0.4	0.4	0.3	0.5	0.4	0.3
Mg	1.1	1.0	0.9	0.8	0.9	0.9	0.8	0.7	0.8	0.8	0.8	1.0	1.0	0.9
Ca	2.3	2.6	2.7	2.1	2.6	2.6	11.1	2.1	2.2	9.4	9.4	2.3	2.1	10.9
Ti	1.1	1.1	1.1	0.9	1.2	1.0	0.6	0.6	0.6	0.7	0.7	0.8	0.9	0.4
P	0.2	0.4	0.6	0.4	0.4	0.5	4.2	0.4	0.5	3.3	3.3	0.5	0.4	4.0
S	0.2	0.2	0.2	0.1	0.1	0.3	0.4	0.2	0.2	0.4	0.4	0.3	0.3	0.4
LOI	41.7	47.0	45.2	46.8	52.6	52.5	36.2	39.2	39.2	48.4	48.4	53.4	53.0	45.7
As ppm	181	159	199	213	169	219	193	224	236	170	170	234	207	151
B	214	176	200	200	193	203	162	213	212	137	132	183	174	108
Ba	1711	1261	4273	1250	2552	2684	3727	868	910	1882	1869	1268	1541	1506
Be	7.8	1.7	4.5	2.6	3.8	5.9	9.0	1.6	1.9	2.9	3.0	5.9	6.7	4.5
Bi	--	37.7	29.2	30.6	31.9	22.8	--	26.4	28.4	--	--	--	--	--
Br	27	28	21	30	25	31	29	27	31	31	27	27	27	30
Cd	--	6	4	4	4	4	--	5	--	--	--	--	--	--
Cl	9048	9731	7640	8975	9167	9768	8142	9199	9376	8876	8497	9909	9508	7767
Co	6265	10110	3689	4750	3659	3419	1797	5783	5960	3830	3621	7581	5427	2735
Cr	13	35	<12	19	18	<13	27	15	14	16	13	13	18	13
Cu	1735	546	1232	801	1066	1510	959	409	422	527	507	298	536	526
Ga	--	10	12	10	9	9	--	9	7	--	--	--	--	--
Ge	<12	<12	<12	<13	<13	<13	<12	<12	<12	<13	<13	<13	<13	<13
Hf	12	5	12	9	13	15	12	4	4	7	7	4	10	--
Li	2	<1	1	<1	4	<1	5	1	2	<1	<1	<1	3	1
Mo	408	403	343	396	303	395	291	445	466	481	475	540	449	526
Nb	54	60	75	49	68	83	40	24	29	37	39	47	53	34
Ni	3940	4614	2894	3338	2865	2826	1978	3439	3522	3961	3778	3797	3769	4605
Pb	996	1148	998	1226	1017	906	1016	1201	1260	1165	1133	1573	1412	972
Sb	29	31	48	44	43	57	47	31	31	38	38	35	43	35
Sc	5.2	4.8	5.8	4.8	5.2	5.5	8.1	6.0	6.5	4.1	4.1	4.8	3.8	3.3
Sr	1325	1177	1590	1179	1484	1535	1604	1114	1237	1660	1621	1456	1399	1455
Te	44.3	57.3	55.3	44.8	56.1	52.8	40.4	33.0	33.9	60.1	64.4	54.1	67.6	49.8
Th	5.7	19.6	9.8	11.1	9.1	2.7	7.7	20.0	20.0	8.4	7.7	14.3	10.4	1.4
Tl	--	192	134	130	126	151	--	118	125	--	--	--	--	--
U	10.5	11.9	11.6	12.9	11.1	12.0	9.9	13.8	13.3	11.9	11.6	12.2	12.0	10.2
V	798	506	665	609	569	750	539	644	637	608	595	653	635	543
W	84	87	82	85	69	94	52	80	82	67	68	103	100	84
Zn	576	523	588	498	527	686	485	429	439	576	558	479	540	625
Zr	708	368	863	519	819	992	636	351	371	315	358	417	504	295
Hg ppb	<6	<6	<6	<6	<7	<6	<6	<6	<6	<7	<7	<7	<6	<6
Interval	0-12	0-7	0-70	0-15	15-36	36-55	0-18	0-5	0-5	0-112	0-112	0-13	13-28	28-74
Type	Bulk UC	Bulk	Bulk	Layer	Layer	Layer	Bulk	Bulk	Bulk	Bulk	Bulk	Layer	Layer	Layer

Table 13 continued

	D7-1E	D7-2A	D7-2B	D7-2C	D7-2D	D7-2E	D7-2F	D7-7C	D7-9A	D7-9B	D7-9B[1]	D7-9C	D7-9D	D7-10A
Fe Wt%	10.4	13.5	14.8	15.8	15.3	13.3	8.0	9.2	16.4	14.7	14.2	17.3	15.4	15.0
Mn	19.3	22.4	21.5	24.8	23.3	12.0	16.4	16.9	22.2	24.5	23.8	22.3	21.5	20.1
Fe/Mn	0.6	0.6	0.8	0.7	0.8	1.2	0.6	0.6	0.9	0.8	0.8	1.0	0.9	0.9
Si	0.9	1.9	3.9	2.8	1.5	1.1	0.7	1.4	2.3	2.3	2.4	3.1	1.2	3.2
Na	1.2	1.4	1.2	1.4	1.7	1.3	1.4	1.3	1.4	1.6	1.6	1.4	1.3	1.6
Al	0.1	0.4	0.6	0.6	0.4	0.3	0.1	0.6	0.6	0.5	0.4	0.9	0.4	0.8
K	0.2	0.4	0.5	0.5	0.5	0.2	0.4	0.4	0.4	0.5	0.4	0.5	0.3	0.5
Mg	0.7	0.9	0.8	0.9	1.1	0.7	0.7	0.9	1.0	1.0	1.1	1.0	0.9	1.1
Ca	13.0	12.5	2.3	2.6	2.6	14.1	13.5	10.9	3.4	2.2	2.2	2.2	2.1	2.0
Ti	0.5	0.6	0.7	0.9	1.1	0.3	0.4	0.6	0.9	0.9	0.9	1.0	0.7	0.9
P	4.8	4.0	0.5	0.5	0.6	5.4	4.9	4.1	0.8	0.4	0.4	0.4	0.4	0.4
S	0.4	0.4	0.2	0.2	0.2	0.3	0.4	0.3	0.3	0.3	0.3	0.3	0.3	0.3
LOI	41.2	42.9	36.1	37.2	42.2	22.5	40.4	28.9	54.5	53.6	54.4	54.1	56.5	55.9
As ppm	147	161	215	209	225	203	123	145	207	195	197	222	250	199
B	108	136	207	179	164	127	95	110	160	162	166	169	157	167
Ba	1951	1632	1019	1462	1945	1237	1392	1958	1628	1375	1327	1643	1739	1327
Be	5.9	2.6	1.8	2.7	3.8	3.3	1.7	3.1	7.1	5.4	4.6	7.3	8.7	2.5
Bi	--	34.2	29.1	37.1	27.2	7.2	36.8	64.4	--	--	--	--	--	35.9
Br	25	26	25	29	30	23	23	19	39	26	28	38	46	28
Cd	--	4	5	5	5	3	4	4	--	--	--	--	--	5
Cl	7264	9345	9570	11183	10214	7953	8190	6963	10646	12192	12194	10834	12437	10305
Co	2933	3362	6693	5406	4804	1365	2229	3637	5594	8690	8541	4381	4308	5790
Cr	<12	21	23	20	<12	12	<12	18	27	25	29	33	14	27
Cu	286	549	297	584	744	602	499	625	901	489	460	734	1112	509
Ga	--	9	10	9	11	6	6	13	--	--	--	--	--	8
Ge	<12	<12	<11	<12	<12	<11	<12	<11	<13	<13	<13	<13	<13	<13
Hf	6	7	6	10	11	7	6	6	10	8	8	14	13	8
Li	<1	<1	<1	1	<1	<1	2	6	<1	<1	3	3	1	3
Mo	453	433	424	432	580	443	436	495	466	486	480	360	673	372
Nb	34	46	46	58	77	45	30	44	57	34	26	76	58	57
Ni	2773	3362	3160	3817	3820	2239	3805	3482	4044	4462	4297	3507	4480	3705
Pb	1202	995	1325	1241	1034	452	872	1313	1191	1492	1432	1196	1046	1220
Sb	32	38	34	43	57	50	32	37	52	38	37	55	67	39
Sc	3.1	4.8	4.8	5.2	3.1	7.9	4.3	8.8	6.2	4.3	3.8	6.8	5.9	5.0
Sr	1706	1607	1257	1427	1649	1482	1490	1613	1408	1375	1327	1434	1344	1319
Te	78.3	46.5	51.0	67.5	64.3	46.3	46.8	77.6	79.2	79.2	73.6	85.3	69.6	70.8
Th	8.8	3.2	15.9	9.7	3.8	<0.5	2.7	8.2	9.3	11.7	11.4	8.5	1.4	11.8
Tl	--	142	135	176	210	104	123	111	--	--	--	--	--	163
U	10.9	9.8	11.1	14.6	14.0	13.2	9.0	9.0	12.0	11.7	12.0	13.3	11.5	12.9
V	613	592	680	618	705	581	461	582	602	589	610	561	742	607
W	22	78	82	87	130	87	57	41	114	101	104	102	184	80
Zn	548	491	405	503	587	439	510	577	585	518	497	527	679	473
Zr	315	506	453	566	585	440	299	355	561	432	407	622	568	498
Hg ppb	<6	<6	<6	<6	<6	<5	<6	<6	<6	<6	<7	<7	<7	<7
Interval	74-112	0-116	0-9	9-45	45-56	56-61	61-122	Cement in	0-65	0-7	0-7	7-32	32-64	0-31
Type	Layer	Bulk	Layer	Layer	Layer	Layer	Layer	Breccia	Bulk	Layer	Layer	Layer	Layer	Bulk

Table 13 continued

	D8-1A	D8-1B	D8-1C	D8-1D	D8-1D[1]	D8-1E	D8-1F	D9-1A	D9-5A	D11-1A	D11-2A	D12-1-1	D12-2-1A	D13-1A
Fe Wt%	11.2	13.2	14.5	12.5	12.9	16.5	10.4	14.0	15.2	18.8	19.3	10.8	16.6	14.2
Mn	16.8	21.4	22.1	19.3	19.8	16.2	21.7	20.7	24.4	21.1	23.4	19.2	25.3	17.9
Fe/Mn	0.9	0.8	0.9	0.9	0.9	1.3	0.6	0.9	0.8	1.1	1.0	0.7	0.9	0.8
Si	1.5	2.1	2.3	1.4	1.4	1.6	1.0	1.9	2.7	3.1	3.0	1.8	4.8	2.7
Na	1.2	1.4	1.6	1.4	1.1	1.3	1.5	1.5	1.8	1.4	1.6	1.3	1.8	1.2
Al	0.3	0.3	0.5	0.2	0.2	0.4	0.3	0.4	0.5	1.0	0.7	0.3	1.3	0.6
K	0.4	0.5	0.5	0.4	0.4	0.3	0.5	0.5	0.5	0.5	0.5	0.5	0.8	0.4
Mg	0.8	0.9	0.9	0.9	0.7	0.8	0.9	1.0	1.1	1.1	1.1	0.8	1.1	0.8
Ca	1.7	2.0	2.1	1.9	2.0	1.7	5.8	6.7	2.4	2.4	2.5	2.0	3.2	1.9
Ti	0.7	0.8	1.0	0.9	0.9	0.7	0.6	0.7	0.9	1.1	1.1	0.8	1.1	0.9
P	0.4	0.4	0.4	0.2	0.2	0.4	1.8	2.2	0.4	0.5	0.4	0.3	0.8	0.4
S	0.3	0.3	0.3	0.2	0.2	0.3	0.4	0.4	0.3	0.2	0.2	0.2	0.3	0.3
LOI	57.5	53.9	54.4	46.5	--	59.4	50.6	44.6	59.0	41.4	45.8	41.1	49.4	52.3
As ppm	186	210	195	199	199	239	153	173	189	216	224	184	190	190
B	181	194	181	178	173	186	124	158	170	180	184	168	218	181
Ba	1236	1145	1545	1615	1528	1594	1714	1658	1442	2065	2311	770	1052	1361
Be	3.3	1.8	3.4	4.3	4.2	6.0	2.8	3.3	2.3	5.3	5.3	1.3	5.7	4.1
Bi	39.8	35.5	39.0	31.9	33.5	19.4	55.4	37.7	36.1	28.8	28.4	31.2	--	33.8
Br	31	26	34	36	34	36	29	25	32	30	30	24	29	28
Cd	5	5	4	5	5.3	4	6	5	6	4	4	5	--	5
Cl	11092	9436	10286	10845	10919	12417	10320	9282	10162	10348	9888	8446	9023	9923
Co	5220	6920	5468	5478	5590	3546	4169	4295	7574	3721	4248	8285	7893	4561
Cr	21	17	<13	16	17	19	<13	<12	<13	34	16	<12	77	15
Cu	1087	507	840	1145	1173	1328	1368	845	636	1453	1453	404	492	1783
Ga	8	7	5	6	9	8	8	7	7	10	9	6	--	9
Ge	<13	<13	<13	<12	<12	<13	<13	<12	30	<12	<12	<12	<13	<13
Hf	8	8	8	14	12	13	8	7	7	17	14	5	5	14
Li	1	1	1	4	1	3	1	4	1	5	1	2	5	2
Mo	549	541	519	561	570	606	615	504	504	451	512	402	385	452
Nb	40	42	53	55	53	49	40	48	62	64	76	29	41	48
Ni	4261	4220	4195	3925	4012	3466	5524	3998	4447	3577	3553	3705	3515	3577
Pb	1073	1350	1221	1031	1046	799	1023	1123	1442	1061	1019	1074	1129	933
Sb	44	35	40	48	47	56	37	41	36	53	53	28	29	45
Sc	6.1	5.1	5.8	5.0	4.7	8.2	4.9	5.3	4.9	4.9	4.3	5.3	11.3	7.9
Sr	1071	1287	1416	1255	1215	1186	1407	1597	1550	1513	1677	1062	1345	1164
Te	56.6	44.6	50.4	55.5	51.7	52.7	34.7	45.5	59.6	53.5	49.4	37.5	35.9	48.6
Th	<0.7	8.8	10.3	<0.6	<0.6	<0.7	3.1	6.9	16.2	3.4	3.6	38.0	36.8	5.4
Tl	222	190	201	239	242	182	242	192	202	137	152	168	--	168
U	11.1	14.2	11.8	13.3	13.9	8.9	9.8	11.0	14.3	12.0	12.3	10.7	10.8	10.4
V	686	675	606	709	714	821	574	629	573	703	755	507	582	631
W	111	106	94	104	102	108	104	92	101	114	111	82	51	105
Zn	587	503	575	650	660	700	646	567	528	643	642	425	458	557
Zr	427	380	499	561	571	620	467	514	515	905	867	241	348	651
Hg ppb	<7	<7	<6	<6	<6	<7	<6	<6	<7	<6	<6	8	8	13
Interval	0-71	0-7	7-32	32-36	32-36	36-61	61-71	0-105	0-30	0-30	0-30	0-3	0-2.5	0-85
Type	Bulk	Layer	Layer	Layer	Layer	Layer	Layer	Bulk	Bulk	Bulk	Bulk	Bulk	Bulk	Bulk

Table 13 continued

	D13-1B	D13-1C	D13-1D	D13-2A	D13-5A	D13-5A[1]	D13-20-1A	D14-1A	D15-1A	D15-1A[1]	D15-2A	D15-2B	D15-2C	D15-2D
Fe Wt%	14.6	12.7	14.3	18.9	13.4	13.1	12.3	15.8	18.2	18.2	14.8	16.6	16.6	14.4
Mn	20.3	17.1	16.6	20.6	18.9	17.7	20.8	20.9	22.5	22.5	17.1	22.4	21.2	16.1
Fe/Mn	0.9	0.9	1.2	1.1	0.8	0.8	0.8	1.0	0.9	0.9	1.1	0.9	1.0	1.1
Si	3.5	2.9	2.1	4.2	1.6	1.5	2.5	3.6	3.1	3.1	2.6	3.0	3.9	1.7
Na	1.3	1.1	1.1	1.4	1.0	1.0	1.2	1.3	1.7	1.9	1.1	1.4	1.5	0.9
Al	0.5	0.6	0.7	0.9	0.3	0.3	0.5	0.7	0.6	0.7	0.6	0.6	1.0	0.4
K	0.5	0.4	0.4	0.5	0.3	0.3	0.4	0.5	0.5	0.5	0.4	0.4	0.5	0.3
Mg	0.9	0.8	0.8	0.9	0.8	0.7	0.9	1.0	1.0	1.0	0.8	0.9	1.0	0.8
Ca	2.0	1.8	1.8	2.2	7.9	8.0	2.5	6.2	2.3	2.3	1.8	2.2	2.2	1.7
Ti	0.9	0.9	0.8	1.0	0.9	0.8	0.9	0.8	1.3	1.3	0.9	1.2	1.2	0.8
P	0.4	0.3	0.4	0.5	2.5	2.4	0.3	0.4	0.5	0.5	0.4	0.4	0.4	0.3
S	0.3	0.3	0.3	0.3	0.2	0.3	0.3	0.2	0.2	0.2	0.3	0.3	0.2	0.3
LOI	48.7	48.2	55.6	49.4	34.2	--	51.4	40.3	36.5	36.9	47.7	52.4	43.7	53.9
As ppm	190	163	197	204	170	159	168	190	241	231	201	193	170	217
B	204	171	170	201	146	138	157	201	214	215	197	184	171	183
Ba	1238	1281	1459	1801	2310	2061	1143	964	1959	1933	1380	1429	1553	1481
Be	2.7	3.8	5.1	9.5	5.5	5.1	2.1	1.5	8.4	7.9	9.3	6.7	7.6	10.3
Bi	36.3	35.4	31.9	--	67.7	67.3	43.2	25.3	31.4	31.5	--	--	--	--
Br	24	28	30	31	22	22	18	26	33	30	33	28	32	32
Cd	6	4	5	--	3	3.5	7	7	6	--	--	--	--	--
Cl	8785	9925	10631	9860	6886	6761	7097	12708	11569	10949	10138	9653	9964	10307
Co	5278	5013	3995	4010	3477	3318	8168	6746	5223	5289	4592	6461	4769	4470
Cr	20	<13	13	13	17	14	<13	25	16	13	30	27	<12	27
Cu	743	1583	2484	1430	1234	1144	1368	387	619	646	745	555	786	917
Ga	9	9	9	--	12	10	9	8	9	--	--	--	--	--
Ge	<13	<13	<13	<13	<11	<11	<13	<12	<11	<12	<13	<13	<12	<13
Hf	9	13	17	14	10	10	9	6	9	8	13	6	11	14
Li	<1	1	3	3	1	2	<1	1	<1	<1	<1	1	4	1
Mo	428	397	482	425	462	453	436	334	452	449	378	405	329	433
Nb	51	52	46	64	55	45	57	46	66	59	46	55	63	57
Ni	3367	3681	3679	3001	2707	2582	4748	3420	3288	3368	2961	3526	3289	2912
Pb	1170	932	786	1005	1778	1744	1147	1162	1340	1343	1120	1351	1063	967
Sb	38	40	51	47	60	59	50	26	47	46	46	37	36	51
Sc	5.8	6.3	9.7	6.9	8.3	7.8	4.4	7.1	6.4	6.5	5.8	4.8	5.6	6.6
Sr	1291	1090	1105	1341	1586	1257	1089	1235	1627	1644	1123	1351	1323	1063
Te	41.0	52.1	52.4	45.0	56.2	59.0	73.2	67.1	51.3	52.5	57.0	51.6	65.4	65.3
Th	8.1	8.7	2.8	6.6	15.9	17.0	12.9	16.6	9.7	11.0	6.0	8.8	11.5	2.9
Tl	172	175	164	--	113	117	219	165	181	--	--	--	--	--
U	11.6	13.4	8.8	13.4	10.5	10.8	9.9	10.3	15.3	14.9	13.4	13.4	11.7	10.1
V	666	541	633	654	618	605	548	563	659	666	626	575	540	711
W	89	85	120	105	125	125	85	63	93	90	72	63	55	83
Zn	466	513	625	571	505	496	501	455	553	556	543	510	496	625
Zr	503	681	736	724	622	691	387	479	584	606	531	515	585	585
Hg ppb	23	19	<7	<6	<6	<6	<6	11	<6	<6	<6	<6	<6	<6
Interval	0-28	28-40	40-85	0-50	Breccia	Breccia	0-33	0-2	0-32	0-32	0-48	0-11	11-32	32-50
Type	Layer	Layer	Layer	Bulk	Clast	Clast	Bulk PSC	Bulk	Bulk	Bulk	Bulk	Layer	Layer	Layer

[1] Duplicate analysis of sample

Table 14. Hydroscopic water-free (0% H_2O^-) gold and platinum-group element composition of Fe-Mn crusts in ppb, from Table 12

	D2-1A	D2-1D	D2-1E	D3-2A	D3-3A	D3-4A	D7-1A	D7-1B	D7-1C
Au	6	6	<6	<6	<6	<6	51	7	<6
Ir	5	5	5	5	5	5	5	5	8
Os	<2	3	<2	<2	<2	<2	<4	3	<3
Pd	7	<3	2	<2	5	<2	3	3	<3
Pt	371	245	326	157	323	184	320	238	317
Rh	20	23	17	12	20	12	22	14	23
Ru	14	13	10	16	25	22	10	21	21
Interval	0-70	25-45	45-70	0-14	0-30	0-7	0-112	0-13	13-28
Type	Bulk	Layer	Layer	Bulk	Bulk TC	Bulk	Bulk	Layer	Layer

	D7-1D	D7-1E	D8-1A	D13-1A	D13-1B	D13-1C	D13-1D	D15-1A	Means
Au	<6	<6	<7	10	<6	<6	11	543	<41
Ir	8	2	5	5	5	5	8	5	5.3
Os	<3	<2	3	<3	3	<3	<3	<3	<2.7
Pd	5	2	8	8	5	5	8	5	<4.5
Pt	257	294	360	573	165	490	611	326	327
Rh	20	18	24	28	14	26	32	21	20
Ru	10	5	19	21	20	20	24	21	17
Interval	28-74	74-112	0-71	0-85	0-28	28-40	40-85	0-32	–
Type	Layer	Layer	Bulk	Bulk	Layer	Layer	Layer	Bulk	All

Table 15. Statistics for 27 bulk Fe-Mn crusts from cruise KODODS 97-4; data from Table 13

	N	Mean	Median	SD[1]	Min[2]	Max[3]
Fe Wt%	27	15.1	15.0	2.9	10.2	20.4
Mn	27	21.4	21.7	3.3	13.3	27.3
Fe/Mn[4]	27	0.71	–	–	0.6	1.3
Si	27	2.8	2.7	1.0	1.3	4.8
Na	27	1.4	1.4	0.2	1.1	1.8
Al	27	0.6	0.6	0.3	0.2	1.3
K	27	0.5	0.5	0.1	0.4	0.8
Mg	27	0.9	1.0	0.1	0.7	1.1
Ca	27	4.3	2.5	3.1	1.7	12.5
Ti	27	0.9	0.9	0.2	0.6	1.3
P	27	1.1	0.5	1.2	0.2	4.2
S	27	0.3	0.3	0.0	0.2	0.4
H_2O^-	27	23.4	24.2	7.1	0.0	34.8
LOI	27	46.4	45.8	6.1	36.2	59.0
As ppm	27	189	190	22	144	241
B	27	180	180	27	136	226
Ba	27	1714	1632	748	770	4273
Be	27	4.6	3.3	2.7	1.3	9.5
Bi	18	33.9	34.0	5.4	25.3	43.2
Br	27	28	28	4	18	39
Cd	18	5.1	5.0	0.8	3.9	6.8
Cl	27	9544	9478	1163	7097	12708
Co	27	5364	5155	1789	1797	10110
Cr	27	22	19	13	12	77
Cu	27	890	745	436	387	1783
Ga	18	9	9	1	6	12
Ge	27	14	12	6	11	38
Hf	27	9	8	3	4	17
Li	27	2	1	1	1	5
Mo	27	440	436	68	291	586
Nb	27	51	54	13	24	76
Ni	27	3727	3640	688	1978	5006
Pb	27	1114	1123	120	933	1442
Sb	27	40	38	8	26	53
Sc	27	5.8	5.4	1.6	3.3	11.3
Sr	27	1400.2	1408.3	206.0	1062.1	1677.0
Te	27	51.3	50.4	11.7	31.9	79.2
Th	27	10.6	8.4	9.1	0.6	38.0
Tl	18	172	9	1	6	12
U	27	11.7	11.1	1.4	9.8	15.3
V	27	622	608	68	506	798
W	27	85	85	18	48	114
Zn	27	541	557	63	425	648
Zr	27	542	514	172	241	905
Au ppb	8	79	6	176	6	543
Hg	27	7	6	2	6	13
Ir	8	5	5	0	5	5
Os	8	3	3	1	2	4
Pd	8	5	5	2	2	8
Pt	8	327	325	119	157	573
Rh	8	20	20	5	12	28
Ru	8	19	20	4	10	25
Depth[5]	27	2035	2005	411	1675	3225
Thickness[6]	27	45	32	34	2	116

[1]Standard Deviation; [2]Minimum; [3]Maximum; [4]Ratio of Fe and Mn means, not a mean of the summation of ratios; [5]Water depth in meters; [6]Crust thickness in millimeters

Table 16. Statistics for 33 Fe-Mn crust layers from cruise KODODS 97-4; data from Table 13

	N	Mean	Median	SD[1]	Mlin[2]	Max[3]
Fe Wt%	33	14.1	14.7	3.1	8.0	21.7
Mn	33	21.2	21.5	3.3	12.0	27.5
Fe/Mn[4]	33	0.67	–	–	0.4	1.3
Si	33	2.3	2.3	1.2	0.7	5.3
Na	33	1.4	1.4	0.2	0.9	1.7
Al	33	0.5	0.5	0.3	0.1	1.2
K	33	0.4	0.5	0.1	0.2	0.5
Mg	33	0.9	0.9	0.1	0.7	1.2
Ca	33	4.3	2.3	4.1	1.7	14.1
Ti	33	0.8	0.8	0.2	0.3	1.2
P	33	1.2	0.4	1.6	0.2	5.4
S	33	0.3	0.3	0.1	0.1	0.4
H_2O^-	33	25.8	27.7	5.6	6.6	32.8
LOI	33	48.3	50.8	7.3	22.5	59.4
As ppm	33	193	199	33	115	250
B	33	166	178	32	95	207
Ba	33	1572	1506	355	1019	2684
Be	33	4.6	4.3	2.2	1.5	10.3
Bi	20	34.2	35.5	10.8	7.2	56.5
Br	33	29	28	5	23	46
Cd	20	4.7	4.6	0.9	2.6	6.1
Cl	33	9713	9768	1570	6104	12437
Co	33	4991	4804	1780	1365	8912
Cr	33	18	14	8	12	48
Cu	33	771	602	466	270	2484
Ga	20	8	9	2	5	11
Ge	33	13	13	1	11	13
Hf	30	9	9	4	2	17
Li	33	2	1	1	1	4
Mo	33	490	482	92	303	673
Nb	33	50	49	13	30	83
Ni	33	3896	3805	787	2239	5524
Pb	33	1150	1170	249	452	1613
Sb	33	42	40	9	27	67
Sc	33	5.1	4.9	1.5	3.1	9.7
Sr	33	1386	1407	163	1063	1706
Te	33	56.3	52.8	11.1	34.7	85.3
Th	33	6.2	4.9	4.3	0.5	15.9
Tl	20	179	179	41	104	251
U	33	11.7	11.8	1.8	8.8	15.7
V	33	629	633	77	461	821
W	33	94	94	27	22	184
Zn	33	563	548	76	405	700
Zr	33	508	504	153	295	992
Au ppb	9	7	6	1	6	11
Hg	33	7	6	4	5	23
Ir	9	6	5	2	2	8
Os	9	3	3	0	2	3
Pd	9	4	3	2	2	8
Pt	9	327	294	131	165	611
Rh	9	21	20	5	14	32
Ru	9	16	20	6	5	24
Depth[5]	33	1907	1763	247	1675	2300
Thickness[6]	33	21	18	15	4	61

[1]Standard Deviation; [2]Minimum; [3]Maximum; [4]Ratio of Fe and Mn, not a mean of the summation of ratios; [5]Water depth in meters; [6]Crust thickness in millimeters

Table 17. Concentrations of yttrium and rare earth elements (ppm) in Fe-Mn crusts from cruise KODOS 97-4

	D2-1A	D2-1A[1]	D2-1B	D2-1C	D2-1D	D2-1E	D2-4A	D3-2A	D3-4A	D4-1A	D4-1B	D4-1C
Y	252	218	135	111	177	340	150	108	134	123	124	100
La	219	202	164	192	198	234	177	225	217	197	193	181
Ce	850	776	622	870	732	1070	769	819	1030	754	703	728
Pr	32.9	31.4	25.8	32.4	33.7	30.7	29.3	43.9	46.3	34.7	34.5	31.8
Nd	147	146	120	143	151	139	129	188	199	152	151	141
Sm	32.1	29.6	26.1	32.1	33	29.3	28.5	43.5	47.8	33.9	34.9	31.4
Eu	6.92	6.58	5.63	6.87	6.85	6.26	5.96	9.01	9.82	7.26	7.39	6.48
Gd	38.2	37.2	31.3	35.2	37.3	38.2	32.8	45.1	47.5	36.1	38.3	33.9
Tb	5.1	5.1	4.2	4.9	5	4.9	4.5	6.4	6.7	4.8	5.2	4.6
Dy	33.1	32.9	29	30.5	32.3	33.2	28.3	38.4	41	29.8	33.2	28.6
Ho	7.51	7.31	6.56	6.42	7.02	8.04	6.2	7.57	8.07	6.16	6.77	5.8
Er	23.3	23	19.9	18.6	21.4	25.2	19	21.8	23.3	18	19.9	17.2
Tm	3.2	3.3	2.9	2.8	3	3.6	2.7	3.1	3.4	2.6	3	2.5
Yb	21.6	20.0	19.6	18.1	19.3	23.1	17.7	20.7	22.7	17.9	19.6	17.0
Lu	3.32	3.33	3.06	2.79	2.95	3.65	2.76	3.01	3.33	2.73	3.02	2.57
Σ REE	1423	1324	1080	1396	1283	1649	1253	1475	1706	1297	1253	1232
Ce*	2.3	2.2	2.2	2.5	2.0	2.8	2.4	1.9	2.4	2.1	2.0	2.2
Interval	B 0-70	B 0-70	L 0-10	L 10-25	L 25-45	L 45-70	B 0-65	B 0-14	B 0-7	B 0-70	L 0-15	L 15-36

	D4-1D	D4-5B	D4-5B[1]	D7-2A	D7-2B	D7-2C	D7-2D	D7-2E	D7-2F	D7-7C	D7-10A
Y	93	167	176	153	186	138	101	184	199	511	125
La	172	244	252	184	240	224	186	232	166	328	143
Ce	607	633	673	730	809	828	752	270	705	1530	682
Pr	31.7	48.5	50.6	31.4	41.7	38.3	35	39.7	24.8	46.9	22.9
Nd	136	218	227	136	188	170	149	176	113	206	101
Sm	30.8	49.4	53.4	30.7	42.5	38	32.7	38.4	22.9	41.6	21.6
Eu	6.2	10.6	11	6.29	9.33	7.79	6.79	8.12	5.11	8.97	4.68
Gd	31.9	52.6	55.3	33.7	47.7	41.2	34.2	40.2	29.1	56.3	26
Tb	4.2	7.1	8	4.3	6.6	5.6	4.6	5.9	4	7.2	3.6
Dy	26.7	46.8	49.4	28.3	42.4	34.9	27.8	36.4	25.9	48.1	22.4
Ho	5.34	9.43	10	6.1	9.14	7.48	5.44	7.43	5.76	11.1	4.98
Er	15.5	27.5	29.1	18.4	26.9	22.5	16	22.5	18.5	36.5	15.8
Tm	2.2	3.7	4.2	2.6	3.9	3.1	2.2	3.1	2.6	5	2.3
Yb	15.1	24.7	26.2	17.6	26.3	21.2	14.4	20.2	16.1	32.6	15.4
Lu	2.25	3.85	4.04	2.62	3.92	3.18	2.14	3.11	2.6	5.27	2.41
Σ REE	1087	1379	1453	1232	1497	1445	1268	903	1141	2364	1068
Ce*	1.9	1.3	1.4	2.2	1.8	2.0	2.1	0.6	2.5	2.8	2.7
Interval	L 36-55	B 0-5	B 0-5	B 0-116	L 0-9	L 9-45	L 45-56	L 56-61	L 61-122	Cement	B 0-31

Table 17 continued

	D8-1A	D8-1B	D8-1C	D8-1D	D8-1D[1]	D8-1E	D8-1F	D9-1A	D9-5A	D11-1A	D11-2A
Y	152	154	117	110	117	103	261	162	123	112	80
La	224	214	213	222	235	209	203	211	177	195	179
Ce	658	594	648	752	787	462	918	755	604	635	625
Pr	40.6	37.9	40.9	43	44.4	38.1	35.1	36	31.3	36.7	36.8
Nd	178	173	178	189	194	164	157	156	137	160	156
Sm	39.1	37.3	40.1	41.9	42.8	36.7	33.6	33.7	30.9	36	35.8
Eu	8.43	8.24	8.54	8.63	8.92	7.53	7.39	7.12	6.79	7.55	7.32
Gd	42.4	44.2	43.7	44.2	45.6	38.2	40.9	38.6	34.9	38.7	36.2
Tb	6	6.2	6.3	6.3	6.4	5.3	5.6	5.4	5	5.5	5.1
Dy	36.9	40.3	38.5	38.8	38.7	32.1	36.9	33	31.8	32.6	30.7
Ho	7.64	8.33	7.73	7.7	7.65	6.37	8.25	7.1	6.72	6.45	5.98
Er	23	25.2	22.7	22	22.9	18.5	25.8	21.6	20.3	19.8	16.9
Tm	3.2	3.5	3.2	3.2	3.3	2.5	3.6	3.1	2.9	2.7	2.4
Yb	20.6	23.0	20.3	20.1	20.2	16.3	23.2	20.0	19.0	17.6	15.5
Lu	3.16	3.47	3.00	2.94	3.1	2.48	3.71	3.06	2.96	2.73	2.3
Σ REE	1291	1219	1274	1401	1460	1039	1502	1331	1111	1196	1155
Ce*	1.6	1.5	1.6	1.8	1.8	1.2	2.5	2.0	1.9	1.7	1.8
Interval	B 0-71	L 0-7	L 7-32	L 32-36	L 32-36	L 36-61	L 61-71	B 0-105	B 0-30	B 0-30	B 0-30

	D12-1-1	D13-1A	D13-1B[1]	D13-1C	D13-1D	D13-5A	D13-5A	D13-20-1A	D14-1A	D15-1A	D15-1A[1]
Y	134	204	159	127	140	239	231	112	151	154	156
La	244	239	236	205	181	367	359	162	228	247	253
Ce	879	788	742	759	631	1750	1680	843	769	776	783
Pr	55.3	43.9	43.3	38.9	33.5	59.6	59.5	31.3	45.8	46.6	46.7
Nd	236	193	196	168	150	258	257	135	205	193	198
Sm	57.4	43.3	42.8	37.9	32	51.7	50	31	46.7	39.4	38.5
Eu	11.7	9.2	9.45	8.1	7.16	10.8	10.5	6.65	9.99	9.3	10.1
Gd	54.3	48.2	46.6	41	36.6	58.3	58.3	34.3	49.4	44	44.8
Tb	8	6.8	6.6	5.8	5.2	7.8	7.8	4.8	7.1	7	6.8
Dy	47.2	43.9	42.4	34.8	31	47.5	47.7	29.2	42.8	38.3	40.4
Ho	9.04	9.04	8.64	6.93	6.41	9.89	9.91	6.02	8.27	8.4	8.5
Er	25.4	27.4	25.9	21	19.8	29.3	29.4	18.1	25	23.3	23.9
Tm	3.5	3.8	3.7	3.1	3	4.1	4.2	2.6	3.5	3.4	3.4
Yb	22.0	24.9	23.4	19.3	18.5	26.5	26.5	16.8	22.2	15.5	15.6
Lu	3.25	3.82	3.66	3.05	3.1	4.29	4.25	2.66	3.54	3.5	3.4
Σ REE	1656	1484	1431	1352	1158	2685	2604	1324	1466	1453	1477
Ce*	1.7	1.8	1.7	2.0	1.9	2.7	2.6	2.7	1.7	1.7	1.7
Interval	B 0-3	B 0-85	L 0-28	L 28-40	L 40-85	Breccia Clast	Breccia Clast	B 0-33	B 0-2	B 0-32	B 0-32

Intervals are measured from the outer surface of the crust; B = bulk, L = layer; Ce* = 2Ce/La+Pr from chondrite normalized data

[1]Duplicate analysis of sample

Table 18. Correlation coefficient matrix for 27 bulk crusts listed in Table 13; n=27, except for Bi, Cd, Ga, and Tl = 18; Au, Os, Pd, Pt, Rh, and Ru = 8; the zero correlations for 27 points, 18 points, and 8 points at the 95% confidence level are |0.380|, |0.468|, and |0.706|, respectively

	Fe	Mn	Fe/Mn	Si	Na	Al	K	Mg	Ca	Ti	P	S	As	B	Ba	Be	Bi	Br	Cd	Cl	Co	Cr	Cu	Ga
Mn	0.284																							
Fe/Mn	0.586	-0.514																						
Si	0.831	0.198	0.554																					
Na	0.318	0.601	-0.175	0.267																				
Al	0.798	0.163	0.593	0.917	0.321																			
K	0.411	0.506	0.057	0.628	0.677	0.673																		
Mg	0.34	0.663	-0.121	0.227	0.77	0.379	0.579																	
Ca	-0.35	-0.146	-0.156	-0.402	-0.115	-0.337	-0.301	-0.103																
Ti	0.674	0.521	0.163	0.599	0.464	0.585	0.563	0.491	-0.624															
P	-0.355	-0.227	-0.105	-0.429	-0.127	-0.338	-0.338	-0.174	0.963	-0.623														
S	-0.484	-0.386	-0.063	-0.462	-0.141	-0.338	-0.331	-0.177	0.706	-0.682	0.777													
As	0.672	-0.122	0.575	0.494	0.179	0.451	0.135	0.016	-0.543	0.44	-0.499	-0.522												
B	0.65	0.222	0.338	0.771	0.193	0.599	0.51	0.054	-0.652	0.642	-0.669	-0.722	0.598											
Ba	0.493	-0.107	0.555	0.302	-0.091	0.361	-0.091	0.005	0.274	0.125	0.353	0.08	0.151	-0.036										
Be	0.524	-0.111	0.555	0.394	0.147	0.477	0.107	0.076	-0.121	0.357	-0.016	-0.03	0.455	0.378	0.402									
Bi	-0.662	0.083	-0.541	-0.683	-0.019	-0.556	-0.351	0.09	0.244	-0.292	0.361	0.699	-0.689	-0.719	-0.182	-0.254								
Br	0.128	-0.107	0.199	-0.105	0.252	0.012	-0.052	0.14	-0.089	0.089	-0.024	0.09	0.415	0.028	-0.063	0.497	-0.116							
Cd	-0.382	0.093	-0.239	-0.178	0.066	-0.311	0	0.075	-0.051	-0.056	-0.223	0	-0.188	-0.078	-0.469	-0.272	0.337	-0.045						
Cl	0.163	0.022	0.091	0.005	0.213	0.008	0.051	0.239	-0.209	0.154	-0.322	-0.236	0.414	0.228	-0.333	0.07	-0.306	0.593	0.256					
Co	-0.293	0.412	-0.47	-0.036	0.22	-0.094	0.385	0.234	-0.448	0.233	-0.534	-0.382	-0.18	0.128	-0.627	-0.416	0.249	-0.144	0.711	0.077				
Cr	0.146	0.245	0.072	0.33	0.262	0.483	0.612	0.283	-0.04	0.243	-0.04	-0.017	0.032	0.245	-0.158	0.124	-0.137	0.212	-0.041	0.114	0.239			
Cu	0.455	-0.077	0.376	0.352	-0.048	0.422	0	0.077	-0.379	0.382	-0.32	-0.218	0.241	0.281	0.31	0.462	-0.022	-0.048	-0.308	-0.134	-0.267	-0.245		
Ga	0.343	0.242	0.165	0.321	-0.363	0.385	-0.17	0.052	0.12	0.27	0.154	-0.108	-0.039	0.091	0.652	0.267	-0.014	-0.188	-0.272	-0.284	-0.347	0.153	0.283	
Ge	-0.303	0.116	-0.297	-0.282	0.039	-0.301	-0.121	0.209	0.179	-0.279	0.176	0.347	-0.373	-0.334	-0.08	-0.252	0.415	0.034	0.1	-0.09	0.058	-0.185	-0.213	0.126
Hf	0.608	-0.231	0.632	0.387	-0.12	0.508	-0.086	0.078	-0.286	0.387	-0.214	-0.157	0.448	0.245	0.463	0.634	-0.259	0.199	-0.475	0.039	-0.513	-0.142	0.831	0.374
Li	0.152	-0.112	0.299	0.22	0.181	0.442	0.371	0.233	0.171	-0.068	0.257	0.279	0.022	-0.039	0.185	0.281	0	0.009	-0.302	-0.171	-0.235	0.456	0.09	-0.104
Mo	-0.395	0.216	-0.533	-0.64	0.215	-0.576	-0.246	0.133	0.09	-0.156	0.136	0.215	-0.219	-0.392	-0.237	-0.221	0.5	0.198	-0.065	0.062	-0.03	-0.254	-0.045	-0.152
Nb	0.681	0.439	0.258	0.413	0.35	0.442	0.228	0.548	-0.336	0.716	-0.356	-0.345	0.317	0.199	0.42	0.236	-0.037	0.068	-0.09	0.159	-0.039	-0.092	0.459	0.401
Ni	-0.627	0.345	-0.703	-0.622	0.181	-0.536	-0.093	0.323	0.014	-0.136	-0.02	0.116	-0.529	-0.466	-0.438	-0.44	0.833	-0.051	0.552	-0.038	0.513	-0.126	-0.158	-0.113
Pb	-0.288	0.164	-0.273	-0.32	0.367	-0.326	-0.03	0.264	0.01	-0.091	-0.008	0.091	0.047	-0.229	-0.264	-0.205	0.199	0.301	0.616	0.273	0.377	0.017	-0.6	-0.303
Sb	0.312	-0.311	0.497	-0.023	-0.185	0.148	-0.367	-0.032	-0.105	0.112	0.005	0.16	0.411	-0.199	0.47	0.426	0.096	0.28	-0.256	0.009	-0.462	-0.182	0.498	0.319
Sc	0.244	-0.115	0.332	0.512	0.011	0.506	0.453	-0.061	-0.093	0.058	-0.085	0.068	0.207	0.426	-0.019	0.296	-0.231	0.139	0.078	0.114	0.006	0.553	0.035	0.108
Sr	0.296	0.224	0.095	-0.01	0.431	0.066	0.046	0.388	0.556	0.077	0.581	0.293	-0.007	-0.286	0.612	0.17	-0.075	0.147	-0.357	-0.089	-0.552	-0.077	-0.066	0.273
Te	-0.124	-0.126	0.097	-0.2	-0.074	-0.081	-0.288	0.219	-0.097	0.007	-0.168	0.085	-0.009	-0.353	-0.056	-0.096	0.301	0.223	0.552	0.321	0.214	-0.086	0.001	0.002
Th	-0.12	0.104	-0.113	0.233	0.128	0.153	0.519	-0.029	-0.269	0.078	-0.299	-0.269	0.039	0.249	-0.392	-0.282	-0.255	-0.184	0.282	-0.135	0.666	0.413	-0.427	-0.418
Tl	-0.571	0.072	-0.369	-0.59	0.124	-0.54	-0.112	0.15	0.028	-0.115	0.04	0.422	-0.485	-0.447	-0.299	-0.154	0.831	0.076	0.627	0.051	0.45	-0.135	-0.046	-0.277
U	0.262	0.057	0.148	0.095	0.28	0.008	0.022	0.096	-0.426	0.306	-0.362	-0.243	0.605	0.26	-0.056	0.189	-0.197	0.518	0.082	0.404	0.063	-0.113	-0.186	-0.024
V	0.541	0.071	0.301	0.359	0.274	0.388	0.169	0.231	-0.352	0.421	-0.315	-0.366	0.472	0.482	0.223	0.438	-0.385	0.175	-0.584	0.168	-0.383	-0.183	0.653	0.247
W	-0.008	0.085	-0.131	-0.342	0.07	-0.208	-0.253	0.211	-0.301	0.07	-0.263	-0.07	0.19	-0.245	-0.052	0.021	0.296	0.344	-0.089	0.295	0.003	-0.388	0.378	0.035
Zn	0.111	0.085	0.085	-0.233	0.096	-0.036	-0.183	0.328	0.042	0.185	0.108	0.083	-0.001	-0.222	0.394	0.355	0.226	0.314	-0.289	0.05	-0.389	-0.234	0.466	0.454
Zr	0.833	0.12	0.555	0.536	0.135	0.599	0.097	0.307	-0.227	0.514	-0.206	-0.326	0.493	0.355	0.618	0.519	-0.432	0.108	-0.539	0.102	-0.519	-0.144	0.73	0.454
Au	0.424	0.085	0.231	0.224	0.793	0.228	0.346	0.317	-0.156	0.512	-0.139	-0.296	0.777	0.309	0.551	0.619	-0.417	0.621	0.542	0.655	-0.053	-0.244	-0.28	-0.161
Hg	-0.143	-0.238	-0.019	0.072	-0.132	0.048	0.059	-0.149	-0.109	-0.09	-0.207	-0.048	-0.015	0.081	-0.317	-0.253	-0.217	-0.056	0.249	0.343	0.168	0.081	0.061	-0.257
Os	-0.358	-0.884	0.577	-0.359	-0.054	-0.266	-0.539	-0.702	0.286	-0.33	0.372	0.487	0.232	-0.39	0.224	0.038	-0.148	0.675	0.243	0.272	-0.394	-0.424	-0.036	-0.707
Pd	-0.299	-0.429	0.036	-0.358	-0.354	-0.23	-0.64	-0.287	-0.104	-0.5	-0.051	0.386	0.08	-0.195	-0.274	0.14	0.468	0.215	-0.032	0.349	-0.362	-0.651	0.5	-0.184
Pt	-0.274	-0.584	0.148	-0.261	-0.32	-0.082	-0.667	-0.426	0.007	-0.426	0.067	0.45	0.116	-0.284	-0.114	0.174	0.205	0.256	0.043	0.201	-0.41	-0.724	0.602	-0.117
Rh	-0.312	-0.772	0.414	-0.321	-0.226	-0.147	-0.703	-0.546	0.037	-0.47	0.121	0.49	0.24	-0.28	0.002	0.266	0.202	0.495	0.062	0.338	-0.514	-0.77	0.523	-0.331
Ru	0.498	0.486	0.019	0.465	0.364	0.577	0.549	0.4	-0.836	0.583	-0.849	-0.761	0.466	0.654	-0.242	0.574	-0.241	0.141	0.68	0.511	0.484	0.298	0.558	-0.405
Depth	-0.051	-0.141	0.125	0.236	-0.024	0.24	0.437	-0.164	-0.276	0.02	-0.302	-0.158	0.148	0.246	-0.29	-0.075	-0.225	-0.182	0.235	-0.005	0.363	0.344	-0.092	-0.484
Thick	-0.336	-0.278	-0.118	-0.51	-0.186	-0.4	-0.472	-0.195	0.505	-0.413	0.564	0.675	-0.368	-0.616	0.205	-0.047	0.429	0.078	-0.319	-0.103	-0.517	-0.326	0.044	0.16

Table 18 continued

	Hf	Li	Mo	Nb	Ni	Pb	Sb	Sc	Sr	Te	Th	Tl	U	V	W	Zn	Zr	Au	Hg	Os	Pd	Pt	Rh	Ru	Depth
Li	0.198																								
Mo	-0.207	-0.176																							
Nb	0.521	-0.165	-0.041																						
Ni	-0.442	-0.22	0.695	-0.079																					
Pb	-0.518	-0.113	0.351	-0.072	0.48																				
Sb	0.678	0.106	0.119	0.478	-0.162	-0.078																			
Sc	0.066	0.408	-0.474	-0.194	-0.445	-0.225	-0.119																		
Sr	0.099	0.162	0.263	0.364	-0.075	0.134	0.223	-0.232																	
Te	0.064	-0.284	0.036	0.319	0.353	0.393	0.406	-0.303	-0.091																
Th	-0.487	0.137	-0.383	-0.338	-0.043	0.183	-0.513	0.411	-0.416	-0.201															
Tl	-0.296	-0.144	0.503	0.017	0.811	0.385	0.026	-0.112	-0.157	0.419	-0.118														
U	0.05	-0.222	0.142	0.31	-0.059	0.556	0.209	-0.111	0.094	0.113	-0.001	-0.08													
V	0.587	-0.063	0.163	0.391	-0.178	-0.359	0.254	-0.102	0.181	-0.167	-0.492	-0.366	0.175												
W	0.32	-0.134	0.587	0.381	0.437	0.138	0.544	-0.322	0.014	0.335	-0.401	0.313	0.319	0.304											
Zn	0.488	0.024	0.57	0.424	0.338	-0.027	0.545	-0.35	0.462	0.206	-0.697	0.193	0.092	0.505	0.638										
Zr	0.855	0.128	-0.168	0.724	-0.448	-0.456	0.534	-0.013	0.37	-0.03	-0.513	-0.444	0.1	0.694	0.295	0.497									
Au	0.001	-0.234	-0.026	0.534	-0.327	0.752	0.557	0.082	0.492	0.141	0.085	-0.059	0.956	0.186	0.13	0.022	0.152								
Hg	-0.018	0.008	-0.162	-0.223	-0.052	-0.119	-0.207	0.406	-0.362	0.083	0.239	-0.007	-0.256	-0.189	-0.045	-0.261	-0.127	-0.184							
Os	0.041	-0.104	0.455	-0.445	-0.046	0.328	0.653	-0.233	0.243	0.648	-0.361	0.272	0.255	0.162	0.162	0.381	-0.324	0.271	0.348						
Pd	0.472	0.615	0.6	-0.425	0.255	-0.132	0.658	0.793	-0.406	0.084	-0.785	0.484	-0.204	0.334	0.817	0.689	0.133	-0.023	0.519	0.153					
Pt	0.653	0.706	0.355	-0.397	0.116	-0.172	0.704	0.736	-0.243	0.186	-0.61	0.152	-0.192	0.221	0.671	0.615	0.188	0.002	0.815	0.401	0.842				
Rh	0.571	0.462	0.502	-0.481	0.084	-0.047	0.821	0.571	-0.153	0.337	-0.74	0.308	-0.067	0.402	0.65	0.707	0.104	0.101	0.677	0.614	0.827	0.936			
Ru	0.44	-0.127	-0.532	0.672	-0.106	-0.2	0.142	0.475	-0.532	-0.077	0.213	0.116	0.1	0.278	0.353	-0.126	0.628	0.151	0.115	-0.453	0.164	0.09	-0.003		
Depth	-0.139	0.295	-0.244	-0.292	-0.16	-0.057	-0.148	0.556	-0.452	-0.22	0.71	0.068	-0.143	-0.283	-0.151	-0.428	-0.277	0.217	0.465	0.364	0.783	0.713	0.736	0.268	
Thick	0.042	-0.099	0.479	-0.043	0.215	-0.062	0.345	-0.282	0.403	0.183	-0.578	0.163	-0.143	0.042	0.293	0.486	-0.006	-0.168	-0.025	0.767	0.491	0.667	0.768	-0.594	-0.372

Table 19. Correlation coefficient matrix for 10 bulk crusts ≥ 65mm listed in Table 13; n=10, except for Bi, Cd, Ga, and Tl = 7; Au, Os, Pd, Pt, Rh, and Ru = 4; the zero correlations for 10 points, 7 points, and 4 points at the 95% confidence level are |0.631|, |0.753|, and |0.962|, respectively

	Fe	Mn	Fe/Mn	Si	Na	Al	K	Mg	Ca	Ti	P	S	As	B	Ba	Be	Bi	Br	Cd	Cl	Co	Cr	Cu	Ga
Mn	0.324																							
Fe/Mn	0.53	-0.535																						
Si	0.915	0.056	0.672																					
Na	-0.018	0.627	-0.443	-0.316																				
Al	0.951	0.092	0.668	0.989	-0.256																			
K	0.565	0.412	0.299	0.492	0.381	0.462																		
Mg	0.148	0.815	-0.419	-0.15	0.641	-0.103	0.35																	
Ca	-0.455	0.202	-0.56	-0.49	0.415	-0.527	-0.124	0.293																
Ti	0.818	0.241	0.506	0.816	-0.023	0.85	0.476	0.015	-0.641															
P	-0.511	0.122	-0.527	-0.523	0.387	-0.563	-0.161	0.25	0.993	-0.671														
S	-0.701	-0.244	-0.42	-0.717	0.164	-0.75	-0.307	0.072	0.723	-0.898	0.75													
As	0.695	-0.183	0.701	0.64	-0.203	0.721	0.134	-0.264	-0.804	0.729	-0.814	-0.691												
B	0.642	-0.095	0.618	0.73	-0.415	0.738	0.302	-0.307	-0.882	0.733	-0.879	-0.846	0.74											
Ba	0.73	0.161	0.588	0.842	-0.185	0.806	0.546	0.053	-0.173	0.666	-0.188	-0.608	0.309	0.501										
Be	0.411	0.129	0.237	0.251	0.112	0.37	-0.19	0.211	-0.436	0.502	-0.421	-0.508	0.644	0.381	0.154									
Bi	-0.857	0.173	-0.642	-0.881	0.268	-0.892	-0.198	0.405	0.264	-0.617	0.282	0.546	-0.681	-0.594	-0.682	-0.805								
Br	-0.218	-0.181	-0.037	-0.391	0.116	-0.277	-0.526	-0.015	-0.191	-0.069	-0.187	0.073	0.36	-0.203	-0.54	0.48	0.628							
Cd	-0.446	0.315	-0.432	-0.507	0.466	-0.5	0.194	0.307	-0.107	-0.019	-0.121	0.091	-0.225	-0.224	-0.493	-0.43	0.731	0.578						
Cl	-0.212	-0.158	-0.128	-0.378	0.066	-0.299	-0.314	-0.213	-0.37	-0.163	-0.387	0.049	0.34	0.032	-0.711	0.112	0.457	0.717	0.478					
Co	-0.051	0.311	-0.204	-0.262	0.301	-0.183	0.041	0.288	-0.455	0.224	-0.485	-0.279	0.277	0.109	-0.398	0.26	0.667	0.614	0.927	0.676				
Cr	-0.044	0.33	-0.338	-0.306	0.472	-0.188	-0.312	0.175	0.004	0.053	-0.035	-0.162	0.24	-0.172	-0.364	0.456	0.267	0.727	0.322	0.607	0.585			
Cu	0.452	-0.327	0.467	0.572	-0.529	0.578	0.002	-0.506	-0.817	0.528	-0.808	-0.54	0.684	0.818	0.135	0.3	-0.566	-0.058	-0.187	0.212	0.038	-0.233		
Ga	0.453	0.24	0.219	0.579	-0.492	0.537	0.026	0.078	-0.023	0.435	-0.056	-0.462	0.022	0.209	0.717	0.136	-0.357	-0.595	-0.385	-0.753	-0.34	-0.36	0.011	
Ge	-0.392	0.092	-0.368	-0.313	-0.349	-0.375	-0.247	0.295	0.247	-0.415	0.243	0.357	-0.59	-0.361	-0.136	-0.368	0.546	-0.13	0.129	-0.249	-0.005	-0.368	-0.3	0.433
Hf	0.574	-0.325	0.542	0.708	-0.637	0.715	-0.073	-0.453	-0.7	0.573	-0.703	-0.518	0.699	0.713	0.306	0.355	-0.715	-0.024	-0.409	0.031	-0.116	-0.265	0.913	0.331
Li	-0.172	0.121	-0.187	-0.245	0.313	-0.251	0.195	0.411	0.085	-0.217	0.137	0.295	-0.281	-0.05	-0.187	0.099	0.171	-0.289	0.155	-0.217	-0.099	-0.384	0.023	-0.477
Mo	-0.73	0.157	-0.599	-0.842	0.452	-0.817	-0.232	0.266	0.166	-0.444	0.202	0.295	-0.443	-0.375	-0.668	-0.032	0.929	0.325	0.807	0.369	0.541	0.378	-0.408	-0.624
Nb	0.918	0.409	0.443	0.841	0.047	0.854	0.706	0.187	-0.385	0.797	-0.461	-0.66	0.557	0.523	0.705	0.141	-0.61	-0.24	-0.146	-0.178	0.103	-0.039	0.288	0.508
Ni	-0.667	0.292	-0.628	-0.781	0.409	-0.758	-0.227	0.463	0.216	-0.369	0.242	0.258	-0.506	-0.439	-0.528	0.018	0.986	0.315	0.816	0.178	0.552	0.322	-0.512	-0.295
Pb	-0.364	0.317	-0.3	-0.54	0.599	-0.483	-0.033	0.599	0.285	-0.137	0.312	0.149	-0.269	-0.444	-0.183	0.292	0.795	0.405	0.682	-0.02	0.43	0.421	-0.672	-0.188
Sb	0.695	-0.19	0.68	0.622	-0.299	0.705	0.044	-0.2	-0.769	0.617	-0.782	-0.594	0.965	0.694	0.278	0.657	-0.744	0.367	-0.432	0.331	0.207	0.184	0.676	0.082
Sc	0.203	-0.289	0.219	0.291	-0.707	0.277	-0.194	-0.288	-0.577	0.11	-0.592	-0.127	0.341	0.421	-0.106	-0.01	-0.127	0.046	-0.147	0.273	0.093	-0.337	0.709	0.202
Sr	0.093	0.402	-0.12	0.025	0.578	0.005	0.423	0.52	0.713	-0.017	0.7	0.246	-0.417	-0.508	0.396	-0.129	-0.092	-0.324	-0.088	-0.674	-0.373	-0.096	-0.696	0.244
Te	0.3	-0.17	0.452	0.169	-0.017	0.28	-0.207	-0.044	-0.395	0.377	-0.4	-0.329	0.717	0.165	0.055	0.667	-0.34	0.799	-0.089	0.41	0.415	0.58	0.095	0.105
Th	0.45	-0.292	0.649	0.51	-0.309	0.522	0.076	0.044	-0.14	0.32	-0.117	-0.064	0.384	0.143	0.497	0.37	-0.581	0.037	-0.551	-0.428	-0.355	-0.392	0.187	0.518
Tl	-0.697	-0.056	-0.31	-0.711	0.212	-0.705	-0.056	0.134	-0.169	-0.345	-0.151	0.226	-0.252	-0.188	-0.621	-0.46	0.878	0.746	0.816	0.669	0.866	0.314	-0.237	-0.519
U	0.207	-0.023	0.454	0.174	0.089	0.198	0.363	0.149	-0.279	0.422	-0.288	-0.268	0.342	0.073	0.276	0.106	0.245	0.361	0.531	0.056	0.484	0.12	-0.169	0.255
V	0.362	-0.378	0.682	0.474	-0.361	0.468	0.277	-0.55	-0.735	0.414	-0.711	-0.575	0.636	0.829	0.299	0.108	-0.397	-0.132	-0.17	0.241	0.055	-0.122	0.63	-0.161
W	0.13	0.166	-0.077	-0.053	-0.066	0.023	-0.084	0.113	-0.684	0.202	-0.719	-0.324	0.46	0.384	-0.397	0.316	0.489	0.496	0.66	0.755	0.809	0.385	0.446	-0.426
Zn	-0.117	0.155	0.034	-0.104	0.058	-0.085	0.018	0.325	-0.296	0.278	-0.246	-0.375	0.018	0.219	0.16	0.432	0.355	0.115	0.466	-0.201	0.4	0.04	-0.076	0.286
Zr	0.943	0.225	0.499	0.949	-0.215	0.955	0.498	-0.032	-0.543	0.802	-0.592	-0.732	0.647	0.765	0.7	0.302	-0.911	-0.377	-0.476	-0.237	-0.136	-0.214	0.654	0.483
Au	-0.398	-0.805	0.705	-0.108	0.997	-0.115	•	-0.383	0.564	-0.055	0.616	0.531	-0.021	-0.545	0.788	-0.062	-0.999	0.551	•	-0.405	-0.794	0.004	-0.422	-0.419
Hg	-0.028	-0.414	0.051	0.148	-0.422	0.13	-0.284	-0.598	-0.443	0.188	-0.425	-0.128	0.265	0.345	-0.267	0.013	-0.248	0.035	0.106	0.252	0.019	-0.198	0.779	-0.123
Os	-0.044	-0.991	0.956	0.195	0.816	0.236	•	-0.816	0.038	0.324	0.104	0	0.509	-0.016	0.34	0.421	-0.721	0.833	•	0.116	-0.421	0.436	0.024	-0.945
Pd	0.575	0.645	-0.533	0.3	-0.98	0.323	•	0.14	-0.753	0.278	-0.795	-0.728	0.275	0.739	-0.905	0.313	-0.721	-0.4	•	0.577	0.853	0.15	0.626	-0.945
Pt	0.976	0.248	-0.255	0.928	-0.505	0.909	•	-0.206	-0.607	0.861	-0.631	-0.616	0.495	0.619	-0.496	0.718	-0.947	-0.391	•	0.216	0.193	-0.202	0.899	-0.144
Rh	0.938	-0.218	0.257	0.923	-0.293	0.958	•	-0.683	-0.826	0.969	-0.816	-0.845	0.884	0.841	-0.615	0.978	-0.971	0.159	•	0.591	0.329	0.313	0.976	-0.655
Ru	0.819	0.301	-0.196	0.619	-0.805	0.659	•	-0.268	-0.939	0.64	-0.959	-0.93	0.643	0.935	-0.942	0.692	-0.885	-0.137	•	0.733	0.782	0.323	0.89	-0.817
Depth	0.151	-0.354	0.34	0.314	-0.527	0.281	0.077	-0.554	-0.765	0.269	-0.742	-0.424	0.407	0.778	-0.004	-0.04	-0.239	-0.223	0.026	0.284	0.108	-0.325	0.845	-0.194
Thick	-0.276	-0.45	0.026	-0.194	0.085	-0.232	-0.117	-0.331	0.576	-0.527	0.613	0.681	-0.302	-0.451	-0.188	-0.355	-0.266	-0.19	-0.459	-0.145	-0.702	-0.269	-0.175	-0.477

Table 19 continued

	Hf	Li	Mo	Nb	Ni	Pb	Sb	Sc	Sr	Te	Th	Tl	U	V	W	Zn	Zr	Au	Hg	Os	Pd	Pt	Rh	Ru	Depth
Li	-0.152																								
Mo	-0.666	0.362																							
Nb	0.402	-0.33	-0.649																						
Ni	-0.66	0.327	0.932	-0.558																					
Pb	-0.694	0.235	0.693	-0.303	0.807																				
Sb	0.739	-0.237	-0.51	0.517	-0.541	-0.321																			
Sc	0.754	-0.06	-0.384	0.151	-0.347	-0.644	0.474																		
Sr	-0.534	0.135	-0.088	0.167	0.048	0.426	-0.455	-0.718																	
Te	0.237	-0.463	-0.143	0.235	-0.099	0.261	0.71	0.027	-0.159																
Th	0.477	0.047	-0.638	0.302	-0.459	-0.076	0.479	0.252	0.236	0.41															
Tl	-0.514	0.172	0.952	-0.48	0.888	0.701	-0.362	-0.066	-0.355	0.045	-0.626														
U	-0.074	-0.347	-0.025	0.419	0.114	0.418	0.253	-0.115	0.182	0.593	0.34	0.406													
V	0.432	-0.132	-0.218	0.298	-0.428	-0.423	0.558	0.216	-0.523	0.153	-0.062	0.057	0.093												
W	0.3	-0.025	0.244	0.143	0.213	-0.038	0.496	0.567	-0.734	0.333	-0.237	0.776	0.132	0.256											
Zn	-0.146	0.287	0.488	-0.128	0.636	0.672	-0.044	-0.21	0.014	0.153	0.053	0.518	0.381	0.026	0.147										
Zr	0.728	-0.122	-0.752	0.845	-0.719	-0.578	0.647	0.381	-0.089	0.092	0.361	-0.723	0.015	0.454	0.153	-0.147									
Au	-0.323	-0.558	-0.325	-0.538	-0.304	0.498	-0.232	-0.854	0.721	0.698	0.67	-0.706	0.799	-0.164	-0.908	-0.217	-0.525								
Hg	0.689	0.034	-0.136	-0.106	-0.245	-0.571	0.222	0.6	-0.607	-0.123	-0.026	-0.081	-0.303	0.212	0.274	-0.182	0.22	-0.184							
Os	0	-0.707	-0.267	-0.26	-0.634	0.106	0.315	-0.689	0.24	0.903	0.277	0.021	0.533	0.354	-0.545	-0.526	-0.188	0.845	0.128						
Pd	0.499	0.485	0.244	0.668	0.071	-0.675	0.472	0.88	-0.864	-0.562	-0.741	0.021	-0.879	0.357	0.977	-0.004	0.678	-0.966	0.372	-0.686					
Pt	0.98	0.672	-0.635	0.993	-0.644	-0.952	0.585	0.823	-0.531	-0.441	-0.063	-0.878	-0.89	0.104	0.514	-0.738	0.981	-0.439	0.952	-0.183	0.574				
Rh	0.928	0.169	-0.452	0.838	-0.856	-0.937	0.912	0.528	-0.689	0.08	-0.291	-0.481	-0.692	0.57	0.511	-0.878	0.894	-0.22	0.93	0.239	0.451	0.843			
Ru	0.758	0.349	0.008	0.825	-0.353	-0.895	0.789	0.823	-0.95	-0.293	-0.698	-0.257	-0.909	0.578	0.93	-0.406	0.867	-0.763	0.671	-0.329	0.902	0.759	0.786		
Depth	0.606	0.104	-0.095	0.088	-0.271	-0.604	0.374	0.603	-0.782	-0.194	-0.189	0.169	-0.215	0.777	0.459	0.013	0.401	-0.618	0.65	-0.109	0.798	0.66	0.831	0.966	
Thick	-0.153	0.19	-0.178	-0.375	-0.35	-0.256	-0.279	-0.232	0.309	-0.283	0.112	-0.405	-0.427	-0.138	-0.638	-0.637	-0.265	0.961	0.07	0.876	-0.88	-0.173	0.025	-0.597	-0.2

Table 20. Correlation coefficient matrix for 17 bulk crusts ≤ 50mm listed in Table 13; n=17, except for Bi, Cd, Ga, and Tl = 11; Au, Os, Pd, Pt, Rh, and Ru = 4; the zero correlations for 17 points, 11 points, and 4 points at the 95% confidence level are |0.481|, |0.601|, and |0.962|, respectively

	Fe	Mn	Fe/Mn	Si	Na	Al	K	Mg	Ca	Ti	P	S	As	B	Ba	Be	Bi	Br	Cd	Cl	Co	Cr	Cu	Ga
Mn	0.201																							
Fe/Mn	0.547	-0.612																						
Si	0.689	0.256	0.349																					
Na	0.397	0.62	-0.18	0.438																				
Al	0.626	0.149	0.465	0.849	0.46																			
K	0.23	0.599	-0.192	0.615	0.717	0.681																		
Mg	0.379	0.62	-0.08	0.319	0.793	0.52	0.607																	
Ca	0.096	-0.458	0.55	0.152	-0.266	0.159	-0.164	-0.21																
Ti	0.5	0.718	-0.204	0.297	0.556	0.325	0.477	0.609	-0.487															
P	0.13	-0.524	0.593	0.108	-0.234	0.175	-0.195	-0.293	0.903	-0.444														
S	-0.078	-0.499	0.494	0.13	-0.103	0.236	-0.107	-0.165	0.507	-0.441	0.653													
As	0.547	-0.219	0.422	0.132	0.192	0.107	-0.113	-0.012	-0.116	0.117	-0.015	-0.187												
B	0.507	0.387	-0.02	0.643	0.258	0.339	0.405	0.019	-0.246	0.44	-0.287	-0.451	0.321											
Ba	0.563	-0.309	0.694	0.176	0.01	0.291	-0.214	0.039	0.633	0.01	0.778	0.398	0.26	-0.159										
Be	0.569	-0.263	0.68	0.419	0.105	0.482	0.061	0.004	0.168	0.26	0.347	0.303	0.365	0.32	0.617									
Bi	-0.511	0.178	-0.488	-0.488	0.046	-0.279	-0.24	0.158	-0.377	0.09	-0.448	0.736	-0.589	-0.69	-0.137	-0.18								
Br	0.472	-0.033	0.429	0.152	0.352	0.243	0.125	0.237	-0.028	0.218	0.107	0.109	0.567	0.223	0.345	0.581	-0.335							
Cd	-0.521	-0.077	-0.259	-0.233	-0.15	-0.392	-0.281	-0.06	0.475	-0.257	-0.429	0.365	-0.4	-0.24	-0.501	-0.264	0.445	-0.254						
Cl	0.319	0.107	0.166	0.112	0.234	0.07	0.08	0.361	-0.053	0.218	-0.277	-0.336	0.438	0.271	-0.112	0.033	-0.521	0.556	0.154					
Co	-0.715	0.493	-0.837	-0.349	0.136	-0.344	0.308	0.171	-0.387	0.067	-0.513	-0.253	-0.582	-0.163	-0.754	-0.632	0.602	-0.377	0.669	-0.07				
Cr	0.092	0.242	0.09	0.438	0.196	0.603	0.676	0.269	0.136	0.187	0.153	0.211	-0.15	0.207	-0.08	0.043	-0.091	0.14	-0.224	0.014	0.141			
Cu	0.489	0.07	0.323	0.257	0.093	0.365	-0.038	0.266	-0.091	0.341	-0.011	-0.043	0.032	0.055	0.457	0.514	0.164	-0.04	-0.334	-0.287	-0.399	-0.293		
Ga	0.442	0.37	0.213	0.282	-0.207	0.402	-0.185	0.161	-0.035	0.467	0.524	-0.289	0.152	0.282	0.485	0.383	0.003	0.085	-0.161	0.035	-0.284	0.58	0.487	
Ge	-0.114	0.206	-0.156	-0.142	0.392	-0.164	0.015	0.259	-0.097	-0.121	-0.08	0.292	-0.146	-0.277	-0.093	-0.215	0.293	0.244	0.199	0.062	0.225	-0.142	-0.144	-0.431
Hf	0.64	-0.235	0.682	0.194	-0.031	0.405	-0.19	0.193	0.035	0.283	0.156	0.109	0.325	-0.016	0.638	0.686	-0.122	0.337	-0.515	0.017	-0.72	-0.184	0.808	0.443
Li	0.248	-0.265	0.502	0.405	0.118	0.707	0.385	0.162	0.419	-0.117	0.549	0.483	0.043	-0.177	0.416	0.297	-0.097	0.159	-0.454	-0.18	-0.34	0.563	0.103	0.14
Mo	0.191	0.492	-0.368	-0.188	0.399	-0.205	0.016	0.294	-0.66	0.413	-0.568	-0.396	0.333	0.038	-0.181	-0.188	0.071	0.124	-0.364	0.023	0.141	-0.318	0.237	0.138
Nb	0.548	0.453	0.095	0.104	0.43	0.193	0.049	0.667	-0.255	0.704	-0.24	-0.122	0.148	-0.054	0.319	0.238	0.266	0.28	-0.117	0.278	-0.152	-0.16	0.533	0.431
Ni	-0.51	0.513	-0.71	-0.404	0.242	-0.297	0.132	0.41	-0.546	0.188	-0.625	-0.294	-0.412	-0.299	-0.572	-0.533	0.808	-0.316	0.559	-0.072	0.819	-0.121	0.029	-0.029
Pb	-0.321	0.076	-0.298	-0.333	0.301	-0.329	-0.051	0.158	-0.154	-0.111	-0.184	0.122	0.163	-0.249	-0.315	-0.343	0.3	0.255	0.556	0.377	0.403	-0.053	-0.576	-0.279
Sb	0.338	-0.373	0.569	-0.156	-0.123	0.094	-0.4	0.045	0.05	0.098	0.226	0.339	0.438	-0.394	0.559	0.444	0.235	0.267	-0.194	-0.053	-0.527	-0.191	0.479	0.434
Sc	0.187	-0.056	0.349	0.643	0.18	0.582	0.578	-0.038	0.418	-0.076	0.409	0.369	0.056	0.393	0.088	0.342	-0.592	0.209	0.335	0.029	-0.096	0.702	-0.261	-0.144
Sr	0.782	0.187	0.431	0.335	0.545	0.374	0.144	0.475	0.287	0.391	0.367	0.089	0.483	0.082	0.735	0.389	-0.25	0.504	-0.417	0.239	-0.571	0.015	0.295	0.216
Te	-0.281	-0.078	-0.019	-0.339	-0.052	-0.162	-0.268	0.349	-0.067	-0.03	-0.232	0.172	-0.209	-0.548	-0.17	-0.248	0.569	-0.105	0.627	0.319	0.281	-0.156	-0.023	0.04
Th	-0.61	0.15	-0.519	-0.124	0.077	-0.152	0.451	-0.151	-0.07	-0.224	-0.111	-0.038	-0.321	-0.041	-0.596	-0.507	0.067	-0.286	0.272	-0.188	0.672	0.404	-0.661	-0.676
Tl	-0.438	0.267	-0.398	-0.423	0.183	-0.343	-0.014	0.254	0.021	0.163	-0.434	0.589	-0.564	-0.565	-0.129	-0.09	0.83	-0.212	0.716	-0.189	0.673	-0.235	0.039	-0.192
U	0.174	0.042	-0.033	-0.161	0.259	-0.225	-0.166	0.028	-0.453	0.171	-0.3	-0.074	0.634	0.137	-0.087	0.144	-0.096	0.681	-0.11	0.47	-0.096	-0.219	-0.234	0.05
V	0.705	0.215	0.226	0.427	0.376	0.42	0.148	0.359	-0.333	0.467	-0.275	-0.396	0.505	0.53	0.251	0.48	-0.507	0.297	-0.661	0.154	-0.476	-0.208	0.689	0.438
W	0.128	0.113	-0.047	-0.343	0.203	-0.152	-0.173	0.33	-0.485	0.239	-0.411	-0.269	0.349	-0.29	0.025	0.035	0.139	0.293	-0.181	0.208	0.014	-0.464	0.406	0.166
Zn	0.579	0.174	0.343	0.057	0.261	0.291	-0.008	0.501	-0.228	0.537	-0.142	-0.168	0.336	0.007	0.453	0.525	-0.001	0.466	-0.33	0.199	-0.359	-0.173	0.753	0.507
Zr	0.843	0.039	0.585	0.347	0.213	0.45	-0.054	0.396	0.05	0.407	0.103	-0.104	0.43	0.172	0.658	0.568	-0.341	0.403	-0.569	0.21	-0.722	-0.183	0.761	0.472
Au	0.335	-0.637	0.293	-0.062	0.878	0	•	0.333	-0.42	0.87	0.577	•	0.873	0.156	0.647	0.572	-0.268	0.812	0.5	0.949	-0.243	-0.644	-0.408	-0.5
Hg	-0.234	-0.01	-0.053	0.117	0.052	0.056	0.304	0.139	0.245	-0.26	-0.108	-0.089	-0.184	0	-0.431	-0.424	-0.338	-0.168	0.449	0.473	0.34	0.23	-0.521	-0.531
Os	0.335	-0.637	0.293	-0.062	0.878	0	•	0.333	-0.42	0.87	0.577	•	0.873	0.156	0.647	0.572	-0.268	0.812	0.5	0.949	-0.243	-0.644	-0.408	-0.5
Pd	0.356	-0.981	0.845	0.179	0.845	0.408	•	0.577	-0.97	0.302	0	•	0.803	0.4	0.844	0.99	-0.268	0.781	0.5	0.609	-0.436	-0.913	0.465	-0.5
Pt	0.242	-0.953	0.777	0.057	0.816	0.295	•	0.673	-0.981	0.258	-0.077	•	0.764	0.283	0.779	0.966	-0.122	0.835	0.623	0.651	-0.322	-0.861	0.412	-0.366
Rh	0.368	-0.985	0.822	0.162	0.882	0.383	•	0.575	-0.953	0.371	0.059	•	0.841	0.391	0.857	0.987	-0.268	0.815	0.5	0.667	-0.434	-0.922	0.395	-0.5
Ru	-0.452	-0.454	0.313	-0.431	0.156	-0.189	•	0.891	-0.786	-0.465	-0.772	•	0.065	-0.31	0.108	0.521	0.803	0.578	0.988	0.256	0.315	-0.25	0.446	0.629
Depth	-0.323	-0.144	-0.04	0.045	-0.009	0.107	0.413	-0.166	0.066	-0.212	-0.002	0.119	-0.075	-0.067	-0.362	-0.156	-0.151	-0.19	0.234	-0.113	0.314	0.361	-0.361	-0.649
Thick	0.324	-0.259	0.468	-0.032	-0.017	0.057	-0.364	0.057	-0.257	0.211	-0.075	0.341	0.323	-0.149	0.303	0.552	0.434	0.406	-0.093	0.077	-0.443	-0.308	0.463	0.208

Table 20 continued

	Hf	Li	Mo	Nb	Ni	Pb	Sb	Sc	Sr	Te	Th	Tl	U	V	W	Zn	Zr	Au	Hg	Os	Pd	Pt	Rh	Ru	Depth
Li	0.274																								
Mo	0.117	-0.373																							
Nb	0.553	-0.141	0.501																						
Ni	-0.325	-0.376	0.461	0.232																					
Pb	-0.478	-0.227	0.298	0.016	0.406																				
Sb	0.722	0.213	0.277	0.527	-0.146	-0.007																			
Sc	-0.205	0.54	-0.506	-0.392	-0.444	-0.082	-0.251																		
Sr	0.465	0.254	0.272	0.593	-0.353	0.024	0.416	0.07																	
Te	0.041	-0.212	0.005	0.398	0.508	0.455	0.309	-0.402	-0.143																
Th	-0.804	0.099	-0.136	-0.624	0.244	0.237	-0.615	0.416	-0.469	-0.247															
Tl	-0.197	-0.347	0.025	0.328	0.75	0.442	0.116	-0.275	-0.115	0.632	0.138														
U	0.018	-0.262	0.525	0.261	0.03	0.618	0.274	-0.19	0.225	0.078	-0.189	-0.115													
V	0.627	-0.061	0.386	0.43	-0.123	-0.362	0.226	-0.183	0.411	-0.228	-0.616	-0.59	0.176												
W	0.416	-0.125	0.712	0.572	0.442	0.22	0.536	-0.582	0.199	0.302	-0.344	0.088	0.504	0.355											
Zn	0.828	0.049	0.459	0.781	0.094	-0.195	0.65	-0.335	0.518	0.162	-0.704	0.008	0.239	0.674	0.708										
Zr	0.897	0.188	0.239	0.667	-0.313	-0.421	0.55	-0.196	0.696	-0.051	-0.825	-0.341	0.081	0.766	0.417	0.839									
Au	0.058	•	0.82	0.943	-0.227	0.867	0.967	0.471	0.756	0.326	-0.284	0.283	0.977	0.204	0.56	0.401	0.027								
Hg	-0.479	0.011	-0.359	-0.325	0.05	0.212	-0.512	0.341	-0.235	0.23	0.506	0.038	-0.285	-0.395	-0.317	-0.476	-0.391	•							
Os	0.058	•	0.82	0.943	-0.227	0.867	0.967	0.471	0.756	0.326	-0.284	0.283	0.977	0.204	0.56	0.401	0.027	1	•						
Pd	0.704	•	0.103	0.408	-0.139	0.307	0.749	0.953	0.514	0.139	-0.615	0.283	0.508	0.7	0.506	0.835	0.585	0.577	•	0.577					
Pt	0.622	•	0.072	0.452	-0.021	0.37	0.764	0.908	0.438	0.258	-0.513	0.422	0.54	0.609	0.605	0.894	0.487	0.584	•	0.584	0.992				
Rh	0.666	•	0.18	0.479	-0.154	0.376	0.8	0.941	0.559	0.164	-0.606	0.283	0.576	0.677	0.532	0.824	0.551	0.643	•	0.643	0.997	0.99			
Ru	0.248	•	-0.572	0.063	0.63	0.107	0.242	0.441	-0.352	0.572	0.095	0.997	0.078	0.1	0.692	0.913	0.058	0	•	0	0.617	0.687	0.579		
Depth	-0.362	0.307	-0.142	-0.482	-0.02	0.052	-0.191	0.531	-0.311	-0.191	0.766	0.093	-0.246	-0.441	-0.191	-0.414	-0.503	1	0.56	1	0.577	0.584	0.643	0	
Thick	0.688	-0.053	0.27	0.574	-0.089	0.038	0.763	-0.279	0.239	0.355	-0.657	0.318	0.471	0.301	0.488	0.599	0.504	0.615	-0.495	0.615	0.97	0.935	0.972	0.416	-0.336

Table 21. Correlation coefficient matrix for 5 layers from D7-2 listed in Table 13; the zero correlation for 5 points at the 95% confidence level is |0.883|

	Fe	Mn	Fe/Mn	Si	Na	Al	K	Mg	Ca	Ti	P	S	As	B	Ba	Be	Bi	Br	Cd	Cl	Co	Cr	Cu	Ga
Mn	0.596																							
Fe/Mn	0.274	-0.604																						
Si	0.638	0.603	-0.149																					
Na	0.126	0.376	-0.234	-0.444																				
Al	0.885	0.698	0	0.909	-0.189																			
K	0.353	0.941	-0.774	0.58	0.307	0.542																		
Mg	0.635	0.764	-0.223	0.169	0.799	0.423	0.642																	
Ca	-0.778	-0.936	0.35	-0.765	-0.235	-0.852	-0.858	-0.754																
Ti	0.682	0.919	-0.387	0.401	0.639	0.599	0.814	0.955	-0.896															
P	-0.757	-0.948	0.386	-0.759	-0.242	-0.841	-0.876	-0.752	0.999	-0.899														
S	-0.968	-0.738	-0.074	-0.74	-0.149	-0.922	-0.557	-0.702	0.904	-0.785	0.889													
As	0.969	0.45	0.433	0.555	0.137	0.792	0.224	0.611	-0.687	0.604	-0.659	-0.926												
B	0.847	0.709	-0.038	0.931	-0.149	0.964	0.617	0.476	-0.897	0.637	-0.885	-0.929	0.795											
Ba	0.162	0.395	-0.226	-0.434	0.996	-0.155	0.302	0.803	-0.246	0.65	-0.253	-0.172	0.157	-0.138										
Be	0.529	0.051	0.53	-0.309	0.655	0.077	-0.2	0.615	-0.125	0.404	-0.105	-0.39	0.609	0.038	0.678									
Bi	-0.151	0.683	-0.985	0.265	0.178	0.143	0.811	0.242	-0.438	0.437	-0.473	-0.038	-0.337	0.15	0.183	-0.52								
Br	0.708	0.866	-0.297	0.291	0.685	0.569	0.694	0.946	-0.814	0.969	-0.818	-0.758	0.613	0.548	0.715	0.534	0.365							
Cd	0.503	0.97	-0.662	0.655	0.299	0.659	0.986	0.702	-0.931	0.869	-0.944	-0.687	0.381	0.725	0.299	-0.097	0.717	0.758						
Cl	0.735	0.951	-0.416	0.585	0.348	0.777	0.794	0.75	-0.9	0.892	-0.908	-0.807	0.573	0.718	0.392	0.218	0.531	0.908	0.855					
Co	0.651	0.869	-0.418	0.891	-0.02	0.853	0.866	0.537	-0.952	0.736	-0.953	-0.811	0.557	0.92	-0.02	-0.162	0.502	0.607	0.92	0.787				
Cr	0.501	0.555	-0.244	0.972	-0.554	0.843	0.549	0.011	-0.663	0.279	-0.663	-0.6	0.381	0.83	-0.535	-0.469	0.366	0.185	0.6	0.543	0.823			
Cu	0.176	0.052	0.187	-0.611	0.843	-0.242	-0.145	0.568	0.055	0.357	0.057	-0.061	0.197	-0.311	0.87	0.866	-0.208	0.517	-0.115	0.181	-0.356	-0.693		
Ga	0.745	0.854	-0.257	0.616	0.406	0.717	0.8	0.857	-0.951	0.922	-0.945	-0.874	0.719	0.82	0.397	0.281	0.303	0.819	0.874	0.784	0.867	0.458	0.078	
Ge	-0.175	0.491	-0.721	-0.345	0.732	-0.215	0.49	0.491	-0.174	0.491	-0.205	0.102	-0.311	-0.261	0.752	0.109	0.699	0.55	0.408	0.443	0.029	-0.292	0.532	0.159
Hf	0.623	0.638	-0.093	-0.016	0.798	0.352	0.409	0.892	-0.563	0.828	-0.563	-0.596	0.556	0.288	0.838	0.755	0.147	0.932	0.477	0.746	0.287	-0.12	0.782	0.602
Li	-0.956	-0.338	-0.539	-0.549	0	-0.791	-0.086	-0.468	0.585	-0.468	0.556	0.875	-0.98	-0.755	-0.031	-0.584	0.428	-0.506	-0.25	-0.505	-0.469	-0.4	-0.157	-0.583
Mo	0.288	0.313	0.008	-0.3	0.912	-0.07	0.254	0.834	-0.315	0.644	-0.308	-0.315	0.378	0.04	0.887	0.74	-0.075	0.636	0.285	0.265	0.078	-0.485	0.737	0.555
Nb	0.777	0.635	0.068	0.17	0.717	0.491	0.436	0.952	-0.693	0.875	-0.682	-0.776	0.779	0.51	0.733	0.786	-0.026	0.908	0.536	0.701	0.449	-0.008	0.635	0.797
Ni	-0.068	0.736	-0.925	0.051	0.56	0.051	0.818	0.539	-0.476	0.638	-0.508	-0.103	-0.218	0.077	0.562	-0.169	0.914	0.593	0.736	0.594	0.427	0.088	0.164	0.435
Pb	0.419	0.894	-0.684	0.792	0	0.702	0.947	0.452	-0.869	0.685	-0.883	-0.612	0.276	0.754	0.002	-0.361	0.756	0.557	0.95	0.774	0.944	0.787	-0.394	0.744
Sb	0.54	0.075	0.517	-0.288	0.67	0.089	-0.167	0.645	-0.157	0.433	-0.136	-0.413	0.627	0.066	0.688	0.998	-0.511	0.549	-0.063	0.226	-0.128	-0.458	0.853	0.325
Sc	0.003	-0.696	0.788	-0.103	-0.618	-0.053	-0.839	-0.659	0.557	-0.701	0.577	0.208	0.053	-0.198	-0.582	0.083	-0.732	-0.57	-0.776	-0.474	-0.519	-0.046	-0.106	-0.638
Sr	-0.094	-0.041	0.047	-0.758	0.902	-0.489	-0.125	0.509	0.177	0.272	0.174	0.157	-0.036	-0.486	0.901	0.723	-0.126	0.377	-0.141	-0.01	-0.44	-0.841	0.935	0.017
Te	0.684	0.867	-0.34	0.306	0.595	0.592	0.67	0.849	-0.774	0.908	-0.782	-0.715	0.544	0.517	0.642	0.458	0.433	0.974	0.729	0.946	0.578	0.247	0.488	0.714
Th	0.463	0.621	-0.344	0.971	-0.447	0.803	0.671	0.116	-0.734	0.371	-0.735	-0.611	0.368	0.852	-0.448	-0.489	0.437	0.227	0.709	0.54	0.899	0.969	-0.708	0.581
Tl	0.561	0.842	-0.398	0.171	0.798	0.41	0.731	0.976	-0.763	0.97	-0.77	-0.644	0.489	0.436	0.811	0.501	0.426	0.971	0.768	0.822	0.559	0.056	0.543	0.818
U	0.844	0.403	0.372	0.179	0.382	0.572	0.076	0.624	-0.473	0.576	-0.457	-0.72	0.802	0.446	0.442	0.803	-0.261	0.722	0.211	0.633	0.233	0.075	0.612	0.454
V	0.903	0.6	0.199	0.612	0.242	0.774	0.462	0.735	-0.821	0.744	-0.798	-0.941	0.94	0.853	0.239	0.489	-0.136	0.68	0.593	0.621	0.719	0.417	0.112	0.893
W	0.707	0.441	0.244	0.058	0.707	0.359	0.266	0.886	-0.554	0.749	-0.536	-0.689	0.776	0.418	0.706	0.851	-0.234	0.766	0.37	0.491	0.313	-0.153	0.647	0.727
Zn	-0.007	0.395	-0.399	-0.483	0.973	-0.256	0.349	0.717	-0.182	0.591	-0.198	-0.029	-0.039	-0.243	0.975	0.512	0.345	0.648	0.311	0.358	-0.053	-0.541	0.802	0.306
Zr	0.924	0.684	0.121	0.388	0.475	0.719	0.426	0.838	-0.763	0.834	-0.75	-0.894	0.875	0.67	0.516	0.698	-0.022	0.897	0.551	0.818	0.55	0.249	0.49	0.767
Hg	0.025	0.802	-0.932	0.38	0.299	0.264	0.943	0.468	-0.639	0.635	-0.666	-0.25	-0.109	0.348	0.283	-0.39	0.931	0.506	0.875	0.603	0.685	0.4	-0.193	0.583

	Ge	Hf	Li	Mo	Nb	Ni	Pb	Sb	Sc	Sr	Te	Th	Tl	U	V	W	Zn	Zr
Hf	0.584																	
Li	0.408	-0.477																
Mo	0.409	0.715	-0.23															
Nb	0.297	0.913	-0.677	0.805														
Ni	0.882	0.451	0.353	0.318	0.279													
Pb	0.254	0.227	-0.182	-0.019	0.286	0.645												
Sb	0.104	0.756	-0.592	0.772	0.807	-0.154	-0.332											
Sc	-0.664	-0.385	-0.24	-0.557	-0.401	-0.878	-0.641	0.042										
Sr	0.593	0.624	0.115	0.804	0.5	0.259	-0.427	0.721	-0.283									
Te	0.595	0.915	-0.468	0.475	0.817	0.609	0.566	0.461	-0.477	0.304								
Th	-0.245	-0.118	-0.342	-0.34	0.048	0.195	0.867	-0.464	-0.245	-0.786	0.242							
Tl	0.641	0.901	-0.347	0.749	0.886	0.692	0.54	0.525	-0.725	0.485	0.911	0.148						
U	0.091	0.823	-0.819	0.405	0.805	-0.064	0.049	0.791	0.145	0.315	0.741	-0.024	0.576					
V	-0.204	0.541	-0.86	0.503	0.813	-0.001	0.471	0.525	-0.253	-0.03	0.565	0.485	0.619	0.633				
W	0.142	0.807	-0.672	0.873	0.962	0.101	0.104	0.878	-0.323	0.556	0.631	-0.075	0.77	0.732	0.812			
Zn	0.867	0.755	0.168	0.797	0.594	0.687	0.042	0.52	-0.654	0.874	0.598	-0.449	0.766	0.286	0.069	0.542		
Zr	0.175	0.874	-0.825	0.541	0.934	0.182	0.375	0.707	-0.2	0.251	0.869	0.232	0.794	0.919	0.833	0.842	0.369	
Hg	0.612	0.238	0.25	0.17	0.198	0.912	0.859	-0.36	-0.896	-0.083	0.495	0.538	0.595	-0.199	0.163	0.034	0.396	0.139

Table 22. Correlation coefficient matrix for 5 layers from D8-1 from Table 13; the zero correlation for 5 points at the 95% confidence level is |0.883|

	Fe	Mn	Fe/Mn	Si	Na	Al	K	Mg	Ca	Ti	P	S	As	B	Ba	Be	Bi	Br	Cd	Cl	Co	Cr	Cu	Ga
Mn	-0.638																							
Fe/Mn	0.932	-0.867																						
Si	0.552	0.239	0.242																					
Na	-0.38	0.842	-0.602	0.267																				
Al	0.594	0.073	0.344	0.6	0.423																			
K	-0.644	0.993	-0.877	0.234	0.784	0.049																		
Mg	-0.757	0.897	-0.877	0.085	0.686	-0.294	0.875																	
Ca	-0.771	0.433	-0.71	-0.675	0.366	-0.176	0.45	0.321																
Ti	0.292	0.251	0.124	0.721	0.416	0.277	0.177	0.354	-0.655															
P	-0.68	0.366	-0.63	-0.651	0.308	-0.094	0.393	0.205	0.989	-0.725														
S	-0.327	0.346	-0.416	-0.269	0.31	0.31	0.395	0	0.793	-0.671	0.865													
As	0.905	-0.733	0.907	0.463	-0.667	0.223	-0.715	-0.717	-0.87	0.224	-0.796	-0.524												
B	0.741	-0.328	0.627	0.762	-0.356	0.195	-0.323	-0.269	-0.973	0.602	-0.949	-0.686	0.86											
Ba	-0.168	-0.228	0.04	-0.662	0.164	0.024	-0.299	-0.182	0.457	-0.228	0.434	0.159	-0.373	-0.643										
Be	0.645	-0.892	0.849	-0.216	-0.512	0.162	-0.933	-0.821	-0.366	-0.05	-0.32	-0.333	0.575	0.195	0.541									
Bi	-0.867	0.817	-0.935	-0.331	0.699	-0.118	0.816	0.723	0.868	-0.247	0.813	0.638	-0.974	-0.809	0.21	-0.699								
Br	0.518	-0.622	0.676	-0.072	-0.166	0.176	-0.709	-0.473	-0.432	0.352	-0.446	-0.551	0.401	0.219	0.605	0.878	-0.565							
Cd	-0.944	0.431	-0.82	-0.693	0.105	-0.681	0.468	0.535	0.807	-0.567	0.749	0.423	-0.788	-0.756	0.133	-0.551	0.763	-0.585						
Cl	0.611	-0.912	0.824	-0.304	-0.565	0.163	-0.936	-0.889	-0.244	-0.235	-0.178	-0.168	0.54	0.095	0.547	0.98	-0.644	0.775	-0.466					
Co	-0.195	0.573	-0.392	0.596	0.222	-0.206	0.593	0.67	-0.343	0.546	-0.408	-0.353	-0.005	0.469	-0.81	-0.727	0.093	-0.514	0.062	-0.814				
Cr	0.626	-0.825	0.752	0.066	-0.942	-0.185	-0.772	-0.729	-0.617	-0.182	-0.545	-0.407	0.869	0.628	-0.351	0.513	-0.862	0.201	-0.39	0.538	-0.082			
Cu	-0.091	-0.499	0.19	-0.817	-0.215	-0.128	-0.531	-0.448	0.451	-0.54	0.465	0.217	-0.192	-0.61	0.909	0.65	0.044	0.52	0.196	0.713	-0.924	-0.015		
Ga	-0.1	-0.427	0.075	-0.627	-0.605	-0.269	-0.343	-0.514	0.452	-0.97	0.539	0.542	0.014	-0.395	0.11	0.164	0.017	-0.29	0.413	0.344	-0.524	0.412	0.481	
Ge	0.226	0.191	0	0.297	0.196	0.686	0.25	-0.25	0.257	-0.354	0.376	0.791	0.004	-0.108	-0.235	-0.225	0.186	-0.473	-0.134	-0.093	-0.154	-0.086	-0.166	0.343
Hf	0.358	-0.831	0.647	-0.326	-0.68	-0.39	-0.866	-0.516	-0.464	0.052	-0.484	-0.699	0.525	0.294	0.342	0.804	-0.698	0.767	-0.276	0.738	-0.357	0.613	0.477	0.076
Li	0.264	-0.749	0.555	-0.336	-0.62	-0.465	-0.791	-0.395	-0.447	0.112	-0.486	-0.75	0.45	0.273	0.338	0.732	-0.634	0.747	-0.211	0.651	-0.277	0.542	0.44	0
Mo	-0.174	-0.494	0.09	-0.859	-0.476	-0.285	-0.459	-0.509	0.562	-0.907	0.617	0.462	-0.145	-0.609	0.555	0.406	0.082	0.063	0.422	0.553	-0.797	0.218	0.831	0.883
Nb	0.458	-0.309	0.504	0.286	0.046	0.146	-0.406	-0.101	-0.657	0.765	-0.714	-0.802	0.393	0.48	0.269	0.559	-0.53	0.86	-0.642	0.385	-0.015	0.081	0.062	-0.702
Ni	-0.864	0.692	-0.887	-0.471	0.549	-0.172	0.708	0.584	0.947	-0.454	0.913	0.738	-0.948	-0.883	0.249	-0.629	0.975	-0.596	0.831	-0.536	-0.042	-0.752	0.167	0.236
Pb	-0.29	0.811	-0.57	0.622	0.517	0.042	0.83	0.759	-0.089	0.472	-0.138	-0.013	-0.238	0.243	-0.725	-0.879	0.369	-0.658	0.125	-0.932	0.919	-0.371	-0.907	-0.516
Sb	0.658	-0.945	0.879	-0.195	-0.64	0.04	-0.977	-0.822	-0.466	-0.036	-0.423	-0.447	0.666	0.306	0.418	0.982	-0.79	0.843	-0.543	0.956	-0.623	0.644	0.568	0.181
Sc	0.872	-0.813	0.919	0.12	-0.522	0.506	-0.806	-0.967	-0.421	-0.16	-0.303	-0.025	0.753	0.366	0.155	0.812	-0.743	0.533	-0.711	0.854	-0.614	0.636	0.341	0.318
Sr	-0.558	0.886	-0.753	0.074	0.954	0.314	0.853	0.698	0.609	0.138	0.563	0.54	-0.818	-0.567	0.179	-0.621	0.868	-0.368	0.346	-0.62	0.151	-0.967	-0.129	-0.354
Te	0.682	-0.558	0.739	0.382	-0.329	0.076	-0.616	-0.347	-0.889	0.656	-0.91	-0.892	0.736	0.76	-0.025	0.627	-0.833	0.772	-0.755	0.479	0.061	0.495	-0.075	-0.496
Th	0.034	0.732	-0.328	0.806	0.653	0.542	0.74	0.489	-0.123	0.495	-0.119	0.193	-0.112	0.269	-0.596	-0.676	0.281	-0.499	-0.209	-0.711	0.654	-0.417	-0.817	-0.533
Tl	-0.845	0.339	-0.659	-0.707	0.317	-0.601	0.294	0.576	0.634	-0.141	0.52	0.038	-0.8	-0.732	0.576	-0.196	0.652	0.018	0.746	-0.218	-0.103	-0.588	0.443	-0.043
U	-0.235	0.456	-0.349	0.461	0.127	-0.39	0.46	0.671	-0.395	0.591	-0.486	-0.55	0.009	0.471	-0.687	-0.598	0.019	-0.341	0.093	-0.713	0.96	-0.03	-0.802	-0.563
V	0.738	-0.944	0.899	0.023	-0.882	-0.068	-0.925	-0.832	-0.661	-0.078	-0.595	-0.494	0.896	0.601	-0.086	0.76	-0.94	0.508	-0.544	0.756	-0.287	0.944	0.188	0.299
W	0.022	-0.619	0.254	-0.499	-0.909	-0.584	-0.538	-0.497	0.016	-0.702	0.068	0	0.332	0.021	-0.146	0.239	-0.343	-0.156	0.288	0.349	-0.219	0.752	0.265	0.823
Zn	0.168	-0.711	0.459	-0.678	-0.382	-0.085	-0.749	-0.621	0.16	-0.396	0.182	-0.018	0.095	-0.341	0.839	0.845	-0.255	0.71	-0.055	0.877	-0.91	0.212	0.953	0.402
Zr	0.527	-0.812	0.749	-0.287	-0.397	0.111	-0.87	-0.7	-0.293	0.009	-0.271	-0.363	0.44	0.095	0.661	0.981	-0.595	0.934	-0.479	0.942	-0.734	0.37	0.712	0.07
Hg	0.574	-0.498	0.537	0.295	-0.721	0.08	-0.408	-0.612	-0.446	-0.289	-0.335	0	0.744	0.571	-0.636	0.138	-0.616	-0.244	-0.327	0.22	0.081	0.84	-0.302	0.49

	Ge	Hf	Li	Mo	Nb	Ni	Pb	Sb	Sc	Sr	Te	Th	Tl	U	V	W	Zn	Zr
Hf	-0.7																	
Li	-0.791	0.991																
Mo	0.1	0.286	0.227															
Nb	-0.609	0.613	0.642	-0.43														
Ni	0.249	-0.651	-0.605	0.283	-0.658													
Pb	0.143	-0.686	-0.616	-0.782	-0.194	0.229												
Sb	-0.308	0.879	0.813	0.375	0.562	-0.716	-0.839											
Sc	0.322	0.428	0.306	0.32	0.224	-0.646	-0.662	0.791										
Sr	0.31	-0.789	-0.736	-0.264	-0.235	0.766	0.486	-0.752	-0.588									
Te	-0.537	0.731	0.729	-0.385	0.898	-0.914	-0.216	0.693	0.429	-0.595								
Th	0.502	-0.804	-0.785	-0.773	-0.137	0.143	0.861	-0.707	-0.306	0.586	-0.191							
Ti	-0.564	0.074	0.171	0.263	-0.007	0.634	-0.088	-0.231	-0.678	0.403	-0.316	-0.373						
U	-0.423	-0.121	-0.024	-0.751	0.151	-0.119	0.797	-0.475	-0.644	0.031	0.211	0.45	0.054					
V	-0.185	0.777	0.702	0.246	0.332	-0.846	-0.574	0.855	0.772	-0.964	0.666	-0.536	-0.529	-0.194				
W	-0.083	0.439	0.393	0.66	-0.412	-0.156	-0.434	0.355	0.273	-0.745	-0.077	-0.646	-0.097	-0.156	0.613			
Zn	-0.256	0.684	0.636	0.743	0.273	-0.14	-0.979	0.79	0.532	-0.364	0.211	-0.867	0.26	-0.761	0.446	0.311		
Zr	-0.34	0.817	0.765	0.388	0.633	-0.545	-0.876	0.949	0.695	-0.516	0.623	-0.703	-0.025	-0.575	0.648	0.137	0.883	
Hg	0.408	0.09	0	0.113	-0.318	-0.504	-0.045	0.241	0.559	-0.676	0.119	0.01	-0.81	-0.02	0.67	0.642	-0.158	-0.054

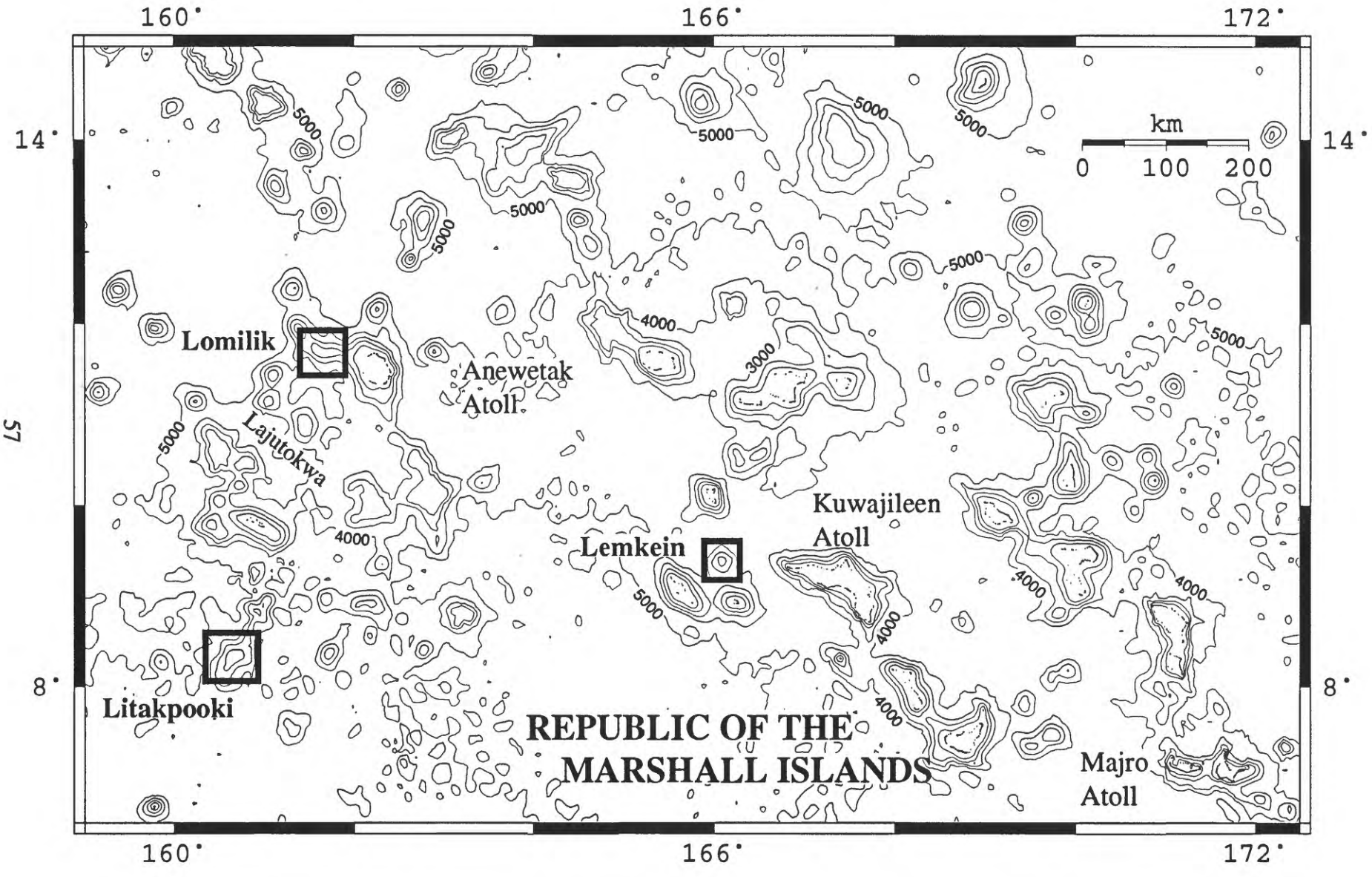

Figure 1. Atolls and Seamounts comprising the Marshall Islands. The three boxed areas enclose Lemkein Seamount, Lomilik Seamount, and Litakpooki Ridge, which were studied during cruise KODOS 97-4

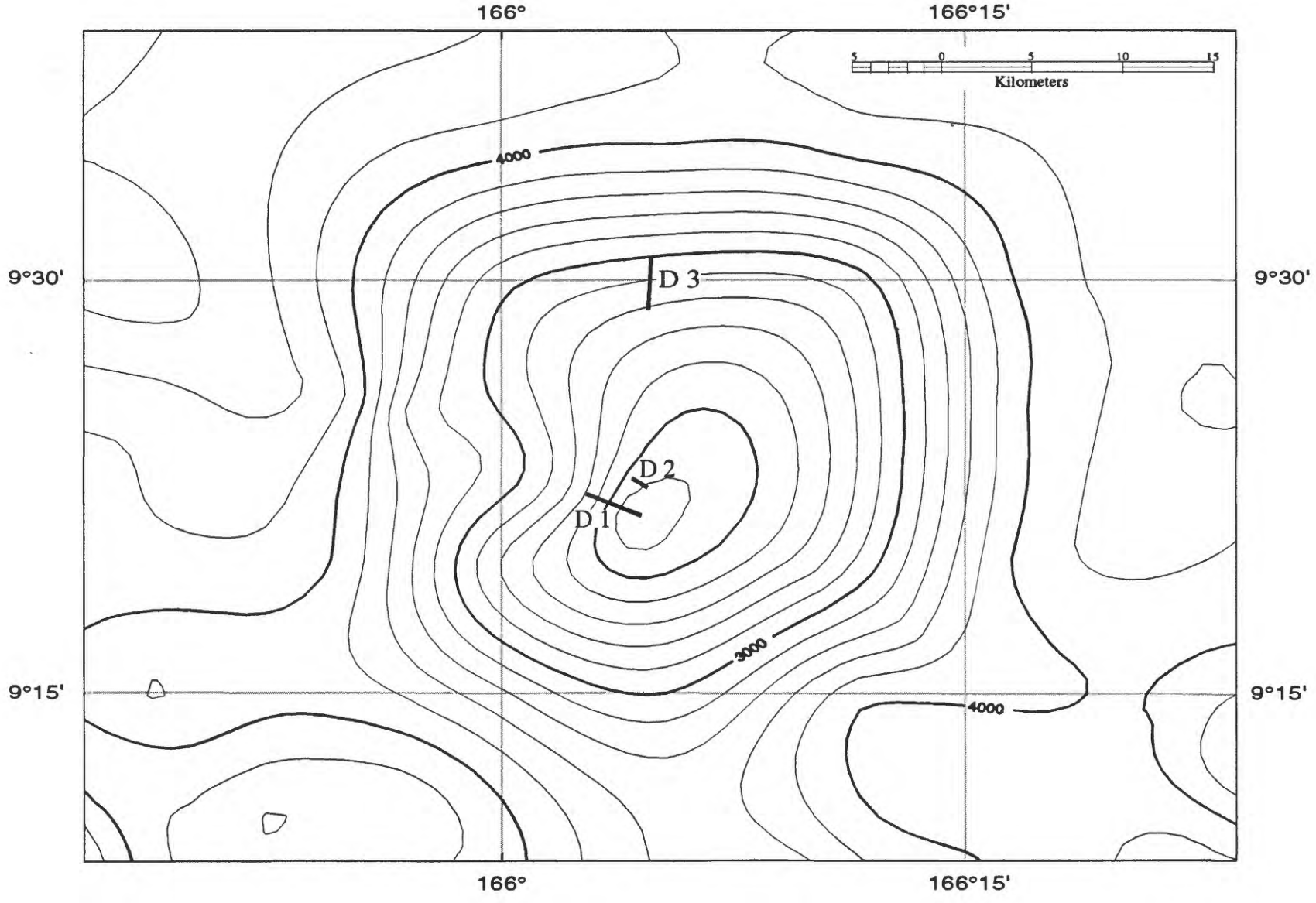

Figure 2. Bathymetry and dredge (D) locations for Lemkein Seamount, located west of Kuwajleen Atoll within the Marshall Islands group; bathymetry is modified from Chase and Menard (1973); contour interval is 200 m

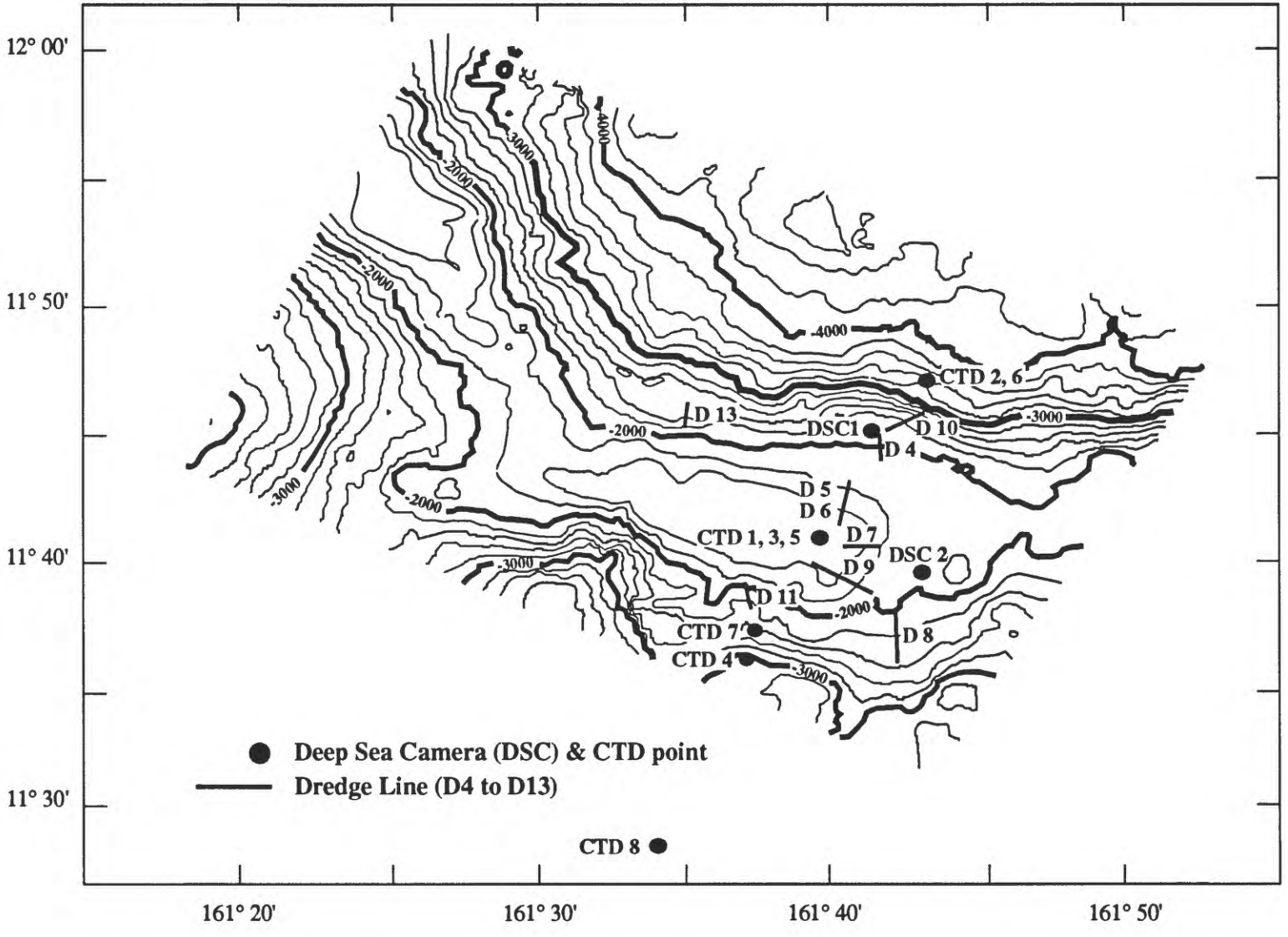

Figure 3. Bathymetry, dredge (D), camera (DSC), and CTD locations for Lomilik Seamount, located west of Anewetak Atoll; contour interval is 200 m

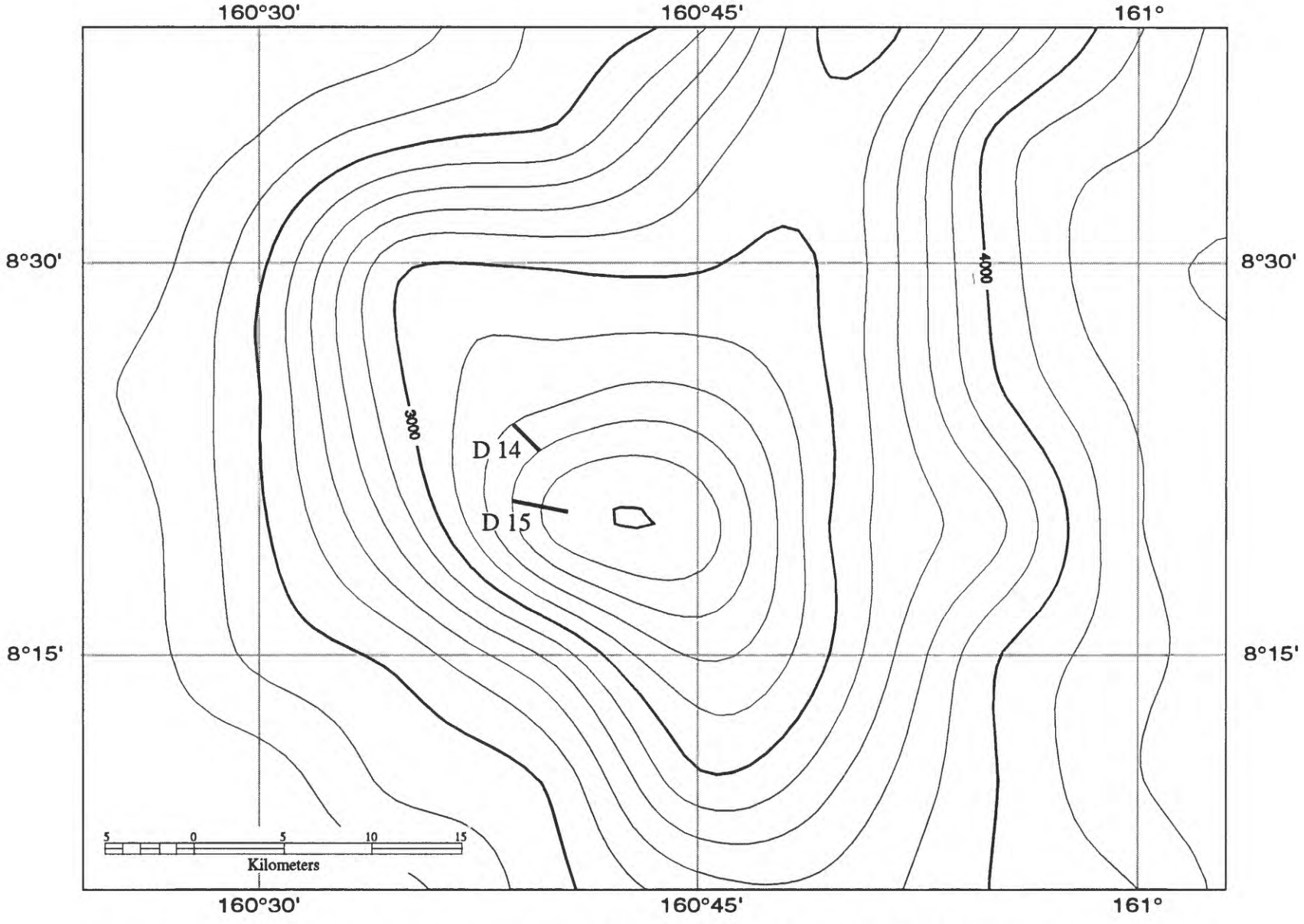

Figure 4. Bathymetry and dredge (D) locations for Litakpooki Ridge, located south of Ujlan Atoll in the Marshall Islands group; bathymetry is modified from Chase and Menard (1973); contour interval is 200 m

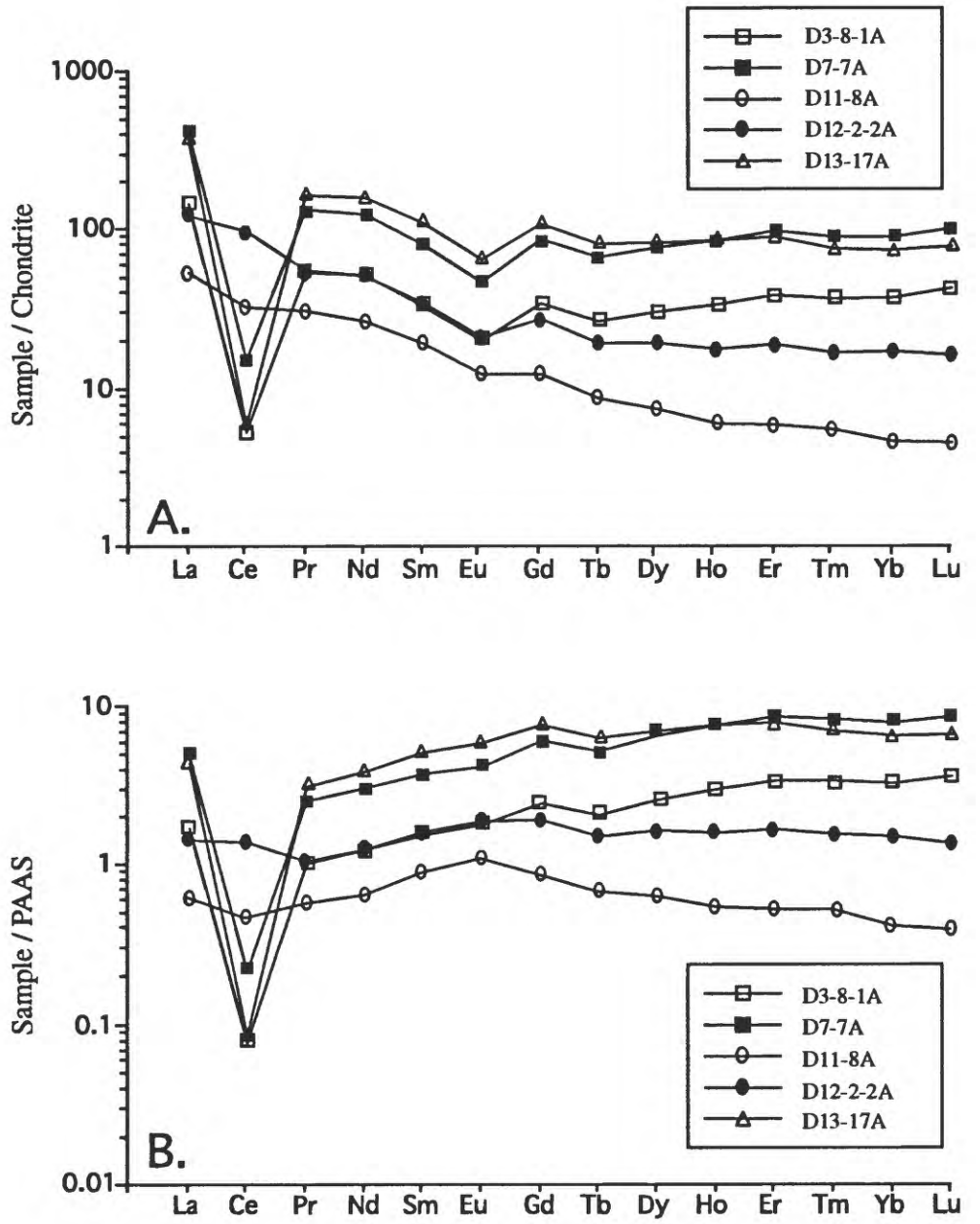

Figure 5. REE plots of substrate samples from dredges D3, D7, D11, D12, and D13, Lemkein and Lomilik Seamounts: (A) Chondrite (Anders and Grevesse, 1989) normalized, and (B) Post Archean Australian Shale (PAAS, McLennan, 1989) normalized

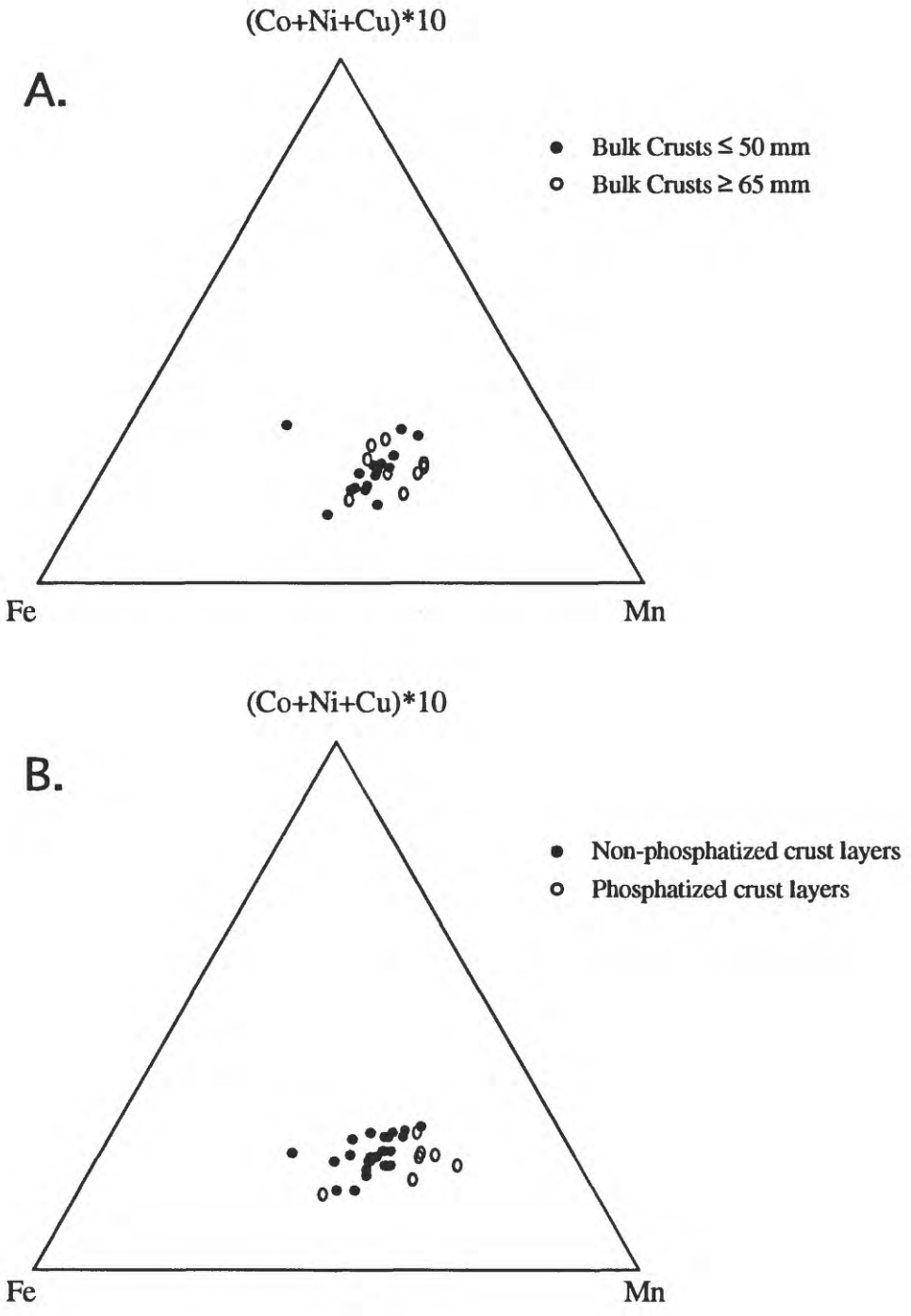

Figure 6. Mn-Fe-(Co+Ni+Cu)*10 ternary diagram after Bonatti et al. (1972) for: (A) bulk crusts, and (B) crust layers

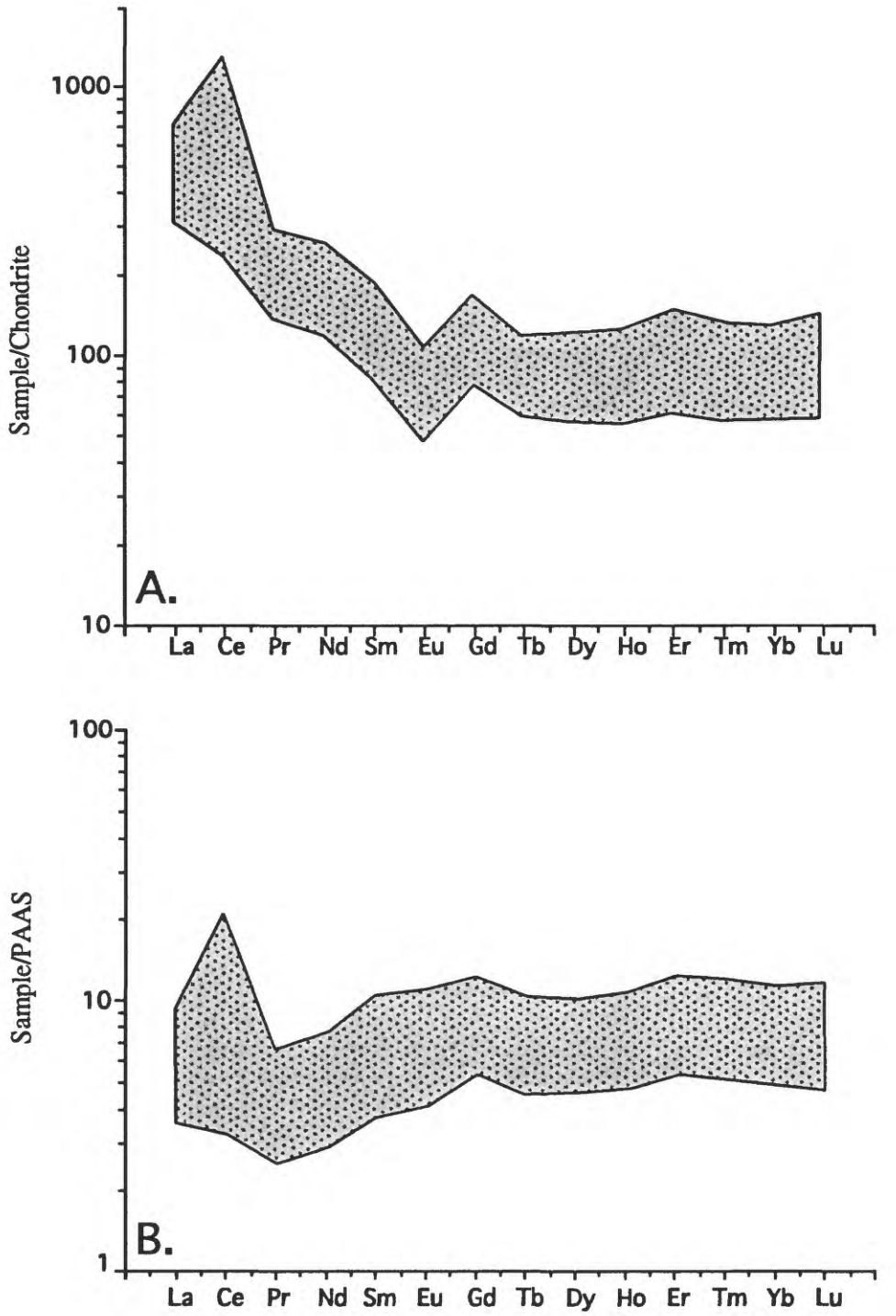

Figure 7. Range of REE plots for 40 Fe-Mn samples: (A) Chondrite (Anders and Grevesse, 1989) normalized, and (B) Post Archean Australian Shale (PAAS, McLennan, 1989) normalized

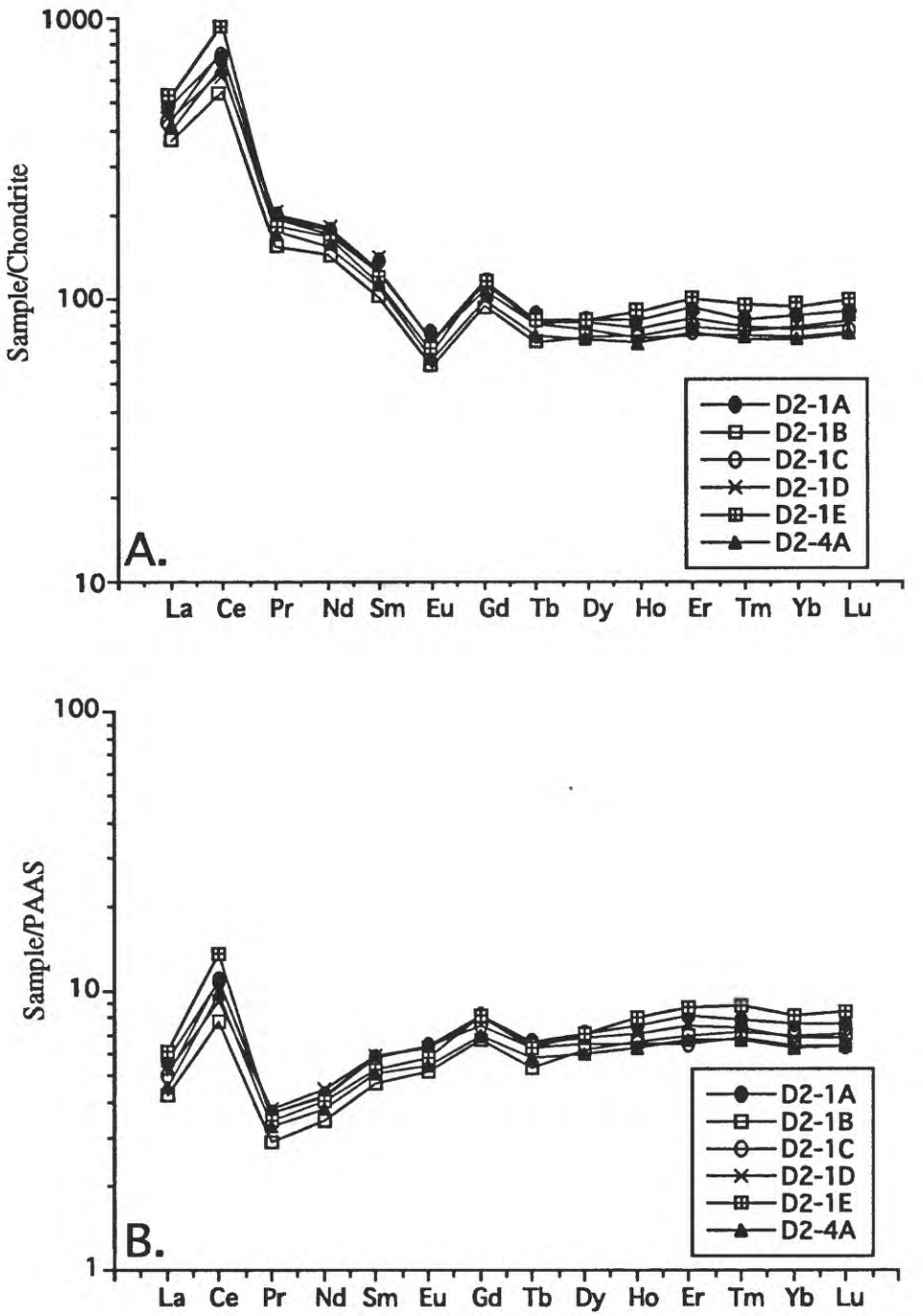

Figure 8. REE plots of bulk crusts and layers from dredge D2, Lemkein Seamount: (A) Chondrite normalized, and (B) PAAS normalized

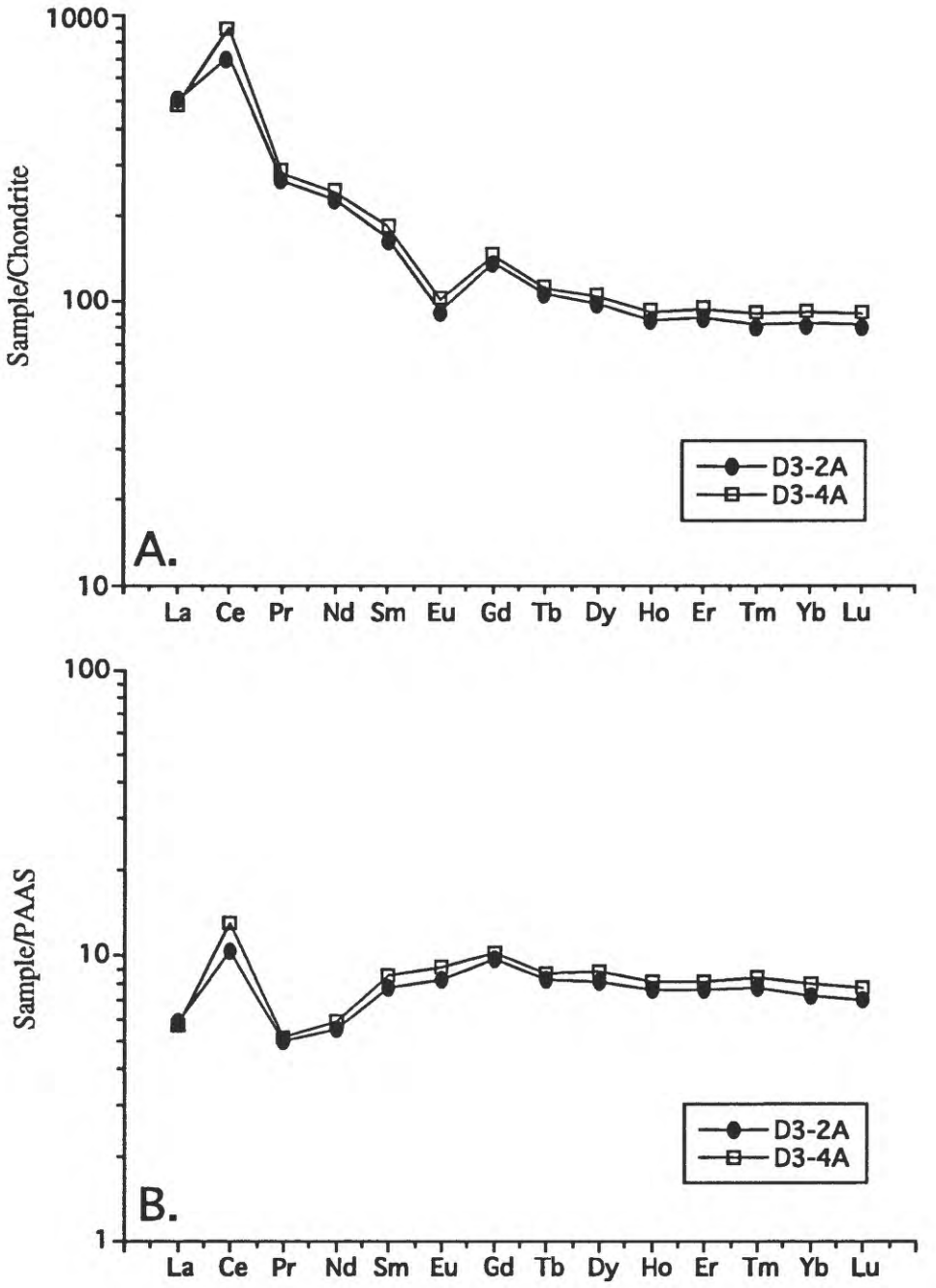

Figure 9. REE plots of bulk crusts from dredge D3, Lemkein Seamount: (A) Chondrite normalized, and (B) PAAS normalized

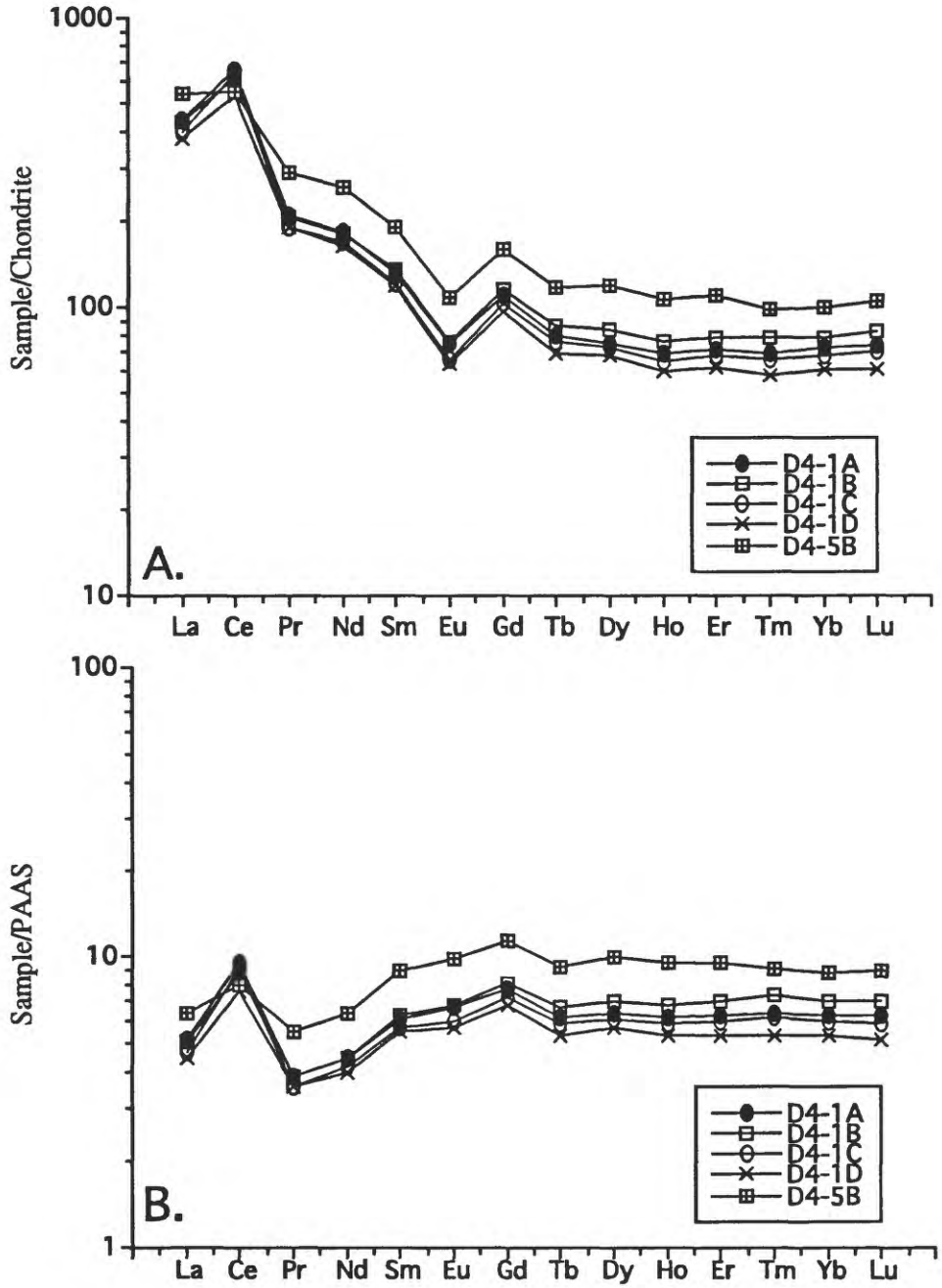

Figure 10. REE plots of bulk crusts and layers from dredge D4, Lomilik Seamount: (A) Chondrite normalized, and (B) PAAS normalized

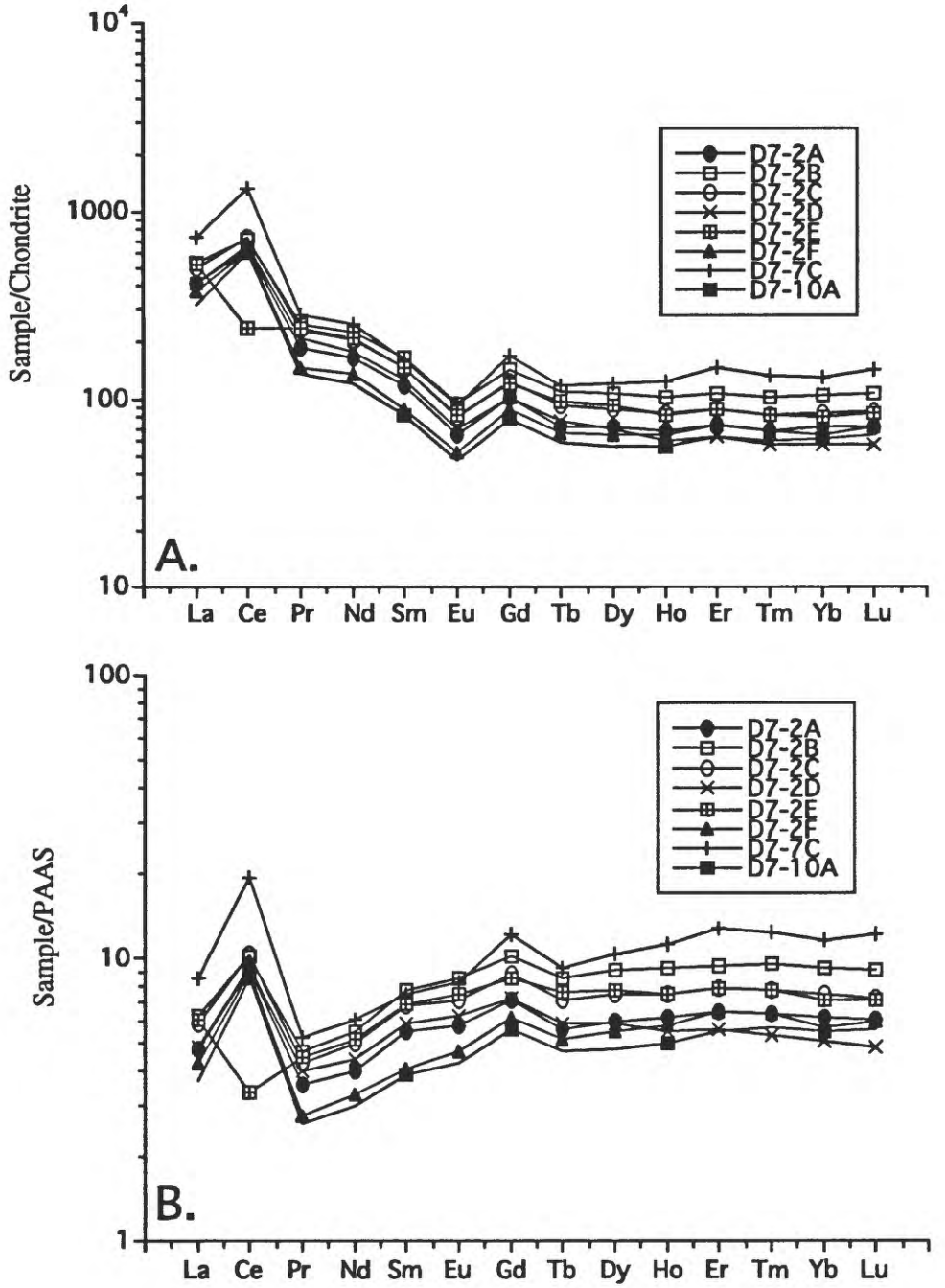

Figure 11. REE plots of bulk crusts and layers from dredge D7, Lomilik Seamount; sample D7-7C is a cement from breccia: (A) Chondrite normalized, and (B) PAAS normalized

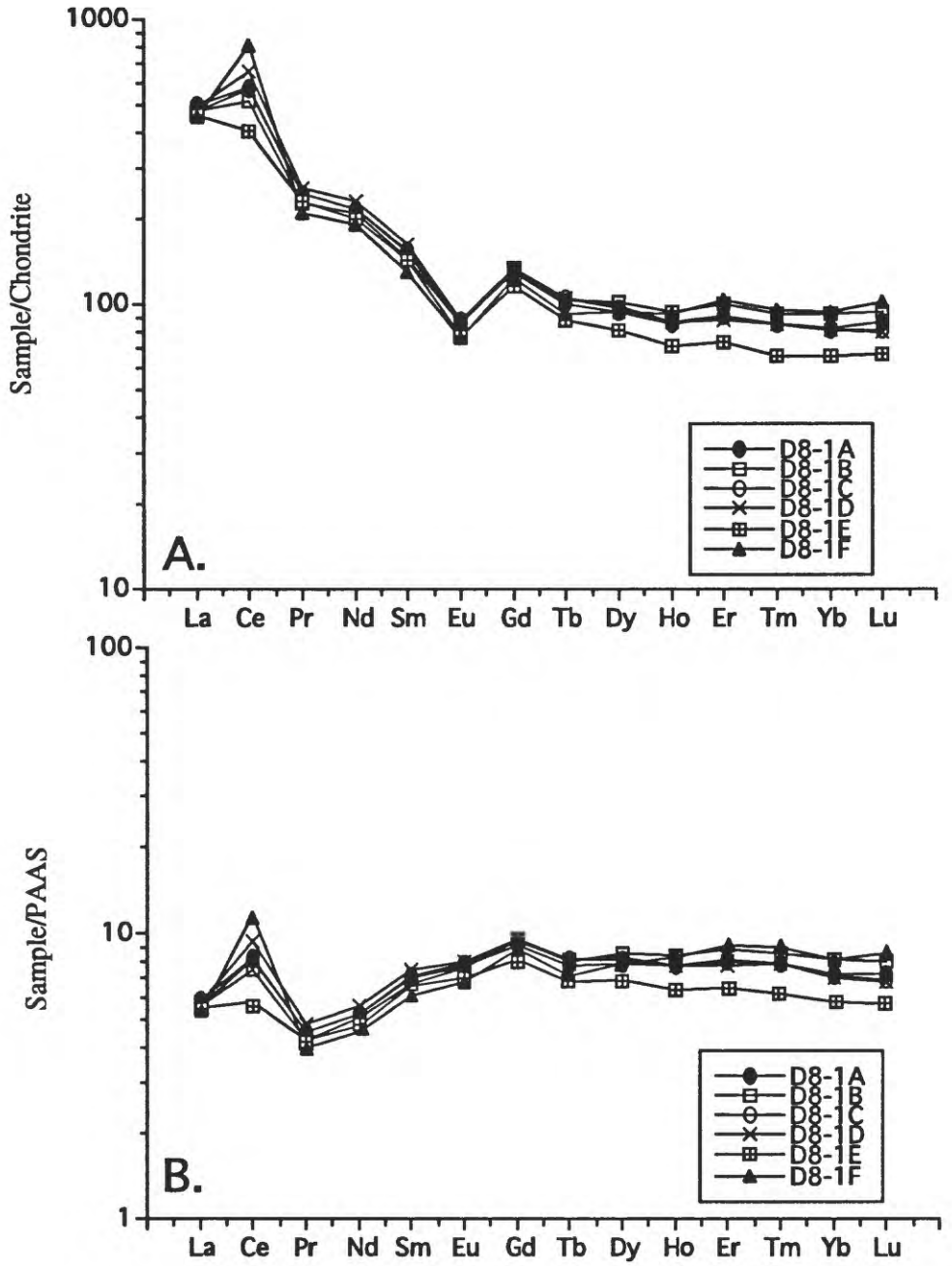

Figure 12. REE plots of bulk crust and layers from dredge D8, Lomilik Seamount: (A) Chondrite normalized, and (B) PAAS normalized

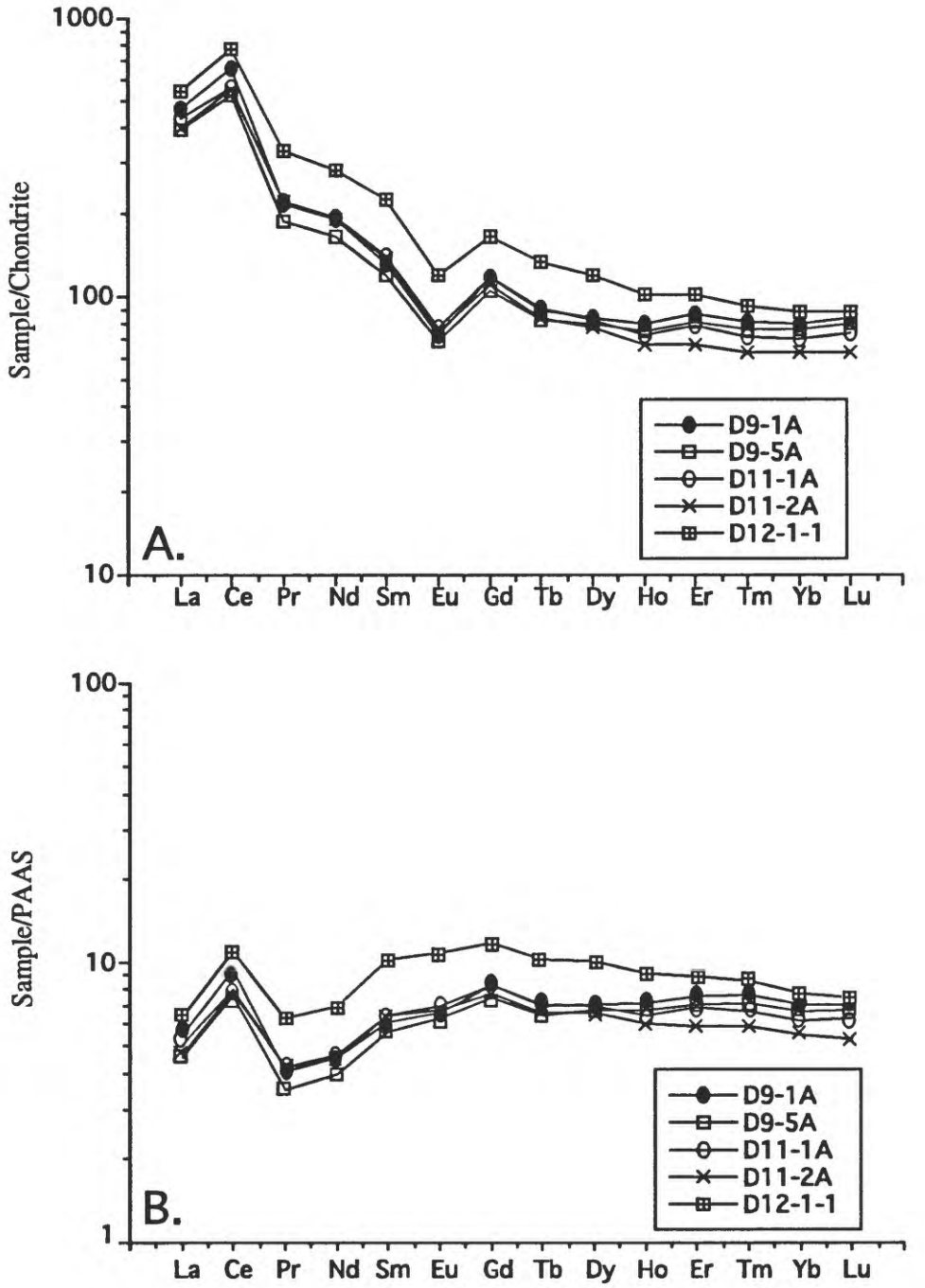

Figure 13. REE plots of bulk crusts from dredges D9, D11, and D12, Lomilik Seamount: (A) Chondrite normalized, and (B) PAAS normalized

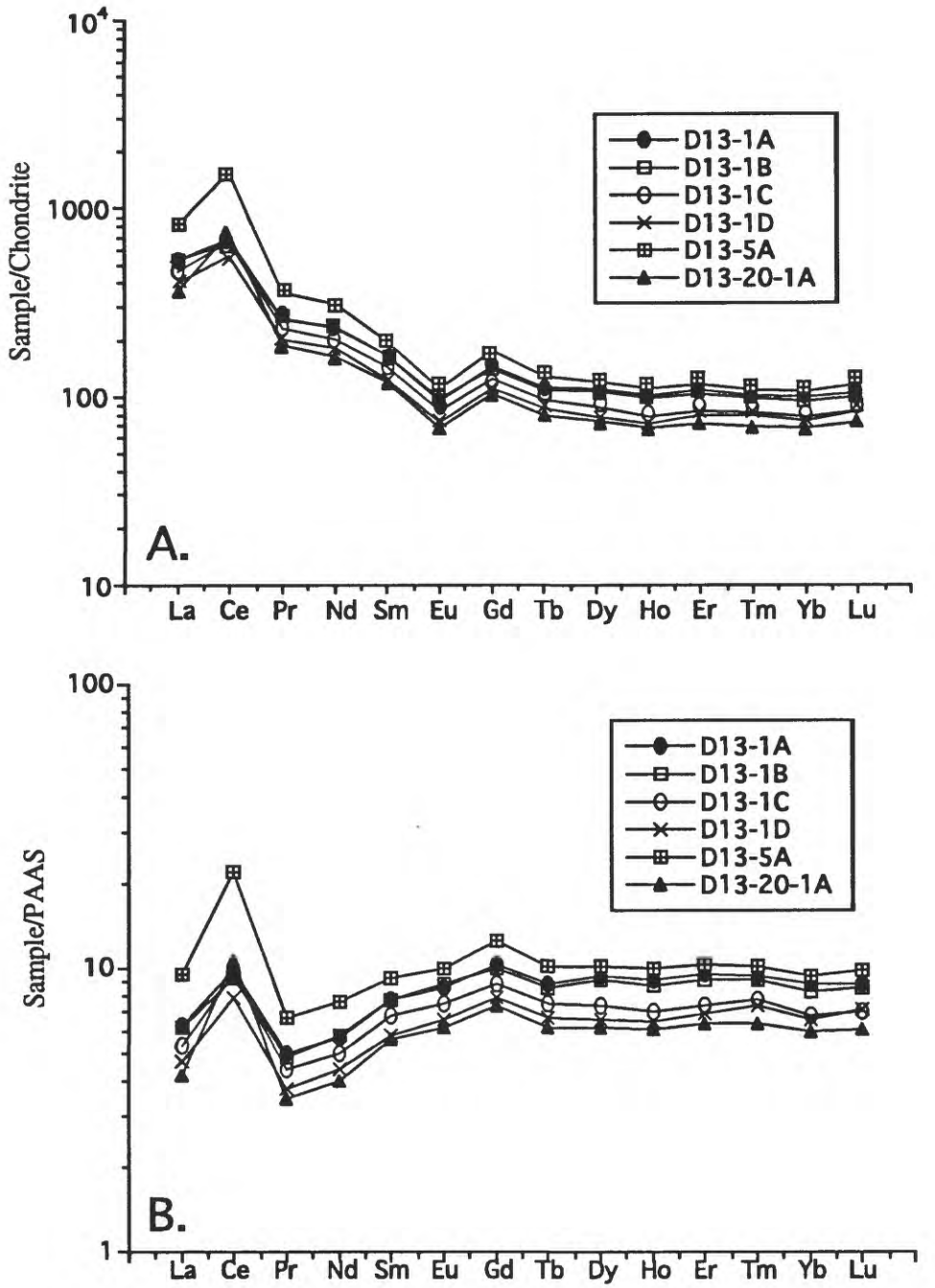

Figure 14. REE plots of bulk crusts and layers from dredge D13, Lomilik Seamount; sample D13-5A is a clast from breccia: (A) Chondrite normalized, and (B) PAAS normalized

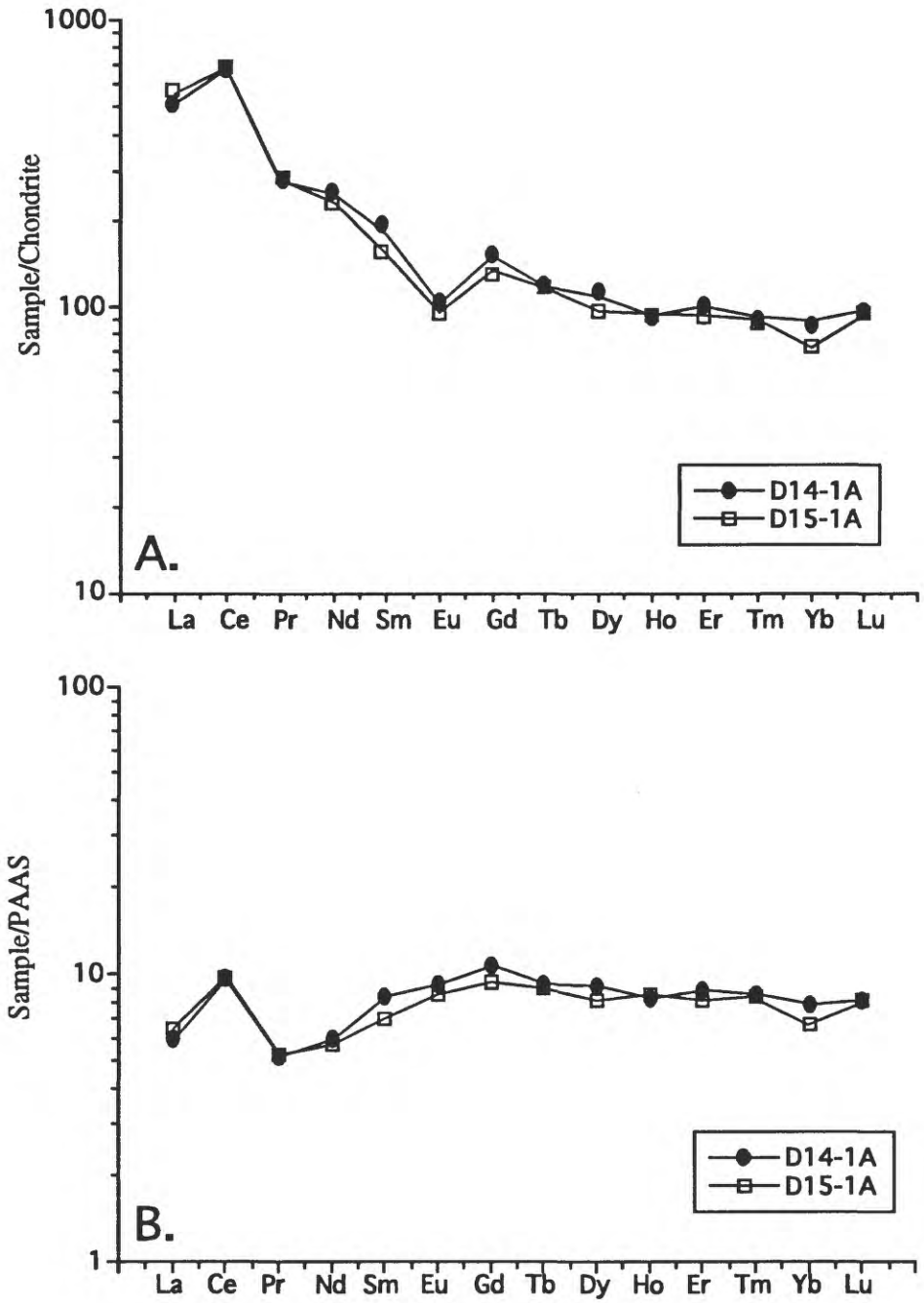

Figure 15. REE plots of bulk crusts from dredges D14 and D15, Litakpooki Ridge: (A) Chondrite normalized, and (B) PAAS normalized